Cumulative population-level effects of habitat loss on seabirds 'Kader Ecologie en Cumulatie 4.0'

Author(s): F.H. Soudijn, S. van Donk, M.F. Leopold, J.T. van der Wal, and V. Hin.

Wageningen Marine Research

WAGENINGEN
UNIVERSITY & RESEARCH

Client: Rijkswaterstaat Water, Verkeer en Leefomgeving
            Attn.: K. Portegies
            Lange Kleiweg 34
            2288GK Rijswijk

This report can be downloaded for free from https://doi.org/10.18174/565601
Wageningen Marine Research provides no printed copies of reports

Wageningen Marine Research is ISO 9001:2015 certified.

© Wageningen Marine Research

Contents

Publiekssamenvatting

In het programma 'Noordzee 2022-2027' worden nieuwe gebieden op zee aangewezen als zoekgebieden voor windenergie. In deze studie is een inschatting gemaakt van de negatieve effecten van habitatverlies op zeevogels door de potentiële nieuwe windparken binnen deze zoekgebieden. De effecten zijn bepaald voor de volgende vogelsoorten: duikers[1], noordse stormvogel, jan-van-gent, aalscholver, eider, zwarte zee-eend, grote stern, zeekoet, alk en papegaaiduiker. Waar, vanwege hun kustgebondenheid, voor aalscholver, eider en zwarte zee-eend alleen een inschatting is gemaakt van aantallen slachtoffers, zijn voor de andere soorten effecten bepaald op populatieniveau.

De schattingen van de effecten van habitatverlies zijn gedaan voor vijf verschillende scenario's: een scenario omvat de al geplande windparken tot en met 2030; drie scenario's voor de windenergiezoekgebieden tot en met 2030, die een ontwikkeling van 10.7, 12.7, en 16.7 GW windenergie doorrekenen bovenop de al geplande windenergiegebieden tot en met 2030; een internationaal scenario waarin alle momenteel geplande windenergiegebieden tot en met 2030 op internationaal niveau zijn meegenomen.

De inschatting van de slachtofferaantallen van habitatverlies is gebaseerd op de overlap tussen vogeldichtheidskaarten van alle bovengenoemde soorten en de windenergie zoekgebieden. De effecten van de geschatte slachtoffers op populatieniveau zijn berekend met populatiemodellen gebaseerd op de meest recente veldgegevens van reproductie en overleving van de betreffende soorten zeevogels. De populatie-effecten van habitatverlies zijn getoetst aan de hand van soortspecifieke normen ('Acceptable Levels of Impacts'; ALIs), die zijn opgesteld door LNV.

De geschatte aantallen jaarlijkse slachtoffers van habitatverlies voor de aalscholver (3), eider (4) en zwarte zee-eend (7), lijken verwaarloosbaar omdat de slachtofferaantallen niet toenemen voor de scenario's met de windenergiezoekgebieden vergeleken met de al geplande windenergiegebieden tot en met 2030. De hoogste aantallen jaarlijkse slachtoffers zijn voorspeld voor de zeekoet (589-1419), alk (165-372) en noordse stormvogel (12-33). Geen van de geschatte populatie-effecten van habitatverlies overschreden de ALIs. De geschatte populatie-effecten van habitatverlies zijn het sterkst voor de zeekoet en de alk.

---

[1] Overwegend roodkeelduiker.

Summary

In the programme 'Programma Noordzee 2022-2027', offshore wind farm (OWF) search areas will be designated as development areas for generating wind energy. An assessment was made of the effect of habitat loss due to offshore wind development in these search areas on the following seabird species: diver spec.[2], northern fulmar, great cormorant, common eider, common scoter, common guillemot, razorbill and Atlantic puffin. For great cormorant, common eider and common scoter, the effects of habitat loss were assessed based on estimated numbers of casualties. For the other species, population models were used to assess the effect of habitat loss on the population level. For northern gannet and sandwich tern, both the effects of habitat loss and the effects of collision mortality were tested together in the population models. Here, the method and calculation of the numbers of casualties due to habitat loss are described. The estimation of the numbers of casualties due to collision mortality are described in Potiek *et al.* (2021a). The population effects of offshore wind farms on seabirds were considered for six different scenarios:
- No offshore wind farms
- Basic: All offshore wind farms planned up to 2030
- 'Rekenvariant I' (Basic+10.7 GW)
- 'Rekenvariant II' (Basic+12.7 GW)
- 'Rekenvariant III' (Basic+16.7 GW)
- International wind farms + Rekenvariant III

The assessment of the effect of OWF search areas on the ten seabird species considered here consisted of the following steps:
1. Data preparation of seabird observations at sea.
2. Calculation of density and dot maps for the seabird species, the choice of map type depends on the data availability.
3. Calculation of the number of casualties due to habitat loss based on the overlap between the bird maps and the wind farm search areas.
4. Development of new population models for northern fulmar and Atlantic puffin and an update of the parameters of the population models for the other five species.
5. Calculation of annual mortality probabilities due to habitat loss for all species. For the northern gannet, an additional estimation of annual mortality from habitat loss was made using an Individual Based Model.
6. Test of the population level effects of annual mortality due to habitat loss and collision mortality for northern gannet and sandwich tern and habitat loss only for the other species. Population level effects were tested against the Acceptable Level of Impact (ALI) thresholds (Potiek *et al.*, 2021a), of which values were defined in a working document by LNV.

For great cormorant, common eider and common scoter, species that reside mostly in nearshore waters, the effects of habitat loss of the wind farm search areas seem negligible as the number of casualties does not increase for the scenarios with new OWF search areas compared to the scenario with the OWFs that are already planned. The estimated total annual numbers of casualties for great cormorant, common eider and common scoter were respectively 3, 4 and 7 for the national scenarios. Most habitat loss casualties in the national scenarios were predicted for common guillemot (annual totals of 588-1419) and razorbill (annual totals of 165-372), followed by northern fulmar (annual totals of 12-33). For the seven species for which population models were used, the number of casualties from habitat loss did not lead to violation of the ALI thresholds. The population growth rates of razorbill and common guillemot were predicted to be most negatively affected by habitat loss. The KEC assessment methodology is continuously in development and updated according to the most recent scientific knowledge. One of the main uncertainties in the methodology are the quality and spatial coverage of the data on bird observations, which vary between species and through time. Furthermore, the method to predict bird densities could be improved, by using spatial statistical

---

[2] Likely to refer mainly to red-throated diver.

models that predict bird density as a function of relevant covariates. In addition, it is recommended to refine the current method such that it can quantify or qualify uncertainty in all of the assessment steps. Finally, the method to calculate the number of casualties from habitat loss needs to be better integrated with the newly designed ALI method. Ideally, a more sophisticated method based on a mechanistic understanding of habitat loss, should be developed. The estimates in this study give the best estimate possible based on the species distribution data and assessment framework available to us at the current moment and are based on the assumption that seabird distributions will not drastically change in the next 30 years.

1   Introduction

Offshore wind farms (OWF) form an important part of the Dutch strategy to comply with the agreements on reducing CO_2 emissions, such as defined in the Paris Agreement. The draft North Sea Programme (NSP) 2022-2027, has mapped out search areas that are eligible for wind farm development in the North Sea. In stage one, the space necessary for achieving the stricter EU climate targets of a 55% CO_2 reduction by 2030 is designated ("Versnelling"). This is elaborated in 1) a reservation of space to facilitate future site decisions for the remainder of the 49% target of 0.7 GW wind energy (Roadmap 2030) in existing wind farm areas, and 2) a reservation of space to facilitate future site decisions for a maximum of 10 GW additional offshore wind energy for the acceleration task (55% EU target) through to 2030. There is a need for the assessment of the cumulative ecological effects on seabirds of the development of wind farm search areas following the framework 'Kader Ecologie en Cumulatie' (KEC), such as previously described by Leopold *et al.* (KEC 2.0, 2014) and Van der Wal *et al.* (KEC 3.0, 2018). Within KEC, the cumulative effects of wind farms are assessed for species with a protected status in nature legislation. The assessment entails existing and planned future wind farm areas.

The main adverse effects of offshore wind farms on seabirds are thought to stem from mortality due to collisions with turbines and displacement from wind farm areas. The latter may lead to a loss of foraging habitat or barriers to both daily and seasonal movements of birds (Drewitt & Langston, 2006; Masden *et al.*, 2010). The species that are assessed for the effects of collision mortality and displacement were chosen based on previous studies of avoidance behaviour and flight altitudes of seabirds (e.g. Dierschke *et al.*, 2016) and expert elicitation regarding the potential locations of the future wind farms. Here, the focus lies on potential adverse effects of wind farms on seabirds in relation to displacement and habitat loss. Another part of KEC 4.0 focuses on the effects of collision mortality (Potiek *et al*., 2021b). The potential adverse effects of wind farms as barriers to movement are not under consideration within KEC. Species that show high avoidance are thought to be more sensitive to displacement and habitat loss, while the species that show low avoidance and typically fly at altitudes within the rotor areas of the turbines are thought to be more sensitive to collision mortality. In the current assessment, the sandwich tern and the northern gannet are assessed for potential adverse effects of both collision mortality and habitat loss.

In the previous assessments the cumulative population-level effects were tested against species-specific Potential Biological Removal (PBR) reference points. The PBR approach was criticized because it implies a fixed level of density dependence in the populations that leads to compensation of mortality which may not actually occur (O'Brien *et al.*, 2017). Thresholds based on actual population models that explicitly consider the population dynamics of species are considered more reliable (Potiek *et al.*, 2019). Therefore, thresholds were developed, in the form of Acceptable Levels of Impacts (ALIs) that are based on matrix population models (Potiek *et al*., 2021a). The current KEC assessment will test the population-level effects of offshore wind farms on seabirds against the species-specific ALI values defined by LNV in a working document. All other steps in the assessment follow the methodology previously described by Leopold *et al.* (KEC 2.0, 2014) and Van der Wal *et al.* (KEC 3.0, 2018).

2 Study outline

The study focuses on the assessment of the effects of habitat loss on ten seabird species (Table 1). Another part of KEC focusses on estimating the effects of collision mortality (Potiek *et al*., 2021b). Within the current study, density maps were created for both the bird species that are under assessment for habitat loss (Table 1) and for collision mortality (Table 2). The study consists of the following components:

   a. Dot and density maps for the seabirds that are assessed for the effects of habitat loss and collision mortality;
   b. Population models for seven of the ten species, of which two were newly developed;
   c. Individual based model (IBM) for the northern gannet, which is used as an alternative method to estimate casualties of habitat loss;
   d. Estimated numbers of casualties due to habitat loss per offshore wind farm search area for all ten species based on the overlap of the density maps with offshore wind farm search areas;
   e. Estimated mortality due to habitat loss for the northern gannet based on the IBM;
   f. Estimated population-level effects of habitat loss for five of the ten species and estimated population-level effects based on the combination of habitat loss and collision mortality for two species, the sandwich tern and the northern gannet.

Each component is described in more detail in the following paragraphs.

2.1.1 Bird dot and density maps

Data from the ESAS and MWTL databases were used to create bird dot and density maps for the species under assessment for habitat loss (Table 1) and collision mortality (Table 2). The density maps were created based on the methodology previously described by Leopold *et al.* (2014) and van der Wal *et al.* (2018). Dot maps were created for all species for which the available data were insufficient for full coverage density maps (Table 2). Note that for northern gannet and sandwich tern the effects of both habitat loss and collision mortality were assessed.

Table 1. Data of the seabird species that are under evaluation for habitat loss, including Euring, names and type of density map (0, basic density map, 1, density map with medium spreading of data over an area of 5x5 grid cells, or 625 km^2, see section 3.2.2). The last column indicates the source of the matrix population model, if applicable for that species.

Euring	Scientific Name	NL name	EN name	Type	Population model
59	*Gavia sp. (mainly Gavia stellata and to some extent Gavia arctica)*	Duiker spec.	Diver sp.	0	(van Kooten *et al.*, 2019)
220	*Fulmarus glacialis*	Noordse stormvogel	Northern fulmar	1	This study
710	*Morus bassanus*	Jan-van-gent	Northern gannet	1	(van Kooten *et al.*, 2019)
720	*Phalacrocorax carbo*	Aalscholver	Great cormorant	0	-
2060	*Somateria mollissima*	Eider	Common eider	0	-
2130	*Melanitta nigra*	Zwarte zee-eend	Common scoter	0	-
6110	*Thalasseus sandvicensis*	Grote stern	Sandwich tern	0	(van Kooten *et al.*, 2019)

Euring	Scientific Name	NL name	EN name			Reference
6340	*Uria aalge*	Zeekoet	Common guillemot	0		(van Kooten *et al.*, 2019)
6360	*Alca torda*	Alk	Razorbill	0		(van Kooten *et al.*, 2019)
6540	*Fratercula arctica*	Papegaaiduiker	Atlantic puffin	0		This study

Table 2. Data of the seabird species that are under evaluation for collision mortality, including Euring, names and type of density map (*, dot map; 0, basic density map, 1, density map with medium spreading of data over an area of 5x5 grid cells, or 625 km^2; 2, density map with medium spreading of data over an area of 11x11 grid cells, or 3025 km^2, see section 3.2.2).

Euring	Scientific Name	NL name	EN name	Type
710	*Morus bassanus*	Jan-van-gent	Northern gannet	1
800	*Phalacrocorax aristotelis*	Kuifaalscholver	European shag	*
1530	*Cygnus columbianus bewickii*	Kleine zwaan	Tundra (Bewick's) swan	*
1680	*Branta bernicla*	Rotgans	Brent goose	*
1730	*Tadorna tadorna*	Bergeend	Shelduck	*
4960	*Calidris canutus*	Kanoet	Red knot	*
5320	*Limosa limosa*	Grutto	Black-tailed godwit	*
5340	*Limosa lapponica*	Rosse grutto	Bar-tailed godwit	*
5410	*Numenius arquata*	Wulp	Eurasian curlew	*
6270	*Chlidonias niger*	Zwarte stern	Black tern	*
15820	*Sturnus vulgaris*	Spreeuw	Common starling	0*
5670	*Stercorarius parasiticus*	Kleine jager	Arctic skua	0
5690	*Stercorarius skua*	Grote jager	Great skua	0
5780	*Hydrocoloeus minutus*	Dwergmeeuw	Little gull	0
6110	*Thalasseus sandvicensis*	Grote stern	Sandwich tern	0
6169	*Sterna paradisaea+hirundo*	'Noordse dief'	'Commic tern'	0
6020	*Rissa tridactyla*	Drieteenmeeuw	Kittiwake	1
5910	*Larus fuscus*	Kleine mantelmeeuw	Lesser black-backed gull	2
5920	*Larus argentatus*	Zilvermeeuw	European herring gull	2
6000	*Larus marinus*	Grote mantelmeeuw	Great black-backed gull	2

0* for 15820, Sturnus vulgaris, both a dot map and a density map were made.

2.1.2 Population models

For the great cormorant, common eider and common scoter, no population level effects were estimated because little overlap is to be expected between these species' coastal distributions and the Dutch (plans for) offshore wind farms. Population effects were calculated for the other seven species that were assessed for habitat loss (Table 1). For five of those (divers sp., northern gannet, sandwich tern, razorbill and common guillemot), population models were taken from the study by van Kooten *et al.* (2019) and were updated with the most recently published values for breeding success and survival. For northern fulmar and Atlantic puffin new population models were developed (Table 1). These models have the same structure as the five population models previously described by van Kooten *et al.* (2019).

2.1.3 Habitat loss mortality per scenario

For all ten species, casualties of habitat loss for seabirds were calculated per bimonthly period and OWF area, based on the same assumptions and calculations as the previous assessments described by Van der Wal *et al.* (KEC 3.0, 2018) and Leopold *et al.* (KEC 2.0, 2014). Annual mortalities per scenario (Table 3 and **Figure 3-4**) were calculated based on the estimated number of birds under the footprints of OWFs in each scenario and estimated population sizes (from the density maps) for the

seven species for which population models were available. This study considers four different scenarios for the Dutch EEZ (Table 3): a basic or base scenario, including operational, under construction, pre-construction and/or authorised OWFs and three other scenarios representing possible search areas to be developed up to ca. 2030. These scenarios were provided to WMR by the commissioner (RWS). The OWFs per scenario and OWF specific information are given in Annex 1.

Table 3. Scenario names and wind farms included per scenario, a list of wind farm areas per scenario can be found in Annex 1.

Scenario name	Included wind farms
Null	No wind farms
basic 2030	existing and permitted wind farms in 2030 (10.8 GW)
'Rekenvariant I'	basic + 10.7 GW
'Rekenvariant II'	basic + 12.7 GW
'Rekenvariant III'	basic + 16.7 GW
International	existing and expected international farms up to 2030, national Rekenvariant III scenario included

2.1.4 Individual based model northern gannet

An individual based simulation model (IBM) was used to assess the effect of OWF-induced habitat loss on survival for the northern gannet. For this species, the IBM was used as a second approach to estimate mortality due to habitat loss, next to the mortality estimation based on bird density maps as described in the next section. The IBM model was originally developed within the WOZEP programme (van Kooten *et al.,* 2019). Van Kooten *et al.* (2019) showed that for the northern gannet the mortality estimates by the IBM were likely higher than for the "10% mortality rule" applied in KEC 3.0. Therefore, we estimate the mortality due to habitat loss both with the IBM and the method described previously by Van der Wal *et al.* (KEC 3.0, 2018) and Leopold *et al.* (KEC 2.0, 2014). Only effects of the international and national '*rekenvariant III'* OWF-scenarios were calculated with the IBM due to the time constraints of the project.

2.1.5 Population-level effects

The population-level effects of habitat loss were assessed with species specific population models for five species (Table 1). For the sandwich tern and the northern gannet, the population- level effects of both habitat loss and collision mortality were assessed with population models. The collision mortalities that were used for northern gannet and sandwich tern were calculated by Potiek *et al.* (2021b). Using the models, the population growth rates without OWF were compared to the population growth rates with the additional mortality due to OWFs. The changes in population growth rates for all seven species were then tested against Acceptable Levels of Impact (ALIs) (Potiek *et al.*, 2021a). We report whether the estimated mortality due to OWFs leads to an exceedance of the ALIs for any of the species.

3 Materials and Methods

In short, the methodology to assess the effects of habitat loss on the ten seabird species consists of the following steps:

a. The selection and pre-processing of the data from the international European Seabirds At Sea (ESAS, version 6.1) and Dutch MWTL (Monitoring Waterstaatkundige Toestand des Lands) databases for both the species that are under assessment for collision mortality (Table 2) as well as the species that are under assessment for habitat loss (Table 1).

b. The spatial conversion of the data from the previous step and the creation of dot maps and density maps for both the species that are under assessment for collision mortality (Table 2) as well as the species that are under assessment for habitat loss (Table 1).

c. The development of two new population models and update of the parameter values of five population models.

d. The implementation of an individual based model (IBM) for the estimation of habitat loss mortality for the northern gannet.

e. The calculation of habitat loss casualties per species, bimonthly period, wind farm area and data subset (national/international) based on the overlap between density maps and offshore wind areas.

f. The calculation of annual habitat loss mortality per species and scenario, for the northern gannet based on the IBM (d) as well as on the overlap between density maps and offshore wind areas (e).

g. The assessment of the population level effects of the mortalities due to habitat loss and testing against the Acceptable Levels of Impact (ALIs).

3.1 Data preparation

The selection and pre-processing of data was done in preparation of the creation of dot maps and density maps for both species that are under assessment for collision mortality (Table 2) as well as for the species that are under assessment for habitat loss (Table 1).

3.1.1 Data sources

The European Seabirds At Sea (ESAS) database (version 6.1) that includes mostly ship-based counts of seabirds in the greater North Sea was recently screened and updated by the Brussels 'Instituut voor Natuur- en Bosonderzoek' (INBO). The 'Monitoring Waterstaatkundige Toestand des Lands' (MWTL) database holds aerial surveys covering the Dutch section of the North Sea, and was provided by Bureau Waardenburg. More in-depth information on seabird counts can be found in previous studies (Camphuysen *et al.*, 2004; Van Roomen *et al.*, 2013; Fijn *et al.*, 2020).

3.1.2 Data selection

Counts from 1991 onwards were selected with valid geographical position (latitude and longitude) and a non-zero sampled surface area, until the most recent data available (7-July-2020 for MWTL, 20-December-2019 for ESAS). Each count was assigned to a "period" (bimonthly periods, Table 4) based on the month of survey, which was later used to merge data (Baptist & Wolf 1993). An overview of the spatial effort per data source per bimonthly period can be found in **Figure 3-1**. Spatially, counts were selected that fall within the area of "Southern North Sea" & "Central North Sea" (**Figure 3-2**).

Table 4. Bimonthly periods used for the bird maps.

Period	Months
1	August + September
2	October + November
3	December + January
4	February + March
5	April + May
6	June + July
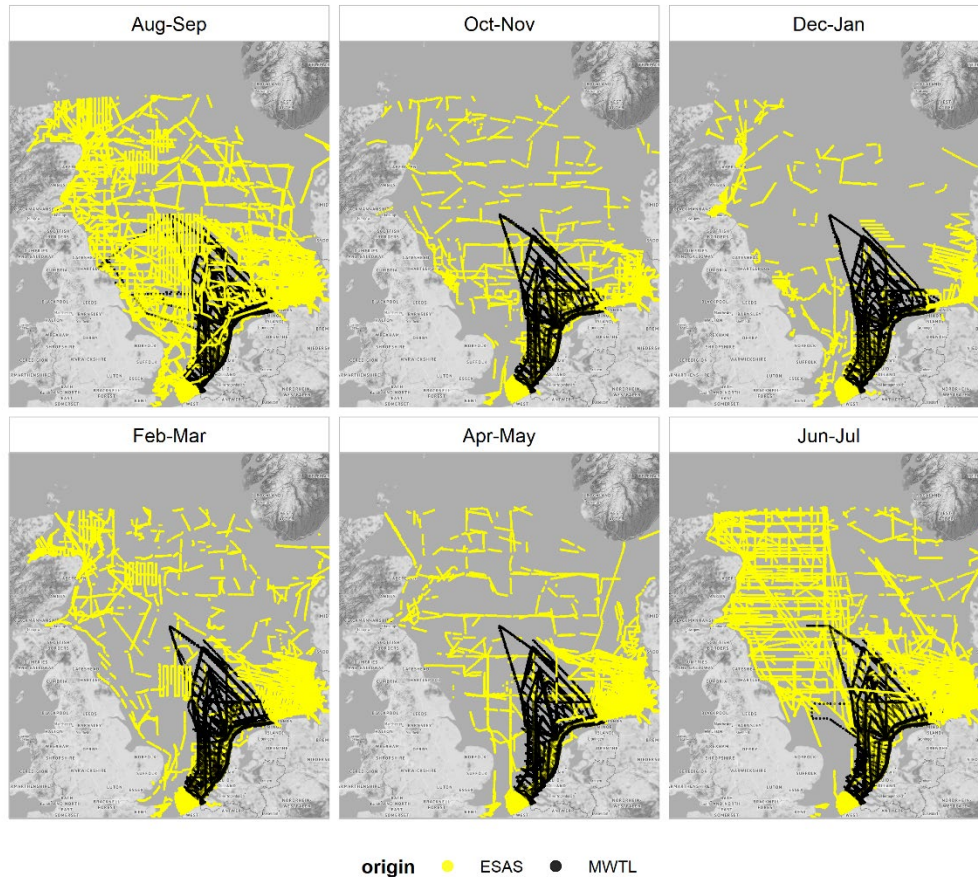
Figure 3-1. *Counting effort of the two data sources used in this study (ESAS in yellow and MWTL in black) per bimonthly period. The background of this map is created with the ggmap package (Kahle & Wickham, 2013).*

In line with the previous KEC-assessments, a number of (sub)species and observations were merged in the dataset because these were often not identified at species level (Table 5). For instance, red-throated divers and black-throated divers have been merged into "diver sp.". Other observations were split into the species that are covered by the overarching term (Table 5). For example, the specifically unidentified common guillemot/razorbills were split based on the known species composition per bimonthly period and position. A grid of 50 by 50 km was used and all observations from 1991 onwards of relevant species were summed per grid cell per bimonthly period to calculate proportions of occurrence.

Counts were conducted in strips; a predetermined area with a certain length, width and hence, surface. Birds that were counted outside this strip, either flying or on the water, were not selected for further analysis. During ship-based counts (ESAS) the snapshot method was used for flying birds (Tasker et al. 1984).

Table 5. Overview of overarching Euring codes and in which species counts are split or joined

Euring code	Name	Split in:	Merged as:
6169	Common tern/Arctic tern		Common tern, Arctic tern ('commic tern')
59	Diver sp.		Red-throated diver, black-throated diver, unidentified diver
5910	*Larus fuscus*		Lesser black-backed gull (all (sub)species/races)
5920	*Larus argentatus*		European herring gull (all (sub)species/races)
6345	Common guillemot/razorbill	Common guillemot, razorbill	
6549	Alcidae	Common guillemot, razorbill, Atlantic puffin	
849	Cormorant sp.	European shag, great cormorant	
5919	Lesser black-backed gull/European herring gull	Lesser black-backed gull, European herring gull	
6009	Unidentified *Larus* gull	Lesser black-backed gull, European herring gull, yellow-legged gull, Caspian gull, great black-backed gull, black-headed gull, common gull	
6049	Unidentified gull	Lesser black-backed gull, European herring gull, yellow-legged gull, Caspian gull, great black-backed gull, black-headed gull, common gull, Black-legged kittiwake	
5709	Unidentified skua	Pomarine skua, Arctic skua, long-tailed skua	
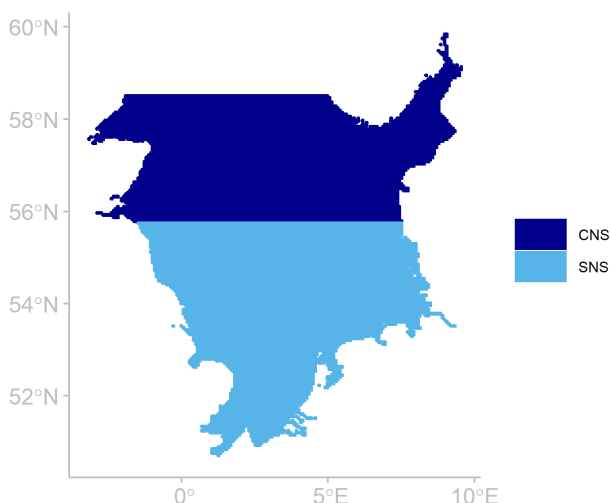
Figure 3-2. *Counts were selected that fall within the area of "Central North Sea" (CNS) & "Southern North Sea" (SNS)*

3.1.3 Distance sampling

Distance sampling is an established method for estimating animal densities (Buckland & Turnock 1992). This method assumes that the probability of detecting an animal decreases with distance. To correct for this distance effect, birds are assigned to distance bins. The first bin is the closest to the ship's or airplane's transect line and the last is the furthest away. Every bin has an estimated standard width.

Standard ship-based counts use a standard strip width of 300 meters perpendicular to the ship with four counting bins with widths of 50m|50m|100m|100m (moving away from the ship). However, there are also counts with strip widths of 100, 150, 200 or 500 meters. All birds in the two closer bins of 50 meter were assumed to be detected, although, in reality there will always be some birds missed. Per species, the potentially missed individuals in the outer bins were estimated by comparing the summed numbers of birds in the first two bins with the numbers seen in each of the outer two bins. This allowed for a correction of birds missed in these outer bands, depending on the species. For each strip width, a separate correction factor was calculated. When relatively more birds were recorded in the outer two bins, resulting in a correction factor for missed birds that was below 1, the factor was set at 1 and actual count values were used. For some large species, such as the common eider, which were presumably always detected in all bins, but for which insufficient numbers of observations were available, the correction factor was also set at 1. Ship counts with a transect width of 100 were left uncorrected, as they only include the two closer bins of 50 meter. The corrections were only calculated for birds counted on the water and not for flying birds: these usually moved over several bins and are presumably relatively easily detected.

Aerial surveys were conducted by MWTL and ESAS. MWTL surveys were conducted without distance estimation until mid-2014 and were left uncorrected in the used dataset. Later MWTL aerial counts were conducted with distance estimation. "Effective strip widths" were calculated by Bureau Waardenburg (Fijn *et al.*, 2019; 2020) and were used to correct the area surveyed, instead of the number of observations. For common eider, common scoter and Arctic skua, no factors were calculated and area surveyed was left uncorrected. Aerial counts conducted by ESAS either used two bins (44 m|91 m|163 m) or three bins (44 m|91 m|163 m|432 m), with the first 44 m left uncounted as this section was obscured from view (directly under the airplane). Number of birds (per meter strip width) in the first two bins were comparable, therefore only birds in the third bin (163 m-432 m) were corrected and counts with only two bins were left uncorrected. Correction factors were calculated in the same way as for the ship counts described above; expected numbers per species based on the first two bins were divided by the actual counted numbers per species. When the correction factor was below 1, the factor was set at 1 and actual counts were used.

Numbers of birds were summed per position key (unique code per transect segment per survey) per species and these sums were, where applicable, multiplied by the calculated correction factors. For ship-based counts, birds within the transect (scored as 'on the water' or 'flying') that were not assigned to a specific bin were added to the totals per position key, after correcting the numbers of birds that were assigned to specific bins. Totals per species per position key were converted to densities (numbers per square kilometer) by dividing the corrected totals by the area surveyed (which is the transect width in kilometers multiplied by the kilometers travelled).

For all species, zeros were added to the dataset at every position where counts had been conducted but where that specific species was not seen.

3.1.4 Count methods & species counted

The ESAS database is collated from surveys with different objectives. In most (standard) surveys, all species were counted. However, some surveys targeted specific species, or groups of species and these are not suitable to evaluate the presence of other species. Furthermore, in ship-based counts, flying birds are not always assigned to a transect ("no snapshot method for flying birds"). For these counting methods, we only included species that are mainly swimming. Within our selection these are the divers, common guillemot, razorbill, Atlantic puffin, common eider and common scoter. All observations of species that were not counted during a specific expedition (including the zeros) were not included in the analyses.

3.2 Density maps and dot maps

Dot maps and density maps were calculated for both the species that are under assessment for collision mortality (Table 2) as well as for the species that are under assessment for habitat loss (Table 1).

3.2.1 Dot maps

During the pre-processing of the raw data from both ESAS and MWTL, it was noted that for a number of species under evaluation for collision mortality, the available data were insufficient for full cover density maps. To determine which species are seen frequently enough to produce density maps, numbers of observations per species were plotted geographically. For species with few observations, the actual counts summed per observation key were mapped instead (Table 2).

3.2.2 Density maps

Seabird density maps were calculated following the methodology described in the previous assessments (KEC 2.0, Leopold *et al.*, 2014; KEC 3.0, Van der Wal *et al.*, 2018). While the previous assessment used data up to 2017 (Van der Wal *et al.*, 2018), in the current assessment for both the international North Sea (INT) and the Dutch EEZ (NAT) maps (**Figure 3-3**), data up to 2020 were used (Table 6). Data from both ESAS and MWTL were used for international density maps, and, in contrast to the previous assessment, only MWTL data were used for the national maps (Table 6). Density maps were calculated both for species that are under assessment for the effect of habitat loss (Table 1) as well as for species that are under assessment for the effects of collision mortality (Table 2). For each bird species fourteen density maps were calculated: a national and international map of each of the six bimonthly periods (Table 4) and of a yearly average.
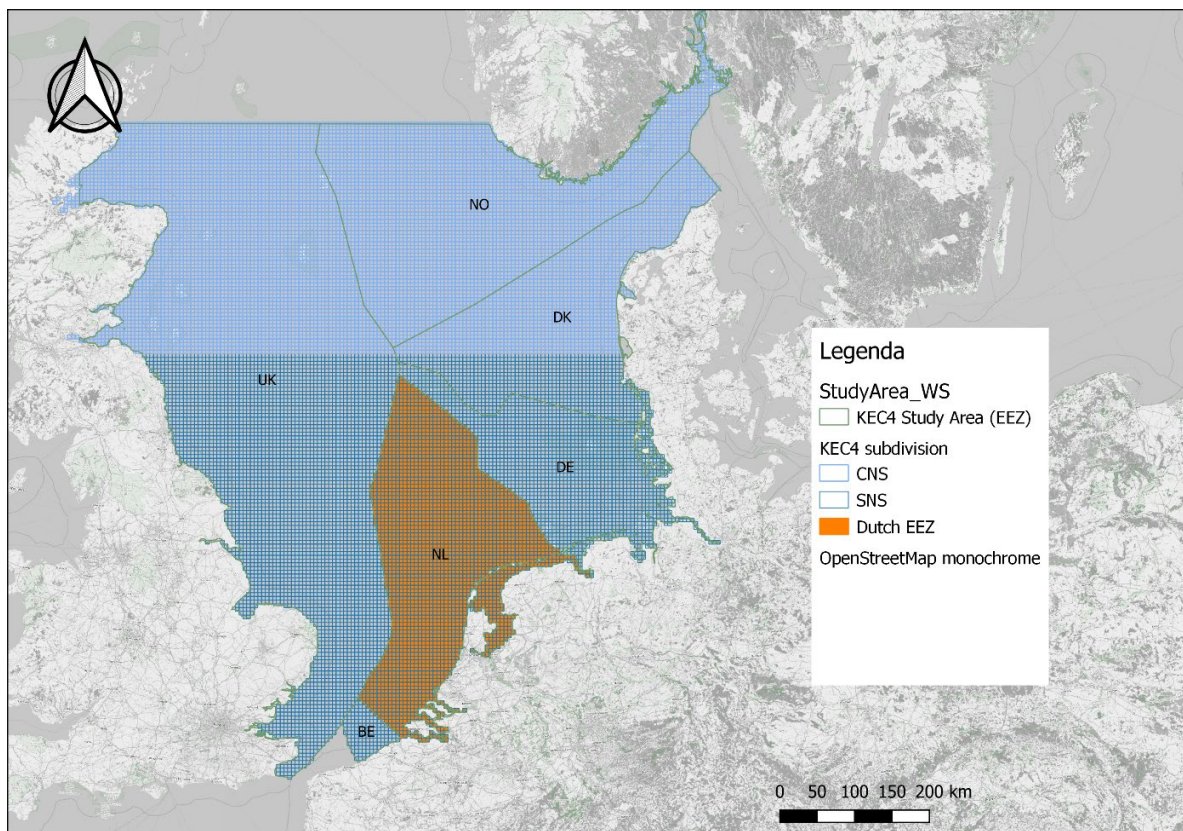
Figure 3-3. *Study area with subdivisions, the Ducth EEZ (national scenarios, indicated in orange) and the international, southern North Sea (international scenarios, green outline).*

The data were converted to grids with grid cells of 5x5 km. For some species, calculated local densities tend to be too high due to clumping behaviour behind fishing vessels (Leopold *et al.*, 2014). For these species, bird densities >10 birds/km^2 were spread at a medium (5 x 5 grid cells) or high (11 x 11 grid

cells) level before the grid interpolation. Whether such spreading of the data was performed is indicated per species in Table 1 and Table 2.

Values per grid cell were averaged per species and bimonthly period across databases. Interpolated gridded density maps were calculated based on inverse distance weighting (with nearest neighbours). A minimum of 5 cells and a maximum of 15 cells were included in the calculation of the value in each cell and cells at a maximum distance of 317 km could be included in the calculation (but with decreasing weight with distance). It was noted that for a few species data are scarce near the Scottish coast, as a result some empty areas were left in the Moray Firth and Firth of Forth. To fill those empty areas the nearest available data (to the East) were propagated westward. GIS processing, including inverse distance weighting, was executed with QGIS (version 3.16.6-Hannover) and Python (version 3.7.0).

Table 6. Data sources and periods used in calculating the seabird density maps for the international (International North Sea; INT) and national (Dutch EEZ; NAT) maps.

	International	National
Source(s)	ESAS + MWTL	MWTL
Period (years)	1991-2020	2000-2020

3.3   Casualties per wind farm area

Figure 3-4 represents an overview of the offshore wind farms (OWF) that were included in the assessment (source: RWS). For the calculations of the casualties per national scenario and per Dutch OWF area in the national tables and figures, the national bird density maps were used. For the calculations of the casualties per international scenario, the international OWF areas and the Dutch OWF areas in the international figures, the international bird density maps were used.

Casualties due to habitat loss were calculated based on the same assumptions as for the previous assessments (KEC 2.0, Leopold *et al.*, 2014; KEC 3.0, van der Wal *et al.*, 2018). The number of casualties C per OWF area and per bimonthly period i due to habitat loss were calculated as:

$$C_i = B_i * \text{RDRS} * E,$$

which depends on the mean bird density in the OWF area B_i per bimonthly period, the estimated area occupied by the OWF E and the relative displacement risk score RDRS (Table 7). These latter scores are taken from Leopold *et al.* (2014; table 4.21*)* and are a combined measure of the vulnerability of a species for habitat loss and the species' sensitivity (Bradbury *et al.,* 2014).

The provided OWF boundaries delineate the outer edges where an offshore wind turbine can be positioned (**Figure 3-4**). For each area occupied/influenced by an OWF, the mean bird densities per bimonthly period (B_i) were calculated based on the density values of the grid cells inside each OWF and inside a 500 m buffer around each OWF. All vector grid-cells that have some overlap with the buffered OWF were included in this mean. The estimated area occupied by the OWF (E) was calculated by multiplying the known area of the OWF by a scale factor. The scale factors are 1 for e.g. fully commissioned OWFs and for most other OWFs that are in a late state of development. The OWF in early development stages, labelled as concept/early planning resp. development zone, mostly have a scale factor well below 1 because the area under consideration is far larger than needed for the amount of power that is planned to be installed. The scale factors were calculated by estimating the required area assuming a future density of 10 MW/km^2 (based on information provided by RWS).
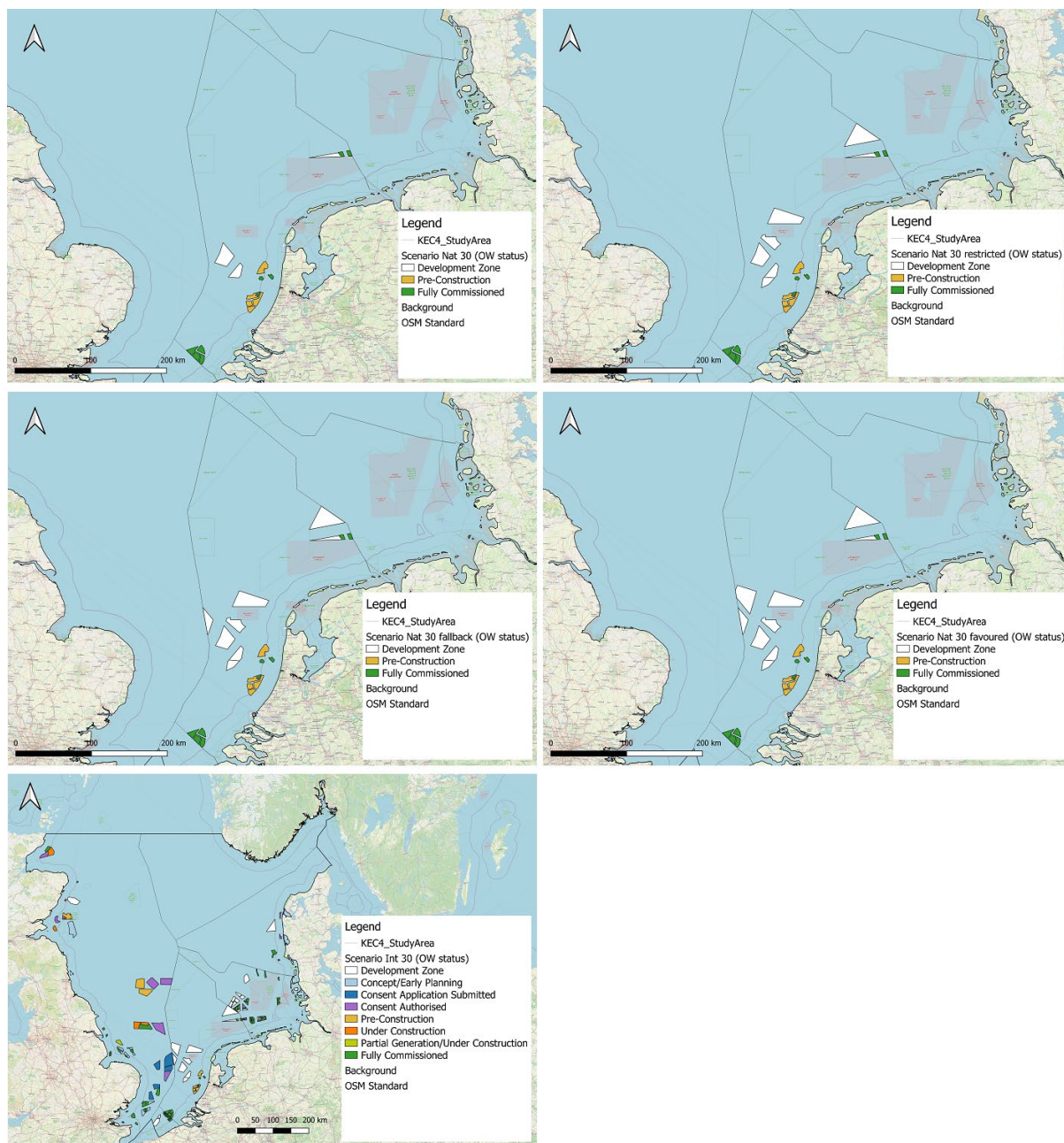
Figure 3-4. *Overview of the OWFs included in the scenarios for the habitat loss calculations.*

Table 7. Relative Displacement Risk Score (RDRS) per seabird species. Values for RDRS were taken from Leopold et al. (2014; table 4.21).

Euring	Scientific Name	English name	RDRS
59	*Gavia sp.*	Diver sp.	0.080
220	*Fulmarus glacialis*	Northern fulmar	0.004
710	*Morus bassanus*	Northern gannet	0.008
720	*Phalacrocorax carbo*	Great cormorant	0.012
2060	*Somateria mollissima*	Common eider	0.048
2130	*Melanitta nigra*	Common scoter	0.080
6110	*Thalasseus sandvicensis*	Sandwich tern	0.024
6340	*Uria aalge*	Common guillemot	0.036
6360	*Alca torda*	Razorbill	0.036
6540	*Fratercula arctica*	Atlantic puffin	0.024

3.4 Individual-based model northern gannet

An individual based simulation model (IBM) was used to assess the effect of OWF-related habitat loss on northern gannet survival. For this species, the IBM was used as a second approach to estimate OWF related mortality, in addition to the mortality estimation based on bird density maps as described in Section 3.3. The IBM model was originally developed within the WOZEP programme (van Kooten *et al.,* 2019). Important constants and characteristics of the IBM are summarized in Table 8.

The IBM model developed by van Kooten *et al*. (2019) was adjusted for the current assessment. The model simulates the energy budget of birds that move around a discretized habitat quality map (grid) of the North Sea. The energy level of each bird is depleted by a fixed amount each time step, and birds replenish their energy level each time step with an amount that is equal to the habitat quality of their location at that time. Birds that run out of energy die from starvation. Movement of birds is random, but the chance of moving to a neighbouring grid cell is proportional to the habitat quality of that grid cell, with a higher probability of moving to a cell with higher habitat quality. Habitat quality of grid cells that contain an OWF is reduced in proportion to the size of the OWF and the avoidance rate of the birds. Survival of a large number of birds from simulations with and without OWFs is compared to estimate habitat loss mortality induced by avoidance of OWF-areas.

3.4.1 Habitat maps

The habitat quality maps (grid) of the North Sea as used within the IBM are scaled versions of the bird density maps produced for the current assessment (section 3.2.2), under the assumption that bird density is proportional to food abundance. This is based on the idea that birds spend more time in foraging locations. Bird density maps were rescaled by truncating the bird density of grid cells that exceeded the 99th quantile of the distribution of positive bird densities across all grid cells. Subsequently, bird densities were rescaled with the maximum bird density on the (truncated) bird density map. This ensured that the maximum habitat quality on the map equalled one.

Birds could move to all grid cells within the KEC4 study area. Other grid cells were marked as land and birds could not move to these areas. The KEC4 study area encompasses the Central and Southern North Sea, as shown in **Figure 3-2** and **Figure 3-3**. In addition, grid cells for which bird density could not be estimated, either because they were not surveyed, or too little data were available, were marked as land.

We produced a unique habitat quality and land map for each bimonthly period, corresponding to the bird density map of that period (Table 4).

3.4.2 OWF maps

Displacement by OWFs was modelled by reducing the habitat quality of grid cells that contained OWFs. Because the chance that a bird moves to a grid cell is proportional to the habitat quality of that grid cell, birds are less likely to move to grid cells that contain OWFs. The reduction in habitat quality of an OWF grid cell is proportional to the tendency of the birds to avoid OWFs, and to the size of the OWF relative to the size of the grid cell (5x5 km).The size of the OWF relative to the total area of the overlapping grid cells is termed $OWF_{fraction}$. The avoidance parameter p captures the tendency of northern gannets to avoid OWF areas. For all grid cells the habitat quality correction factor was calculated as:

$$OWF_{scale} = (1 - p * OWF_{fraction})$$

Because there were several grid cells that contained (parts of) multiple OWFs, this equation was iterated for all OWFs included in each OWF scenario. Consequently, the grid cells that contained multiple OWFs were downscaled multiple times. This led to proportionally lower values of OWF_{scale}, compared to grid cells that contained only a single OWF. Note that $OWF_{scale} = 1$ for grid cells without OWFs. Finally, OWF-adjusted habitat quality maps were calculated by multiplying, for each grid cell, the habitat quality value with the value of OWF_{scale}.

3.4.3 Energetics

Each bird is characterized by its position on the map and its energy level E_t, which changes with time t. Each time step, the energy level is depleted by a fixed amount equal to the bird's field metabolic rate m. We assume that m is constant over time. In addition, birds replenish their energy level according to the habitat quality of their current location. Thus, the acquired energy per time step, I_t, varies with the location of the bird, which changes as birds move around the grid. For each individual bird, the energy level at time step t is calculated from the energy level at the previous time step (E_{t-1}) as:

$$E_t = E_{t-1} + I_t - m$$

The individual dies when $E_t \leq 0$. The units of E, I and m are arbitrary, because we are only interested in the relative effect of displacement from OWFs and not in the absolute energy dynamics. We express E_t in 'normalized habitat quality', and I_t equals the habitat quality of the location occupied by the bird at time t (van Kooten *et al.*, 2019)

3.4.4 Movement

Each time step, a bird can move to a grid cell within the surroundings of its current position, or remain in its current location. Birds were restricted from moving to grid cells on land, as indicated by the land map. Movement is random, but the chance of moving to a surrounding grid cell, or remaining in the current grid cell, is proportional to the habitat quality of that grid cell (**Figure 3-5**). To obtain proper probabilities, habitat qualities of surrounding grid cells were normalized, such that sum of all probabilities equalled one. Following van Kooten *et al.* (2019), we present results for a maximum travel length of 1 grid cell per time step in the main text. In this case, a bird can move to a total of 9 different grid cells ($(1 + 1 + 1)^2 = 9$). In addition, we analysed the effect of a maximum travel length between 1 and 8 grid cells per timestep (Annex 2). For a maximum travel length of 8 grid cells, each individual bird can move to $(8 + 8 + 1)^2 = 289$ different grid cells. With a grid-cell size of 5km by 5km, the maximum travel distance within a single time step (4 hours) equals 56.6 km. In Annex 2, we present results for a maximum travel length of 8 grid cells per timestep, which probably represents a more realistic travel distance for the northern gannet.
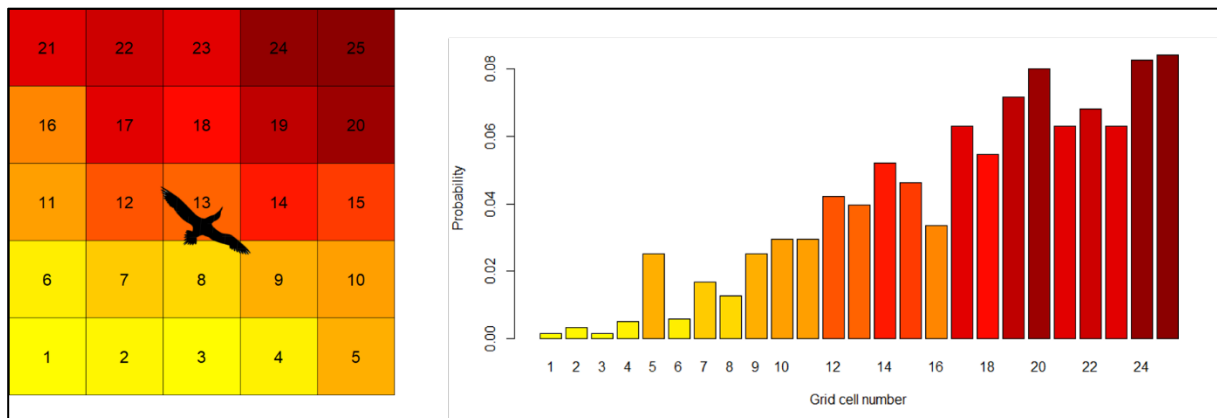
Figure 3-5 The probability of moving to a certain grid cell is proportional to the habitat quality of that grid cell. Left is a sample of the grid with an individual bird in grid cell 13. Colours indicate low (yellow) to high (red) habitat quality. In this illustration, the bird can move at maximum 2 grid cells per time step and samples the surrounding (2 * 2 + 1)² = 25 grid cells. The probability of moving to each of these grid cells is shown in the right panel. Colours correspond to those of the left panel.

Table 8. Constants and variables of the Individual Based Simulation Model for the Northern Gannet

Constant	Value
Dimensions of habitat map (number of grid cells)	219 x 284
Number of grid cells on habitat map	62,196
Number of grid cells within KEC4 study area (excluding 'land' grid cells)	+/- 17,000
Dimension of a single grid cell	5 km x 5 km
Number of birds at start simulation	10,000 individuals
Time period of single simulation	2 months
Length of each time step	4 hours
Number of time steps per simulation (assuming 30 days per month)	360
Number of replicate simulations	1000
Maximum bird movement per time step	1 – 8 grid cells
Baseline annual survival rate	0.9
Bird metabolic rate m	Calibrated
Avoidance parameter p	0.8 or 1.0
OWF scenarios	International 2030 & national *rekenvariant III*

3.4.5   Scenarios and parameters

The avoidance parameter p captures the tendency of northern gannets to avoid OWFs. Following van Kooten *et al.* (2019), we studied two scenarios for the avoidance parameter (Table 8). One scenario assumed complete, 100%, avoidance ($p=1$), and another scenario assumed avoidance of 80% ($p=0.8$).

We applied the northern gannet IBM to estimate the effect of two OWF scenarios: the 'international scenario' and the 'national 2030 Rekenvariant III' scenario (Table 8). For both OWF scenarios, we assumed that individual birds can move across the entire KEC4 study area. Hence, movement of birds in the 'national 2030' scenario was not restricted to the Dutch Continental Shelf and we used the international bird density maps for both scenarios.

Separate OWF-adjusted habitat quality maps were produced for each combination of bimonthly period, OWF scenario and avoidance parameter p, resulting in a total of 24 different OWF-adjusted habitat maps (2 avoidance scenarios x 2 OWF scenarios x 6 bimonthly periods). We additionally studied the effect of varying the maximum travel length of simulated birds over a range of 1 to 8 per timestep of 4 hours (Table 8; Annex 2).

The value of the metabolic rate parameter m was obtained through calibration. The purpose of calibration was to find the value of m that resulted in a predefined survival in absence of OWFs, which was taken to be 0.9 on an annual basis (Table 8; van Kooten *et al.,* 2019). The calibration procedure used the 'bisection method', which is a root-finding algorithm that guarantees convergence. For each value of m, the calibration procedure used the mean survival of 100 replicate simulations. The desired value of m was obtained when the mean survival equalled the predefined survival value of 0.9. The calibration procedure was carried out separately for each of six baseline habitat quality maps that were free of OWFs (one per bimonthly period) times 8 different maximum travel lengths. This resulted in 48 calibrated values of m. Because calibration was performed for each bimonthly period, the annual target survival rate was rescaled to a bimonthly survival S_{bm} according to:

$$S_{bm} = e^{\frac{\ln(S_y)}{6}}.$$

3.4.6 Initialization

Calibration simulations were initialized with 10,000 birds that were assigned an initial position on the grid and an initial energy level. Initial positions were assigned randomly using the spatial distribution of OWF-free habitat quality as probability distribution. Therefore, the initial spatial distribution of birds was proportional to the spatial distribution of habitat quality without OWFs. Following van Kooten et al. (2019), the initial energy level of each bird was equal to the mean habitat quality across the entire grid. Consequently, all birds had the same initial energy level. Simulations with OWFs used the initialization of the corresponding calibration simulation.

3.4.7 OWF simulations

To estimate the impact of OWF-related habitat loss we ran 1,000 replicate simulations for each OWF-adjusted habitat map and maximum travel length, using the corresponding calibrated value of m. A single simulation covered a single bimonthly period with time steps of 4 hours and therefore lasted 360 time steps in total (Table 8). Survival for each bimonthly period was calculated by dividing the number of individuals at the end of the simulation with the initial abundance (10,000 individuals). Because we ran 1,000 replicate simulations, this led to a distribution of survival values. From this distribution we report the 5th, 50th (median) and 95th percentiles in Annex 2. In the main text we only consider the median survival values. We calculated annual survival as the product of all bimonthly survival rates per OWF scenario.

3.4.8 Population effects

Annual OWF-induced mortality was calculated as the difference between the survival probability used for model calibration (0.9; Table 8) and the annual survival as derived from the OWF simulations (see section 3.4.7). Subsequently, we use the northern gannet population model to assess whether OWF-induced mortality led to a violation of the Acceptable Level of Impact (ALI), as defined for the northern gannet (Table 9). Calculation of population effects and comparison with the ALIs was only performed for the maximum travel length of 1 and 8 grid cells per time step (Annex 2).

3.5 Mortality calculation

Annual mortality probabilities due to habitat loss per scenario (Table 3 and **Figure 3-4**) were calculated from the estimated number of casualties per bimonthly period, for each of the species that is under assessment for habitat loss (Table 1). For northern gannet and sandwich tern also the collision mortality probabilities per scenario were considered in the population models. The collision mortality probabilities were taken from Potiek *et al.* (2021b). The effects of habitat loss and collision mortality were considered together in one population model because there is, for both species, only a single North Sea population that is assumed to suffer from both processes. The annual mortality probabilities were used in the population models to assess the population-level effects of the OWF scenarios.

We used the mean number of casualties over the six bimonthly periods to obtain a more robust estimate of the number of casualties. The mean number of casualties per period (M_{period}) was divided by the maximum population abundance over all bimonthly periods (N_{max}) as derived from the density maps. We assumed that the maximum abundance is most representative for the size of the population that suffers from habitat loss. The resulting mortality figure $m_{period} = M_{period} / N_{max}$ was transposed to the annual mortality rate m_{annual} as:

$$m_{annual} = 1 - (1 - m_{period})^6$$

The parameter m_{annual} represents the annual mortality that results from habitat loss as a consequence of displacement from OWF areas. For the calculations of the mortality probabilities for the national

scenarios, abundances based on the national bird density maps were used. For the calculations of the mortality probabilities for the international scenario, the international bird density maps were used.

For the northern gannet IBM, annual mortality from OWF-induced habitat loss was calculated as the difference between the annual survival in the OWF simulations and the background survival value that was used during model calibration without OWFs (Table 8).

For the northern gannet and the sandwich tern, we combined mortality estimates from collisions with mortality from habitat loss by summing both mortality terms. This is a precautionary approach as a fraction of the population will suffer from both types of OWF-induced mortality. Therefore, we also considered the isolated effects of collision mortality and habitat loss on the population growth rate.

3.6 Matrix population models

For the population-level assessment we used population models for seven of the ten species that are under assessment for habitat loss (Table 1). For the northern gannet and the sandwich tern, both the effects of habitat loss and collision mortality were assessed using a population model. The KEC 4.0 uses the same type of population models as used by van Kooten *et al.* (2019). All model details and parameter derivations are described in Annex 3; the models are described in broad terms here.

The models for all species are stage-structured matrix population models that subdivide the population into different life stages. Consequently, the population is described by *the population state vector* that holds the number of individuals within each life stage. Individuals within a particular life stage have the same survival probability and reproductive output. A projection of the population into the future is made by multiplying the population state vector with a matrix that contains the stage-specific rates of survival and reproduction. This matrix is called the projection matrix. The projection matrix is a square matrix with the number of rows and columns equal to the number of life stages. The entry in the ith row and j^{th} column of the projection matrix corresponds to the number of individuals of life stage i that are derived from a single individual in life stage j during one time step. The entries in the projection matrix are derived from species- and age-specific data on reproduction and survival. In KEC 4.0 we use deterministic, density-independent population models, which means that rates of survival and reproduction are independent of time and population abundance. Consequently, the entries of the projection matrix do not change from one time step to the next. Under such conditions, repeatedly multiplying the projection matrix with the population state vector results in an exponentially growing or declining population, with the long-term rate of population growth being solely determined by the projection matrix. This long-term population growth rate, or asymptotic population growth rate, is equal to the dominant eigenvalue of the projection matrix, and denoted by λ. The value of λ indicates the relative change in population abundance; for $\lambda > 1$ the population increases exponentially and for $\lambda < 1$ the population declines exponentially. A population that grows or declines with a rate equal to λ will have a stable stage distribution, i.e. the abundance of each life stage relative to the total population abundance remains constant. The stable stage distribution is equal to the right eigenvector associated with the dominant eigenvalue λ.

3.6.1 General model structure

In (sea)birds, age is an important determinant of survival and reproduction, therefore the categorization of life stages is primarily based on individual age. The number of life stages adopted for each species depends on the available information on age-specific survival and reproduction. A large number of stages can only be used if the available data are of sufficient resolution. Furthermore, it is only useful to consider different life stages if there are sufficiently large differences between those stages in terms of survival or reproduction. Here we describe the setup and analysis of the matrix models in general terms. Per species we discuss the adopted projection matrix and their parameter values.

We follow the matrix models previously described by van Kooten *et al.* (2019) and consider separate summer and winter transition matrices. The summer transition matrix $\mathbf{A_s}$ describes reproduction during the breeding season, *i.e.* the addition of new individuals to the first life stage. During the

breeding season individuals do not die or age: there are no transitions between life stages. Therefore, survival of individuals equals 1. The winter transition matrix $\mathbf{A_w}$ describes survival and transition of individuals during the non-breeding season. If a life stage represents a single age-class, surviving individuals always transit to the next life stage. If a life stage comprises multiple age-classes, surviving individuals can remain in that life stage, although a fraction will transit to the next life stage. For a life stage i that spans multiple ages, P_i is the probability that an individual remains in stage i and is derived by assuming a stable age distribution (Crouse et $al.$, 1987):

$$P_i = S_a \frac{\left(1 - S_a{}^{n_i - 1}\right)}{\left(1 - S_a{}^{n_i}\right)}, \tag{1}$$

Here, S_a is the annual survival probability and n_i is the number of ages covered by life stage i. The probability that an individual survives and transits to stage $i + 1$ is given by:

$$G_i = \frac{S_a{}^{n_i}(1 - S_a)}{(1 - S_a{}^{n_i})}. \tag{2}$$

If stage i would comprise a single age class ($i.e.$ $n_i = 1$), P_i correctly evaluates to zero and G_i to S_a. The annual projection matrix $\mathbf{A}$ is calculated by a matrix multiplication of the winter and summer projection matrices: $\mathbf{A} = \mathbf{A_w} \cdot \mathbf{A_s}$. The order of the seasonal matrices in the matrix multiplication implies that the annual projection matrix projects the number of birds censused after winter and just before the breeding season begins. At this time, all individuals have just aged and new-born individuals of the previous summer have become 1 year old, but the new-borns of the current breeding season have not been censused yet. Turning the multiplication of the seasonal matrices around would result in a different annual projection matrix and a different stable stage structure, but with an identical population growth rate. It would just be looking at the population at a different moment in the year.

In reality, vital rates (reproduction and survival) vary between years, colonies and individuals and this leads to variation in the population growth rate (λ). We allow for such variation by representing each model parameter by a statistical distribution described by a mean value and a standard deviation (SD). In case standard errors (SE) instead of standard deviations were reported, we calculated the standard deviation as $SD = SE \cdot \sqrt{n}$, with n the number of samples. Similarly, the range rule, SD = (max – min) / 4, was used to estimate SD from minimum and maximum values. If 5% and 95% confidence intervals were reported, we back-calculated the standard deviation as: $SD = \frac{CI_{95\%} - CI_{5\%}}{3.92}\sqrt{n}$. We adopt the continuous beta distribution for all parameters that can only vary between zero and one. Parameters that can exceed one, either follow a normal distribution or a truncated normal distribution. The distribution of the population growth rate is derived by calculating a large number of annual projection matrices. For each matrix, every parameter is sampled from its own distribution. Subsequently we calculate λ for every projection matrix. Each parameter is sampled independently and we do not consider covariation between different parameters.

3.6.2   Habitat loss mortality per life stage

The habitat loss mortality was calculated per life stage for the seven species for which a population assessment was performed (Table 1). For the northern gannet and the sandwich tern also the life stage specific collision mortality was calculated. First, we assigned an 'OWF vulnerability' to each life stage. The OWF vulnerability (0 – 1) represents the relative vulnerability of each life stage to OWF-induced mortality and can be used to exclude particular life stages from additional mortality, for example if species do not inhabit the North Sea during certain parts of the life cycle. For the sandwich tern, we set the 'OWF vulnerability' to zero for the first two life stages J_0 (individuals of age 0) and J_{12} (individuals of age 1 and 2). Juveniles (J_0) are only present at the North Sea shortly after fledging and individuals of age 1 and 2 do usually not return to the North Sea in summer. This implies that only sandwich terns of 3+ years old experience OWF-induced mortality. The two adult life stages of the sandwich tern have an OWF vulnerability of 1. For the northern gannet, the stage-specific OWF vulnerabilities were based on the estimated age-distribution of the casualties of OWF collisions and were taken identical as used for the collision mortality assessment of the northern gannet (Potiek et $al.$, 2021b). The vulnerability to OWFs is low (+/- 0.45) for the first two life stages of the northern gannet (age 0 and 1) and increases from age 2 onwards. For all other species, the 'OWF-vulnerability' was set to 1 for all life stages.

The OWF-induced mortality was applied to the survival parameters (S_a, see equations (1) and (2)), and some life stages share the same survival parameter (see parameter derivations in Annex 3). The

OWF vulnerabilities of the life stages that share a survival parameter were aggregated into an OWF vulnerability per survival parameter. This aggregation involved calculating the mean of the stage-specific OWF vulnerabilities, weighted by the stable distribution of each life stage. Parameter-specific OWF vulnerabilities were multiplied with the calculated OWF-induced mortality to arrive at additional mortality rates specific to each survival parameter.

Mortality rates were interpreted as finite probabilities that could vary between zero and one, as opposed to instantaneous rates. Accordingly, survival (S_a) was calculated as the complement of mortality $m = 1 - S_a$. The OWF-affected survival rate, S_{OWF}, was calculated from the OWF mortality, m_{OWF}, and the default survival rate S following:

$$S_{OWF} = S * (1 - m_{OWF})$$

3.7 Population level effects and acceptable levels of impacts

The acceptable levels of impact (ALIs) were defined for each of the species for which population-level effects of habitat loss were calculated (Table 9). For the species without population models (Table 1), no ALI thresholds could be defined. The concept of the ALIs has previously been described by Potiek *et al.* (2021a) and the values for the ALI thresholds were defined in an LNV working document. The values of X and Pt that define the ALI thresholds (Table 9) were defined by LNV based on the IUCN status of the species.

For each species, we generated 1e[5] stochastic annual projection matrices per scenario, including the 'null' scenario without OWF-induced mortality. The population growth rate (λ) was calculated for each annual projection matrix as the real part of the dominant eigenvalue. Several summary statistics were calculated to characterize the resulting distribution of the population growth rates (mean, median, standard deviation and 5% and 95% quantiles). Population models were run using R software (R Core Team, 2020) and the 'KEC4popmodels' R-package (Hin 2021), which was developed for the current project.

Following Potiek *et al.* (2021a), the ALI threshold that was used to test the effect of the OWFs in the population models was calculated for each species based on two factors:
    a. The median population growth rate λ_X that, over 3 generations, or 10 years, whichever period is longer (Potiek *et al.*, 2021a), results in a population abundance that is X% lower than the population abundance with no OWFs (Table 9).
    b. The probability that these lower population abundances are the result of the deployment of OWFs, $P_{causality}$. The values of $P_{causality}$ were compared to the Pt values listed in Table 9. When $P_{causality}$ was found to be larger than Pt, the ALI threshold was exceeded.

To calculate $P_{causality}$ for each scenario, we determined the proportion of the 1e[5] stochastic parameter combinations which resulted in population growth rates below λ_X. This proportion is indicated as P_{impact} for scenarios with OWFs, and as $P_{falsepos}$ for the null scenario. Using these, we calculated the fraction of outcomes $P_{causality}$, which is defined as

$$P_{causality} = \frac{P_{impact} - P_{falsepos}}{P_{impact}}.$$

Table 9. Population-level effects of OWFs are tested against the Acceptable Level of Impact (ALI) thresholds (Potiek et al., 2021a) of which values were defined in a working document by LNV. X signifies how much smaller a population is allowed to be due to the influence of OWFs compared to a population without OWF. More exactly, it defines the population abundance that is deemed unacceptable after three bird generations, as a percentage of the population abundance expected without offshore wind farms. Pt signifies the probability that offshore wind farms are the cause of the violation of the X value that is deemed unacceptable.

Euring	Scientific name	English name	X (%)	Pt	Population status (October 2021)
59	*Gavia sp*	Diver sp	30	0.5	IUCN 27 least concern, NL non breeding favourable (based on *Gavia stellata*)
220	*Fulmarus glacialis*	Northern fulmar	15	0.1	IUCN 27 vulnerable, NL non breeding favourable
710	*Morus bassanus*	Northern gannet	30	0.5	IUCN 27 least concern, NL non breeding favourable
6110	*Thalasseus sandvicensis*	Sandwich tern	30	0.5	IUCN 27 least concern, NL non breeding unfavourable, NL breeding very unfavourable
6340	*Uria aalge*	Common guillemot	30	0.5	IUCN 27 least concern, European population near threatened, NL non breeding favourable
6360	*Alca torda*	Razorbill	30	0.5	IUCN 27 least concern, European population near threatened, NL nonbreeding unknown
6540	*Fratercula arctica*	Atlantic puffin	15	0.1	IUCN 27 near threatened, NL non breeding unknown

4 Results

4.1 Population level effects

The presumed effects of habitat loss on the population level were not found to exceed the ALIs. For the northern gannet (Table 10), exceedance of the ALI is caused by the casualties due to collision mortality, which lead to much higher mortality than habitat loss for this species (Table 14).

Table 10. Outcomes of population level assessment of the species under assessment for habitat loss. The effects of the tested scenarios do (TRUE) or do not (FALSE) exceed the species specific ALIs (see Table 9). The sandwich tern (Thalasseus sandvicensis) and the northern gannet (Morus bassanus) are under assessment for both effects of habitat loss and collision mortality and both were taken into consideration simultaneously for the test against the ALI.

| | *Effects of habitat loss* | | | | | *Effects of both habitat loss and collision mortality* | |
Scenario	*Gavia sp.*	*Fulmarus glacialis*	*Uria aalge*	*Alca torda*	*Fratercula arctica*	*Morus bassanus*	*Thalasseus sandvicensis*
Basic 2030	FALSE	FALSE	FALSE	FALSE	FALSE	TRUE*	FALSE
Rekenvariant I	FALSE	FALSE	FALSE	FALSE	FALSE	TRUE*	FALSE
Rekenvariant II	FALSE	FALSE	FALSE	FALSE	FALSE	TRUE*	FALSE
Rekenvariant III	FALSE	FALSE	FALSE	FALSE	FALSE	TRUE*	FALSE
International	FALSE	FALSE	FALSE	FALSE	FALSE	TRUE*	FALSE

*Exceedance of the ALI for the northern gannet is caused by the casualties due to collision mortality.

4.2 Habitat loss casualties

4.2.1 Casualties per OWF area
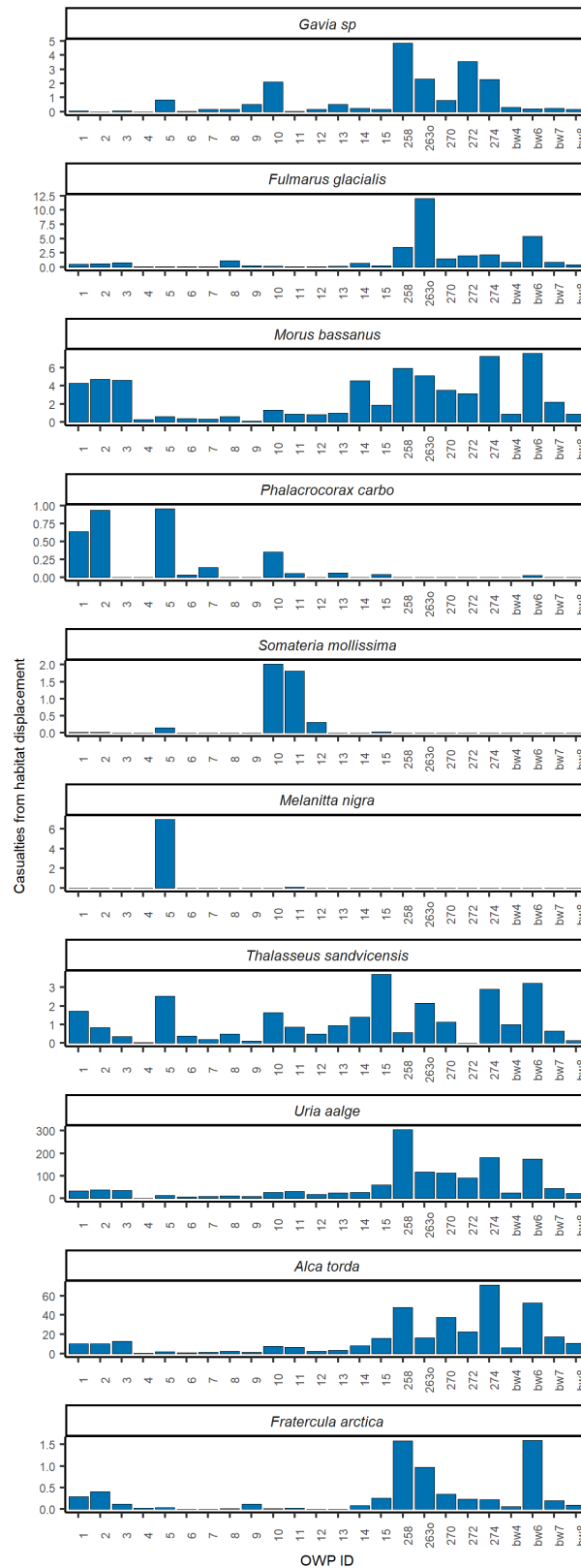
Figure 4-1. *Estimated total number of casualties per year from habitat loss due to Dutch OWFs. Note the different scaling of the vertical axis between the different species. All OWFs are included in the national scenarios. Data represent the national subset (Table 11). Areas corresponding to the OWF IDs are shown in Figure 4-2 and their names can be found in Table 11 and Annex 1.*
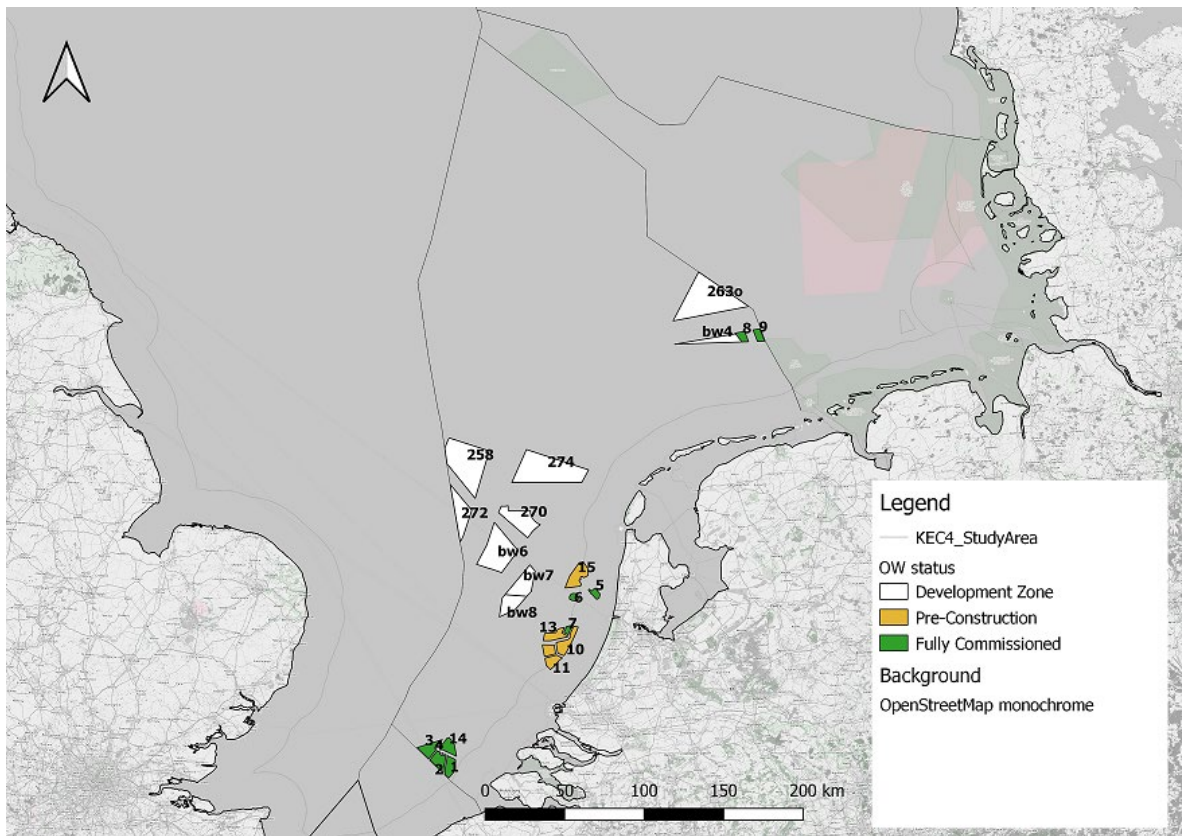
Figure 4-2. *Dutch OWF areas with their OWF IDs*

4.2.1.1   National

The estimated annual number of casualties from habitat loss due to Dutch OWFs is shown per species for each wind farm in **Figure 4-1** and Table 11. Annex 4, Table 44 lists the number of casualties per bimonthly period, species and OWF for all current Dutch OWFs and OWF search areas. There is considerable variation in the annual number of casualties between species and OWF areas. The estimated total number of casualties from habitat displacement across all Dutch OWF areas and species equals 1955 individuals per year for the national subset of the data (Table 11). 72.6% of the total number of casualties per year across the Dutch OWF areas are common guillemots (**Figure 4-1** and Table 11). The second ranked species is the razorbill with 19.0%. All the other species contribute less than 4% of the total estimated number of casualties per year.

Most casualties were predicted for OWF area ' Zoekgebied 1 Noord' (OWF id = 258) with 368.9 casualties per annum (Table 11, **Figure 4-3**), followed by OWF areas 'Zoekgebied 2 Noord' (OWF id = 274) and 'IJmuiden Ver' (OWF id = bw6). Across all species, OWF area 'Zoekgebied 1 Noord' (OWF id = 258) alone is predicted to result in 18.9% of the total yearly number of casualties. Per GW, most casualties are predicted in different OWF areas (Table 12). 'Egmond aan Zee' (OWF id = 5), the 'Borssele' OWF areas (OWF ids = 1 – 4, 14) and 'Hollandse Kust Noord' (OWF id = 15) are predicted to cause most casualties per GW.
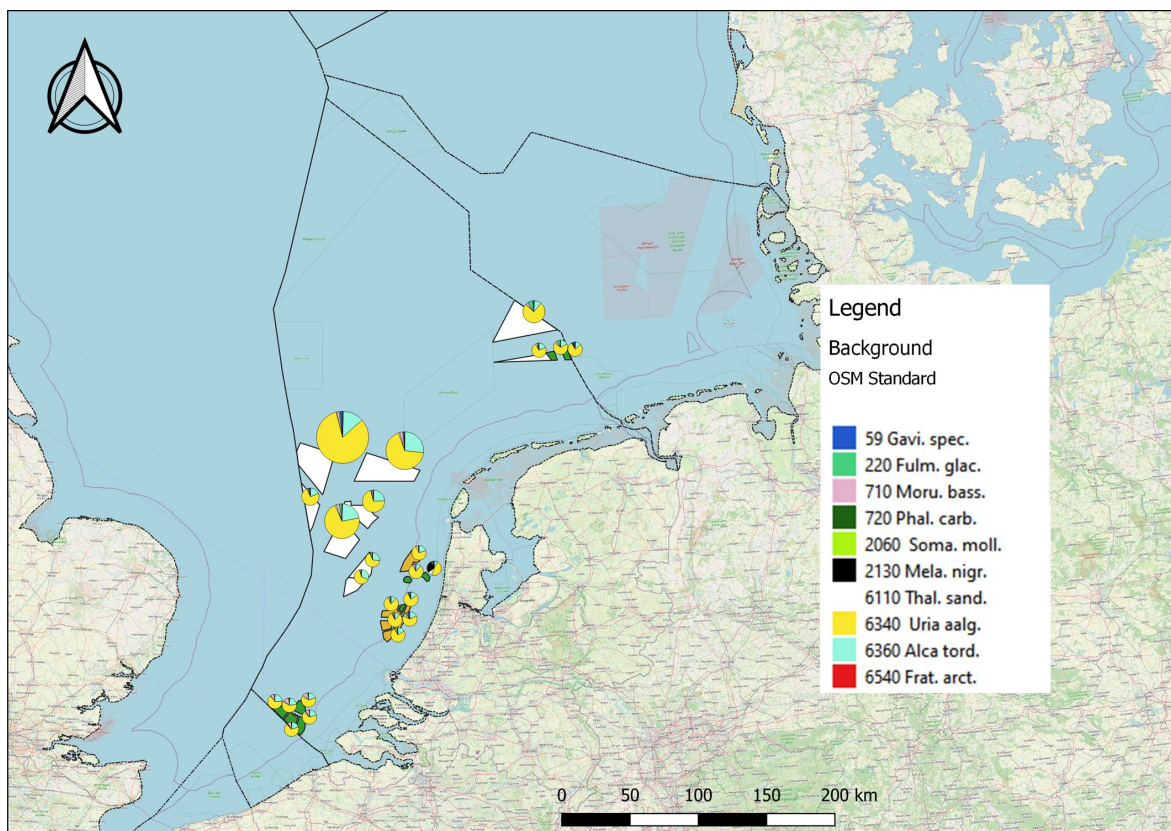
Figure 4-3. Habitat loss casualties by OWF search area. Pie diagram size indicates total number, with segment size representing the proportion per species. The legend indicates the colour per species (Euring and scientific name, abbreviated).

*Table 11. Estimated total annual number of casualties for Dutch OWF areas per species and OWF area. Areas corresponding to the OWF IDs are shown in **Figure 4-2**.*

OWF id	OWF name	Capacity (GW)	Gavia sp	Fulmarus glacialis	Morus bassanus	Phalacrocorax carbo	Somateria mollissima	Melanitta nigra	Thalasseus sandvicensis	Uria aalge	Alca torda	Fratercula arctica
1	Borssele 2	0.38	0.1	0.5	4.3	0.6	0.0	0.0	1.7	33.9	10.3	0.3
2	Borssele 3	0.37	0.0	0.6	4.7	0.9	0.0	0.0	0.8	37.7	10.5	0.4
3	Borssele 4 – Blauwwind	0.37	0.1	0.8	4.6	0.0	0.0	0.0	0.4	34.9	13.1	0.1
4	Borssele Site V -Two towers	0.02	0.0	0.0	0.3	0.0	0.0	0.0	0.0	1.4	0.5	0.0
5	Egmond aan Zee	0.11	0.8	0.0	0.6	1.0	0.1	7.0	2.5	13.1	2.1	0.0
6	Prinses Amaliawindpark	0.12	0.0	0.1	0.4	0.0	0.0	0.0	0.4	7.7	1.1	0.0
7	Eneco Luchterduinen	0.13	0.2	0.0	0.3	0.1	0.0	0.0	0.2	8.5	1.7	0.0
8	Gemini Zee energie	0.30	0.2	1.1	0.6	0.0	0.0	0.0	0.5	10.9	2.8	0.0
9	Gemini Buitengaats	0.30	0.5	0.2	0.1	0.0	0.0	0.0	0.1	9.2	1.5	0.1
10	Hollandse Kust Zuid Holland IV	0.38	2.1	0.1	1.3	0.4	2.0	0.0	1.6	26.4	7.5	0.0
11	Hollandse Kust Zuid Holland III	0.38	0.0	0.0	0.9	0.1	1.8	0.1	0.9	30.9	6.7	0.0
12	Hollandse Kust Zuid Holland II	0.38	0.2	0.1	0.8	0.0	0.3	0.0	0.5	18.9	2.7	0.0
13	Hollandse Kust Zuid Holland I	0.38	0.5	0.1	1.0	0.1	0.0	0.0	0.9	24.3	3.7	0.0
14	Borssele 1	0.38	0.2	0.7	4.5	0.0	0.0	0.0	1.4	26.0	8.2	0.1
15	Hollandse Kust Noord	0.70	0.2	0.2	1.9	0.0	0.0	0.0	3.7	60.2	16.0	0.3
258	Zoekgebied 1 Noord	4.00	4.9	3.5	5.9	0.0	0.0	0.0	0.6	304.6	47.8	1.6
263o	Zoekgebied 5 Oost origineel	4.00	2.3	12.1	5.1	0.0	0.0	0.0	2.1	118.3	16.4	1.0
270	IJmuiden Ver Noord	2.00	0.8	1.4	3.5	0.0	0.0	0.0	1.1	112.2	37.9	0.3
272	Zoekgebied 1 Zuid	2.00	3.6	2.0	3.2	0.0	0.0	0.0	0.0	91.3	22.9	0.2
274	Zoekgebied 2 Noord	4.00	2.3	2.1	7.2	0.0	0.0	0.0	2.9	181.2	71.2	0.2
bw4	Ten noorden van de Waddeneilanden	0.70	0.3	0.8	0.9	0.0	0.0	0.0	1.0	24.3	6.2	0.1
bw6	IJmuiden Ver	4.00	0.2	5.4	7.6	0.0	0.0	0.0	3.2	175.5	52.8	1.6
bw7	Hollandse Kust West	1.40	0.2	0.9	2.2	0.0	0.0	0.0	0.6	44.6	17.5	0.2
bw8	Hollandse Kust West zuidelijke punt	0.70	0.2	0.4	0.9	0.0	0.0	0.0	0.1	22.5	10.7	0.1
	Total		19.8	33.1	62.9	3.3	4.3	7.1	27.5	1418.6	371.9	6.6

*Table 12. Estimated total annual number of casualties for Dutch OWF areas for all species and OWF areas per GW. Areas corresponding to the OWF IDs are shown in **Figure 4-2**.*

OWF id	OWF name	Capacity (GW)	Gavia sp	Fulmarus glacialis	Morus bassanus	Phalacrocorax carbo	Somateria mollissima	Melanitta nigra	Thalasseus sandvicensis	Uria aalge	Alca torda	Fratercula arctica
1	Borssele 2	0.38	0.2	1.3	11.5	1.7	0.0	0.0	4.6	90.1	27.5	0.8
2	Borssele 3	0.37	0.0	1.5	12.9	2.6	0.0	0.0	2.3	102.9	28.7	1.1
3	Borssele 4 – Blauwwind	0.37	0.2	2.1	12.7	0.0	0.0	0.0	1.0	95.4	35.8	0.3
4	Borssele Site V - Two towers	0.02	0.0	2.1	15.2	0.0	0.0	0.0	2.1	71.2	26.2	1.1
5	Egmond aan Zee	0.11	7.8	0.2	5.7	8.9	1.3	64.8	23.4	121.3	19.4	0.3
6	Prinses Amaliawindpark	0.12	0.2	0.5	3.2	0.3	0.0	0.0	3.3	64.5	9.2	0.0
7	Eneco Luchterduinen	0.13	1.4	0.2	2.5	1.1	0.0	0.0	1.6	66.2	13.4	0.0
8	Gemini Zee energie	0.30	0.5	3.7	2.0	0.0	0.0	0.0	1.7	36.4	9.3	0.0
9	Gemini Buitengaats	0.30	1.8	0.7	0.4	0.0	0.0	0.0	0.4	30.7	5.0	0.4
10	Hollandse Kust Zuid Holland IV	0.38	5.5	0.3	3.4	0.9	5.3	0.0	4.3	68.6	19.5	0.0
11	Hollandse Kust Zuid Holland III	0.38	0.0	0.1	2.3	0.1	4.7	0.2	2.2	80.2	17.4	0.1
12	Hollandse Kust Zuid Holland II	0.38	0.4	0.1	2.2	0.0	0.8	0.0	1.3	49.1	7.0	0.0
13	Hollandse Kust Zuid Holland I	0.38	1.3	0.3	2.6	0.2	0.0	0.0	2.4	63.2	9.5	0.0
14	Borssele 1	0.38	0.6	1.8	12.1	0.0	0.0	0.0	3.7	69.1	21.8	0.2
15	Hollandse Kust Noord (Tender 2019)	0.70	0.2	0.3	2.7	0.1	0.0	0.0	5.3	86.0	22.8	0.4
258	Zoekgebied 1 Noord	4.00	1.2	0.9	1.5	0.0	0.0	0.0	0.1	76.2	12.0	0.4
270	IJmuiden Ver Noord	4.00	0.4	0.7	1.8	0.0	0.0	0.0	0.6	56.1	18.9	0.2
272	Zoekgebied 1 Zuid	2.00	1.8	1.0	1.6	0.0	0.0	0.0	0.0	45.7	11.5	0.1
274	Zoekgebied 2 Noord	2.00	0.6	0.5	1.8	0.0	0.0	0.0	0.7	45.3	17.8	0.1
263o	Zoekgebied 5 Oost origineel	4.00	0.6	3.0	1.3	0.0	0.0	0.0	0.5	29.6	4.1	0.2
bw4	Ten noorden van de Waddeneilanden - (Tender 2022)	0.70	0.4	1.2	1.3	0.0	0.0	0.0	1.4	34.8	8.9	0.1
bw6	IJmuiden Ver	4.00	0.0	1.4	1.9	0.0	0.0	0.0	0.8	43.9	13.2	0.4
bw7	Hollandse Kust West - (Tender 2020/2021)	1.40	0.2	0.6	1.6	0.0	0.0	0.0	0.5	31.9	12.5	0.1
bw8	Hollandse Kust West zuidelijke punt	0.70	0.2	0.6	1.2	0.0	0.0	0.0	0.2	32.2	15.3	0.1

4.2.1.2 International

Casualties per bimonthly period, species and international OWF area are presented in a separate document (Electronic supplement E1, E1_Table_KEC4.0_Casualties_IntOWPs_BatchINT_ScenarioOWPs.pdf). The yearly number of casualties per species for all OWF areas are shown in Electronic supplement E2 (E2_Casualties_OWP_Species_INT.pdf), an overview of the casualties per OWF area in **Figure 4-4** and per international EEZ in **Figure 4-5**.

The species with the highest number of estimated victims is the common guillemot in nearly all countries, with the exception of Denmark (**Figure 4-4**). On the Danish EEZ the diver sp. are the hardest hit species (group). This species (group) is also clearly visible within the German pie diagram. For the Dutch, Belgian and UK EEZ, the species with second most casualties is the razorbill. Also per OWF, the casualties mostly consist of common guillemots for international OWFs (**Figure 4-5**). Yet, in the German and Danish OWFs, divers are often the species with most casualties and the same occurs in some southern UK OWFs (**Figure 4-5**). In some German and Danish OWFs, the common scoter is the most common casualty. In a few UK OWFs, this is the razorbill (**Figure 4-5**).
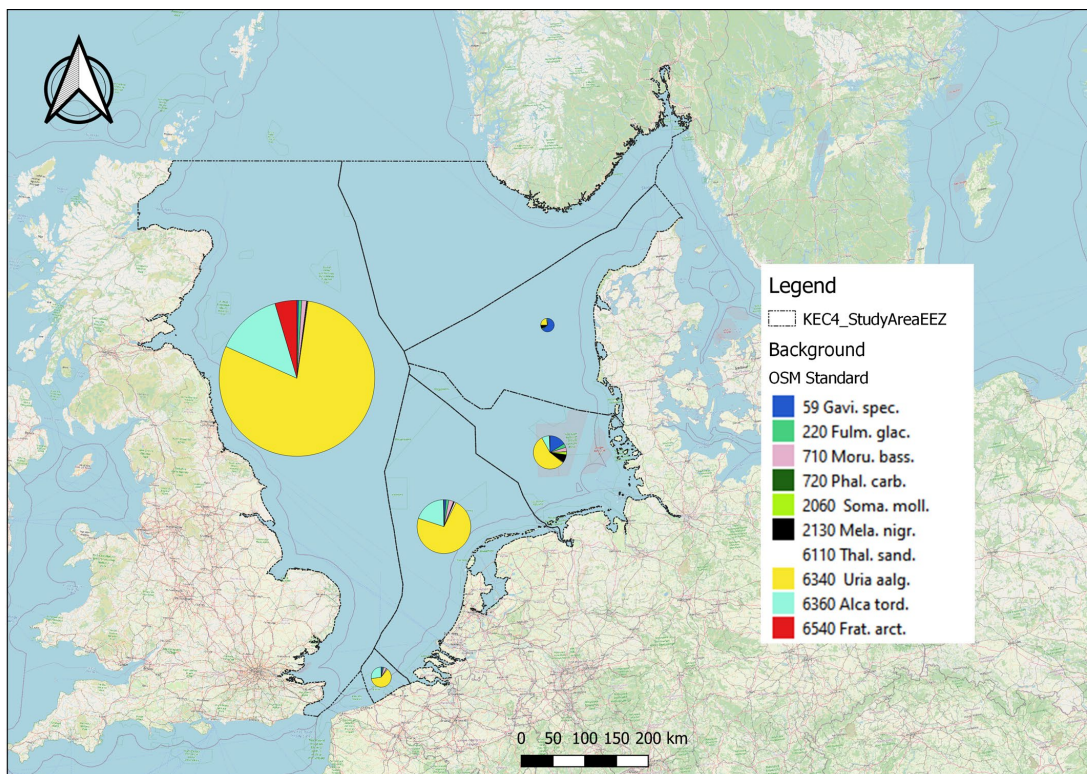
Figure 4-4. *Habitat loss casualties by EEZ. Pie diagram size indicates total number, with segment size representing the proportion per species, per EU member state. The legend indicates the colour per species (Euring and scientific name, abbreviated).*
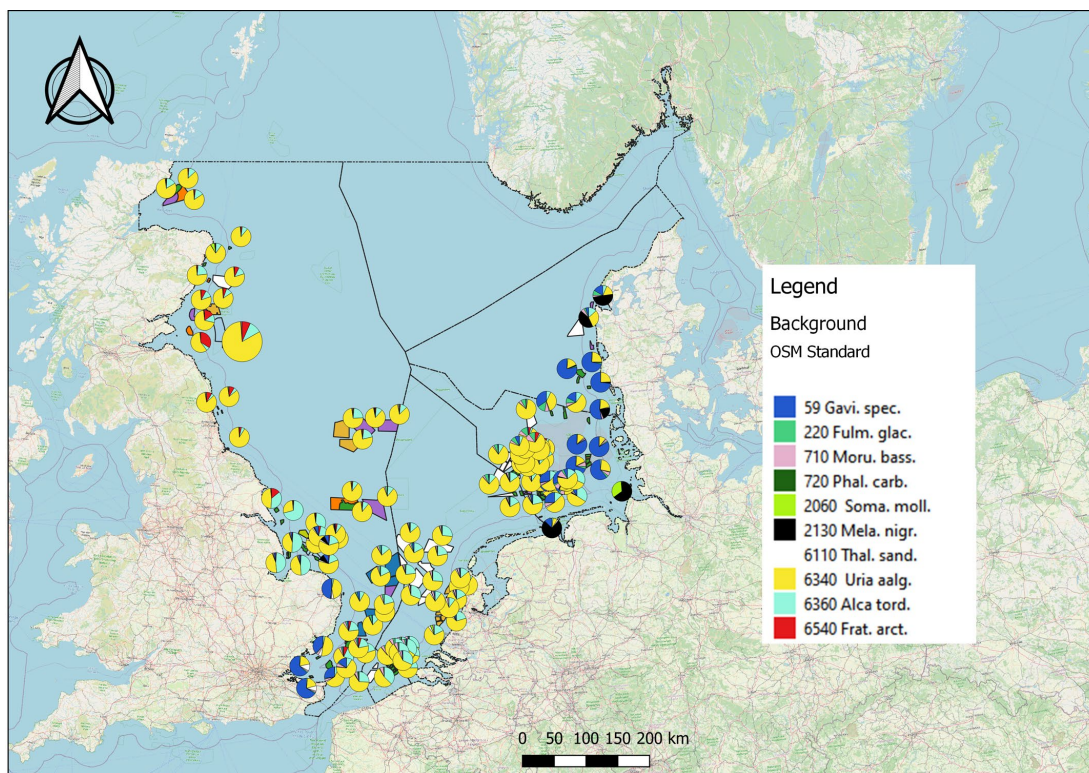
Figure 4-5. *Overview of habitat loss casualties for the international scenario. Size of pie diagrams indicates total number of casualties, segments indicate the proportion per species, per (proposed) OWF. The legend indicates the colour per species (Euring and scientific name, abbreviated).*

4.2.2   Casualties and mortality estimates per scenario

The total number of casualties due to habitat loss per year per OWF scenario are shown in Table 13 for all ten species being evaluated for habitat loss. The total number of casualties across species is lower for the Rekenvariant I and Rekenvariant II scenarios than for Rekenvariant III.

Table 13. Estimated yearly total number of casualties per scenario and species.

Scenario	Gavia sp	Fulmarus glacialis	Morus bassanus	Phalacrocora x carbo	Somateria mollissima	Melanitta nigra	Thalasseus sandvicensis	Uria aalge	Alca torda	Fratercula arctica	Total
Basic 2030	5.8	11.6	37.1	3.3	4.3	7.1	20.6	588.4	165.0	3.2	846.3
Rekenvariant I	11.4	27.6	53.9	3.3	4.3	7.1	26.9	1022.6	301.1	4.8	1463.1
Rekenvariant II	14.9	29.6	57.0	3.3	4.3	7.1	26.9	1114.0	324.1	5.0	1586.2
Rekenvariant III	19.8	33.1	62.9	3.3	4.3	7.1	27.5	1418.6	371.9	6.6	1955.1
International	266.9	171.2	250.7	3.5	34.3	87.2	46.2	14,148.1	2609.6	707.8	18,325.5

Based on the mean numbers of estimated casualties and the maximum population abundances, the mortality due to habitat loss was calculated for the seven species that were assessed at the population level (Table 14). For northern gannet and sandwich tern, we also report population-level mortality from collisions, and total mortality (habitat loss + collisions). The reported mortality probabilities in Table 14 are used as OWF-induced mortality probabilities in the population models. Because the mortality probabilities are relative to the population size as derived from the density maps, they give an indication of how strong each population will be affected by the casualties. While diver sp. were estimated to have less casualties than northern fulmar in the national scenarios, the estimated mortality probability for diver sp. is higher than for northern fulmar (Table 14), because of the higher population abundance of the latter species. The estimated values for the habitat loss mortality are highest for the common guillemot and razorbill. Yet, for the northern gannet, the highest OWF mortality probabilities were estimated, due to the addition of the collision mortalities (Table 14).

Table 14. Estimated annual mortality probability per species and scenario. For northern gannet (Morus bassanus) and sandwich tern (Thalasseus sandvicensis) mortality due to habitat loss (hab.) and collision mortality (coll.) as well as total (tot.) mortality are reported separately.

Scenario	Gavia sp	Fulmarus glacialis	Morus bassanus (hab.)	Morus bassanus (coll.)	Morus bassanus (tot.)	Thalasseus sandvicensis (hab.)	Thalasseus sandvicensis (coll.)	Thalasseus sandvicensis (tot.)	Uria aalge	Alca torda	Fratercula arctica
Basic 2030	0.00102	0.00023	0.00116	0.03657	0.03770	0.00091	0.00142	0.00233	0.00258	0.00267	0.00144
Rekenvariant I	0.00200	0.00055	0.00169	0.05189	0.05351	0.00119	0.00176	0.00294	0.00448	0.00487	0.00217
Rekenvariant II	0.00263	0.00059	0.00179	0.05432	0.05603	0.00119	0.00176	0.00294	0.00488	0.00524	0.00228
Rekenvariant III	0.00348	0.00066	0.00197	0.05893	0.06080	0.00122	0.00183	0.00304	0.00622	0.00602	0.00299
International	0.00826	0.00046	0.00154	0.04223	0.04371	0.00178	0.00249	0.00427	0.00841	0.01142	0.00305

4.3 Diver sp. (*Gavia sp.*)

4.3.1 Diver sp. habitat loss casualties and mortality
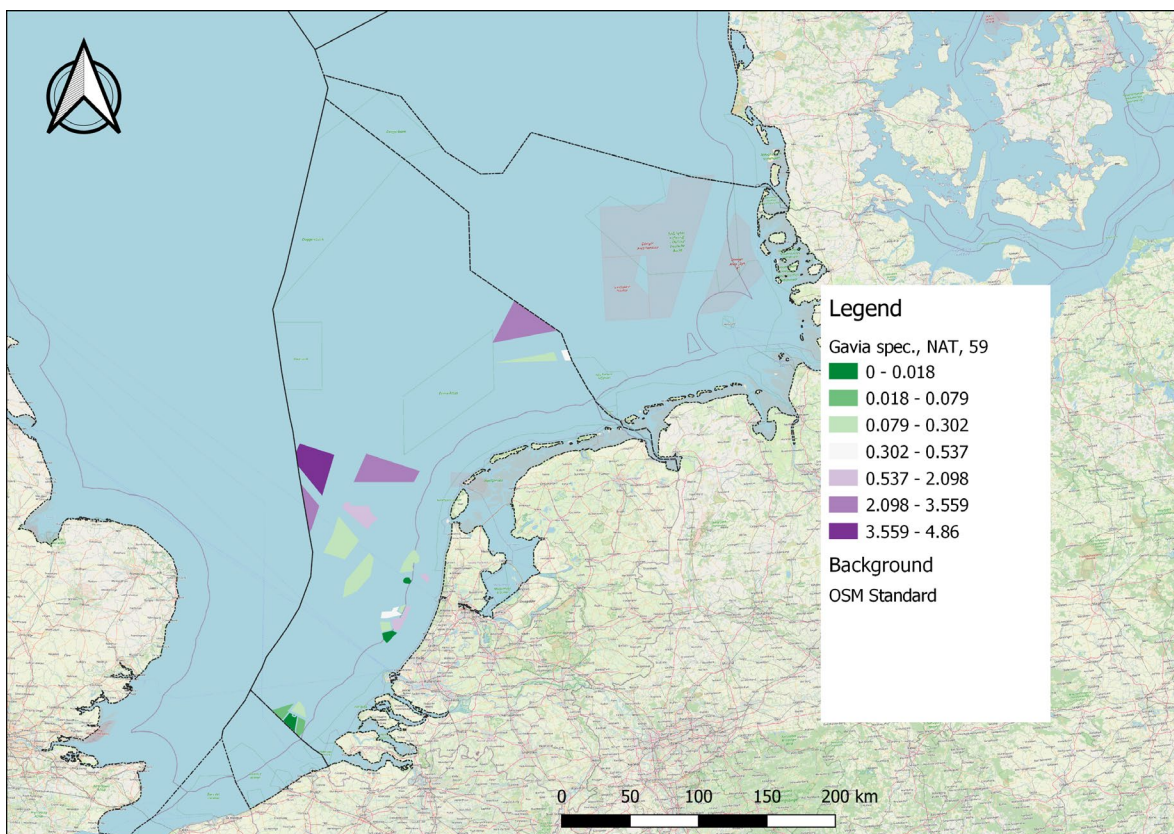
Figure 4-6. *Diver sp. (gavia sp., Euring 20, 30 and 59; note that red-throated diver and black-throated diver are considered together Table 5) total annual habitat loss casualties per OWF included in the national scenarios.*

The national map (**Figure 4-6**) of the numbers of habitat loss diver sp. casualties shows that relatively more casualties are to be expected in the areas that are situated more to the north and further away from the coast. The international map (**Figure 4-7**) shows a similar picture for the Dutch EEZ, with relatively fewer casualties closer to the coast and more to the south. Note that these are based on very low numbers of birds, where relatively small differences may appear large due to the discrete colour scales. Besides, densities of divers are generally highest (but also very low) close to the coast where no wind farms are planned. Internationally, most casualties are predicted to occur along the German and Danish coasts and in the central and northern part of the UK EEZ. Bird density maps of each bimonthly period and of the annual averages can be found in separate documents (Electronic appendices E3 and E4; respectively E3_DensityMaps_19species_NATINT_period.pdf and E4_DensityMaps_19species_NATINT_yearly.pdf).

Figure 4-7. *Diver spec. (Gavia sp., Euring 20, 30 and 59; note that red-throated diver and black-throated diver are considered together Table 5) total annual habitat loss casualties per OWF included the international scenario.*

The estimated number of diver sp. casualties per bimonthly period varies between 1 and 4 divers for the national scenarios and is highest for the 'Rekenvariant III' scenario (Table 15). Using a maximum estimated abundance of 5680 individuals this corresponds to an annual mortality of 0.1% to 0.2% (Table 15). Both mean numbers of bimonthly casualties and maximum abundance are higher in the 'International' scenario. The estimated annual mortality for the international scenario equals 0.8% (Table 15). This leads to an estimated decrease of juvenile and adult survival of 1.35 and 0.96%. The number of casualties per bimonthly period for *Gavia* sp. are shown for each Dutch OWF area in Annex 4, Table 44.

Table 15. Overall, immature (J) and adult (A) mortality (mort) and survival values per scenario for diver sp.. Mortality is derived from mean numbers of casualties per bimonthly period and maximum abundance. Note that red-throated diver and black-throated diver are considered together as diver sp. (Table 5).

Scenario	Mean casualties	Max abundance	Mort	Mort J	Mort A	Survival J	Survival A
null						0.61000	0.86100
Basic 2030	1	5680	0.00102	0.00102	0.00102	0.60938	0.86012
Rekenvariant I	2	5680	0.00200	0.00200	0.00200	0.60878	0.85928
Rekenvariant II	3	5680	0.00263	0.00263	0.00263	0.60840	0.85874
Rekenvariant III	4	5680	0.00348	0.00348	0.00348	0.60788	0.85800
International	45	32,199	0.00826	0.00826	0.00826	0.60496	0.85389

4.3.2   Diver sp. population level effects

The estimated mortality due to habitat loss attributable to OWFs does not lead to a violation of the ALI set for the diver species. Population growth rates estimated for the national scenarios are similar to the null scenario (**Figure 4-8**) and the probability that population abundances lower than the population abundance threshold result from the impact of OWFs is at maximum 3.3% for the national scenarios (Table 16).

Table 16. Population growth rates and ALI statistics for diver sp. (note that red-throated diver and black-throated diver are considered together, see Table 5). Median and 5% and 95% quantiles of the population growth rate ('Lambda') distribution are reported. 'P impact' represents the fractions of the Lambda distributions that are below the threshold of a 30% smaller population abundance compared to the median lambda of the null scenario after 3 generations, which occurs for a Lambda of 1.002. 'P causality' is the probability that the violation of the threshold results from the impact. 'ALI 0.5' shows whether P causality exceeds 0.5, the ALI threshold (see Table 9).

Scenario	Lambda median	Lambda q05	Lambda q95	P impact	P causality	ALI 0.5
Null	1.016	0.725	1.123	0.4551		
Basic 2030	1.015	0.726	1.123	0.4594	0.0094	FALSE
Rekenvariant I	1.012	0.722	1.121	0.4668	0.025	FALSE
Rekenvariant II	1.012	0.721	1.122	0.4685	0.029	FALSE
Rekenvariant III	1.011	0.722	1.121	0.4707	0.033	FALSE
International	1.006	0.719	1.118	0.4890	0.069	FALSE
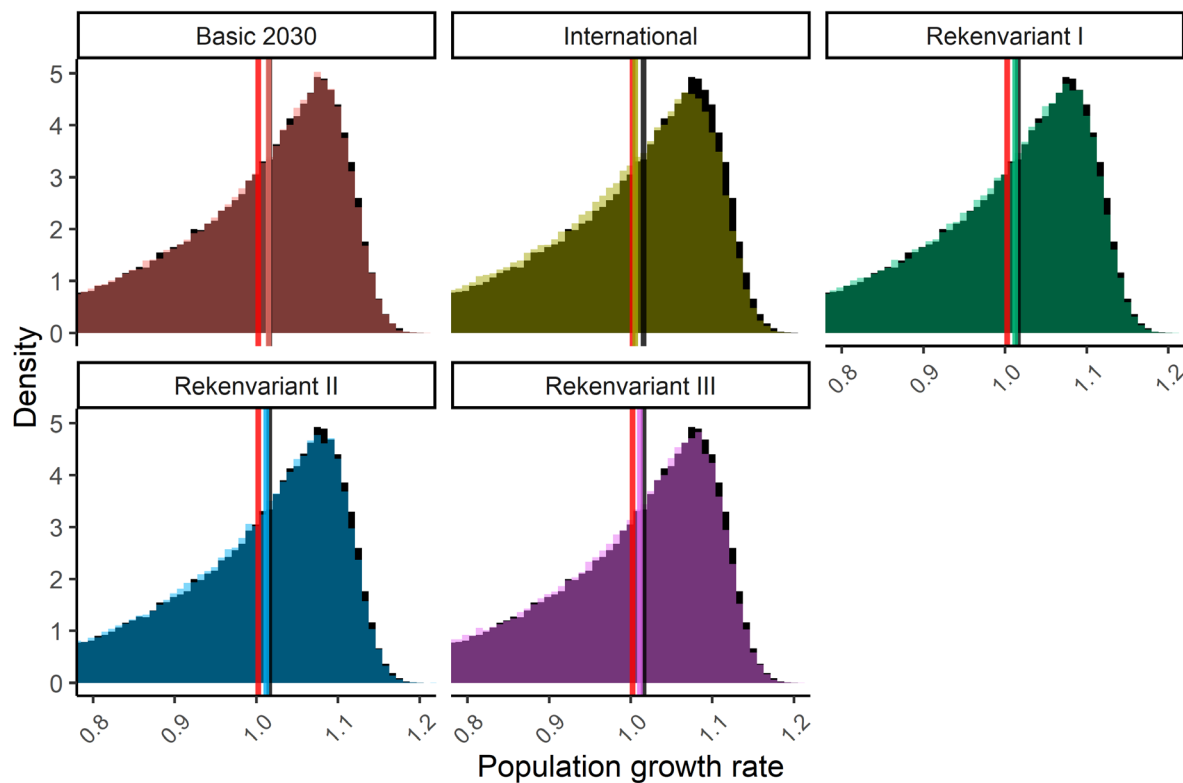
Figure 4-8. *Distribution of population growth rates of diver sp. (note that red-throated diver and black-throated diver are considered together, see Table 5) for the different scenarios. Vertical lines indicate the median population growth rates of the ALI threshold (red), the null scenario (black) and each scenario (colours). The distributions for each scenario (in colours) overlay the distribution of the null scenario (in black).*

4.4 Northern fulmar (*Fulmarus glacialis*)

4.4.1 Northern fulmar habitat loss casualties and mortality
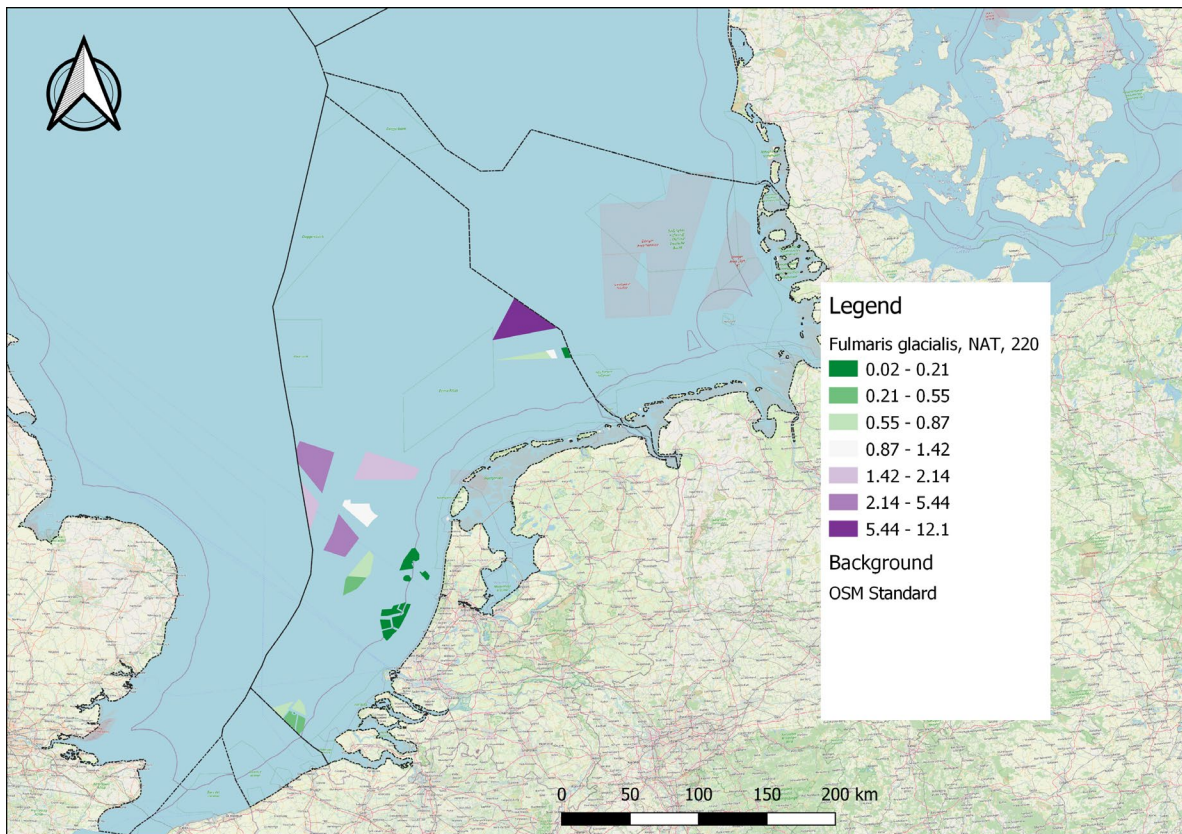
Figure 4-9. *Northern fulmar (Fulmaris glacialis, Euring 220) total annual habitat loss casualties per OWF included in any of the national scenarios.*

For Dutch OWFs, most northern fulmar casualties are predicted in OWF areas further away from the coast (**Figure 4-9**). The international map shows a similar picture with most casualties predicted in OWFs far from the coasts towards the central North Sea (**Figure 4-10**). Bird density maps of each bimonthly period and of the annual averages can be found in separate documents (Electronic appendices E3 and E4; respectively E3_DensityMaps_19species_NATINT_period.pdf and E4_DensityMaps_19species_NATINT_yearly.pdf).
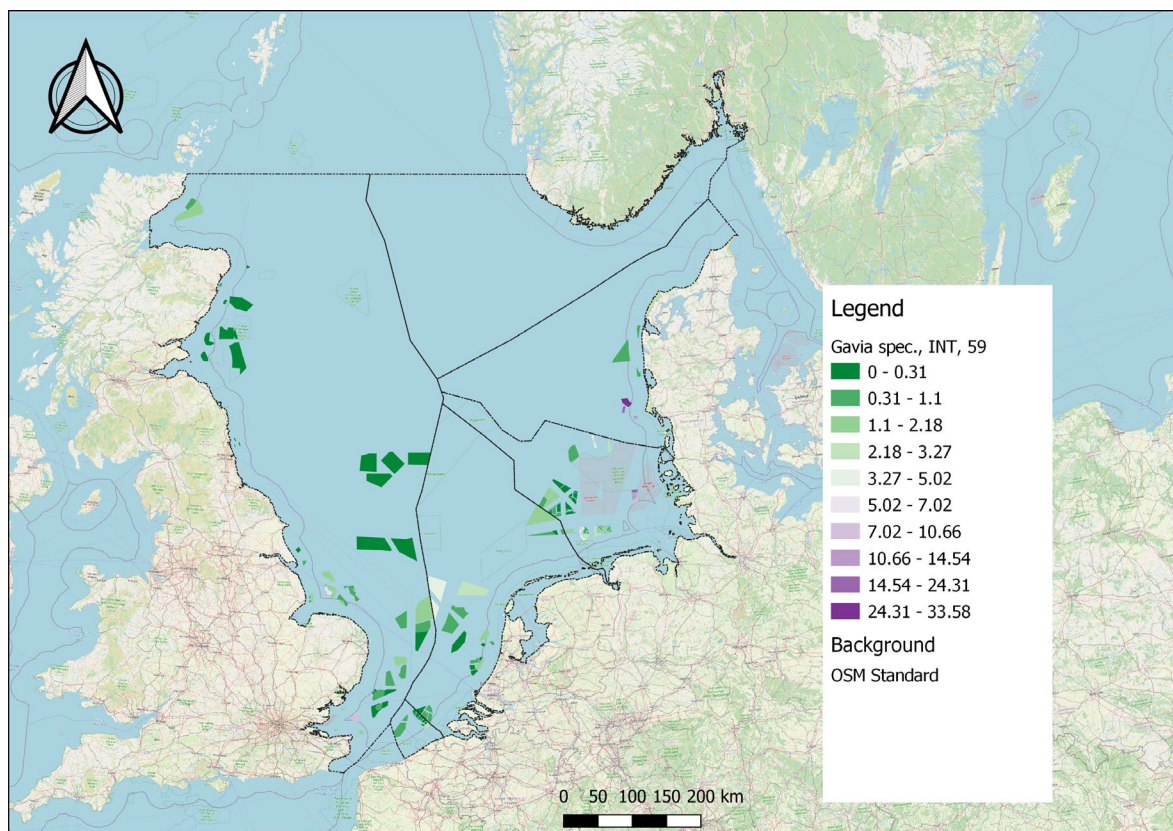
The estimated mean number of northern fulmar casualties per bimonthly period varies between 2 and 6 for the national scenarios and is highest for the 'Rekenvariant III' scenario (Table 17). Using the maximum estimated abundance of 50,376 individuals, this corresponds to an annual mortality of 0.023% to 0.066% due to habitat loss for the national scenarios (Table 17). The estimated mean number of casualties is higher for the 'International' scenario, but because of the large number of northern fulmars in the entire North Sea (estimated at 368,439 individuals), the estimated annual mortality for the international scenario (0.046%; Table 17) is similar to that of the national scenarios. The number of casualties per bimonthly period for the northern fulmar is shown for each Dutch OWF area in Annex 4, Table 44.
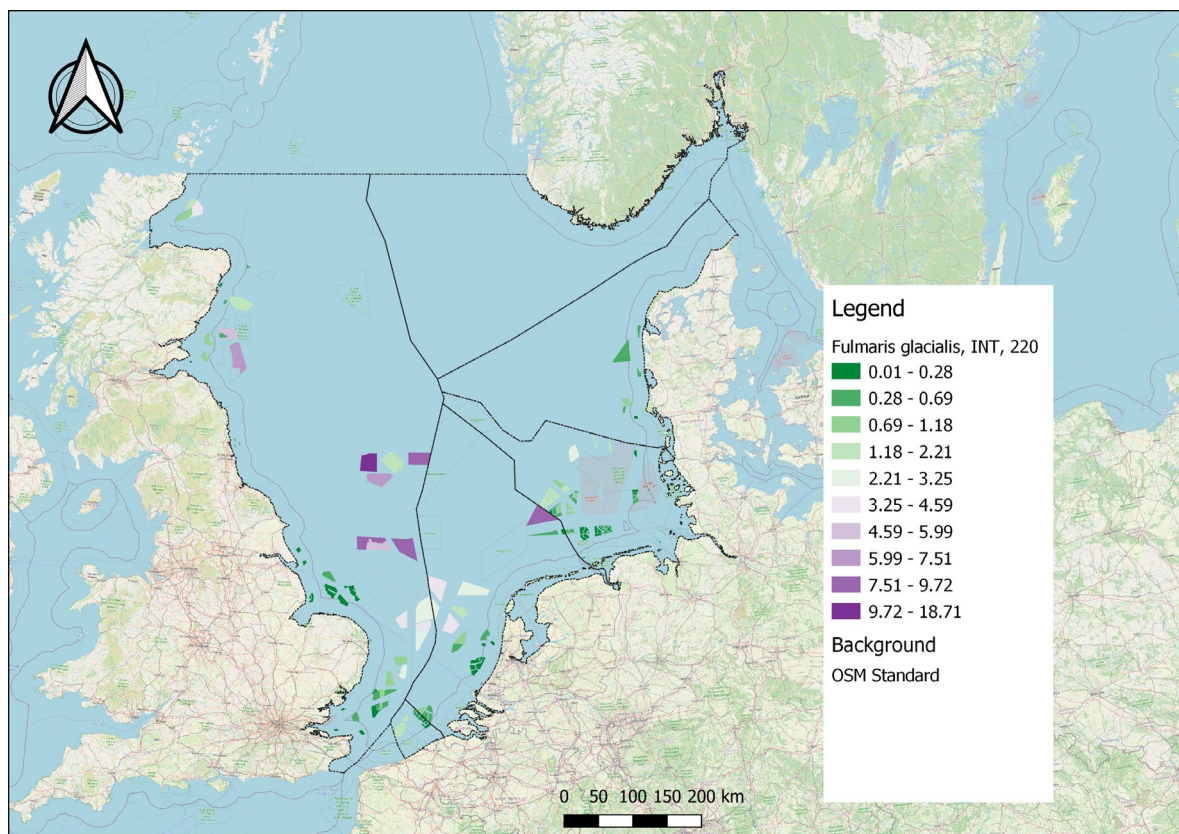
Figure 4-10. *Northern fulmar (Fulmaris glacialis, Euring 220) total annual habitat loss casualties per OWF included in the International scenario.*

Table 17. Overall, immature (J) and adult (A) mortality (mort) and survival values mortality and survival values for the northern fulmar derived from mean numbers of casualties per bimonthly period and max abundance

Scenario	Mean casualties	Max abundance	Mort	Mort J	Mort A	Survival J	Survival A
null						0.88400	0.93600
Basic 2030	2	50,376	0.00023	0.00023	0.00023	0.88380	0.93579
Rekenvariant I	5	50,376	0.00055	0.00055	0.00055	0.88352	0.93549
Rekenvariant II	5	50,376	0.00059	0.00059	0.00059	0.88348	0.93545
Rekenvariant III	6	50,376	0.00066	0.00066	0.00066	0.88342	0.93538
International	29	368,439	0.00046	0.00046	0.00046	0.88359	0.93557

4.4.2 Northern fulmar population level effects

The estimated mortality due to habitat loss attributable to OWFs does not lead to a violation of the ALIs set for the northern fulmar. Population growth rates estimated for all scenarios are similar to the null scenario (Table 18) and the probability that population abundances lower than the population abundance threshold result from the impact of OWFs is below 1.6% for all scenarios (Table 18).
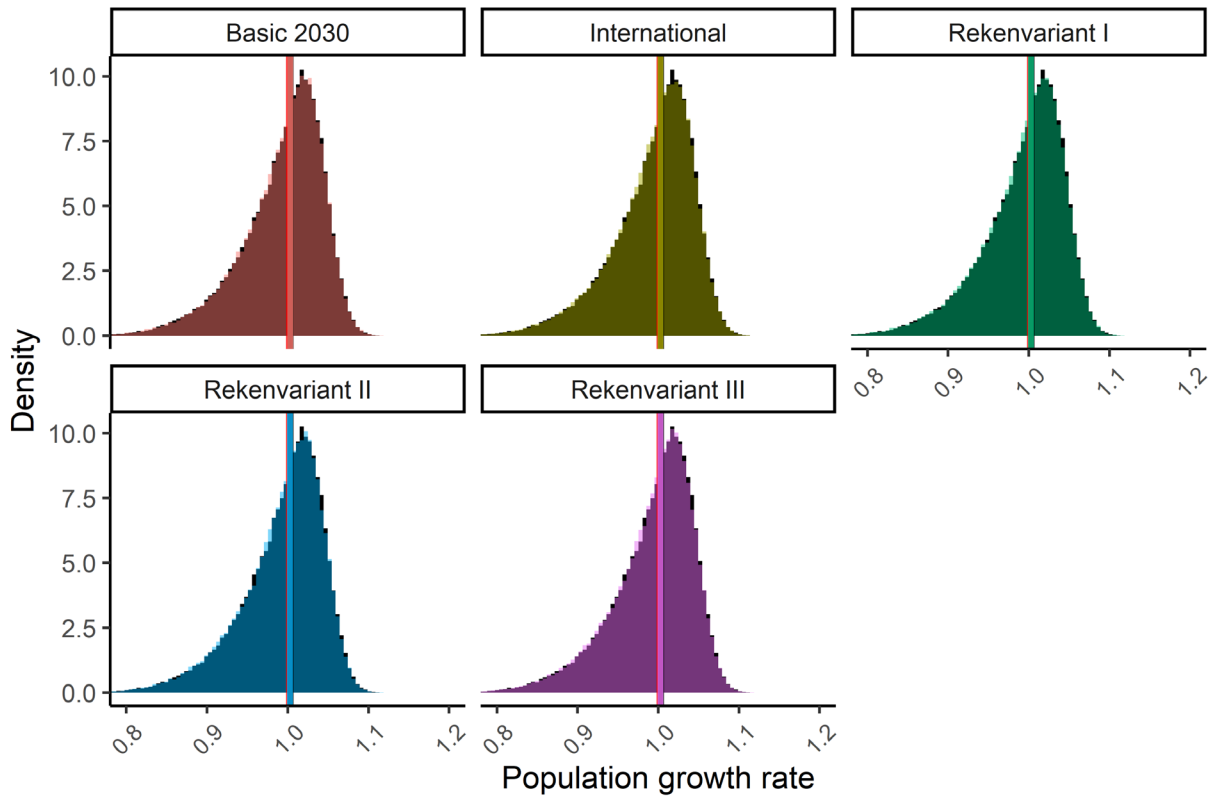
Figure 4-11. *Distribution of population growth rates of the northern fulmar for the different scenarios. Vertical lines indicate the median population growth rates of the ALI threshold (red), the null scenario (black) and each scenario(colours). The distributions for each scenario (in colours) overlay the distribution of the null scenario (in black).*

Table 18. Population growth rates and ALI statistics for the northern fulmar. Median and 5% and 95% quantiles of the population growth rate ('Lambda') distribution are reported. 'P impact' represents the fractions of the Lambda distributions that are below the threshold of a 15% smaller population abundance compared to the median lambda of the null scenario after 3 generations, which occurs for a Lambda of 1.001. 'P causality' is the probability that the violation of the population abundance threshold results from the OWF impact. 'ALI 0.1' shows whether P causality exceeds 0.1, the ALI threshold (see Table 9).

Scenario	Lambda median	Lambda q05	Lambda q95	P impact	P causality	ALI 0.1
Null	1.003	0.896	1.058	0.4806		
Basic 2030	1.003	0.896	1.058	0.4845	0.008	FALSE
Rekenvariant I	1.003	0.896	1.058	0.4880	0.015	FALSE
Rekenvariant II	1.002	0.895	1.057	0.4884	0.016	FALSE
Rekenvariant III	1.003	0.896	1.057	0.4874	0.014	FALSE
International	1.002	0.896	1.058	0.4886	0.016	FALSE

4.5 Northern gannet (*Morus bassanus*)

4.5.1 Northern gannet habitat loss casualties and mortality
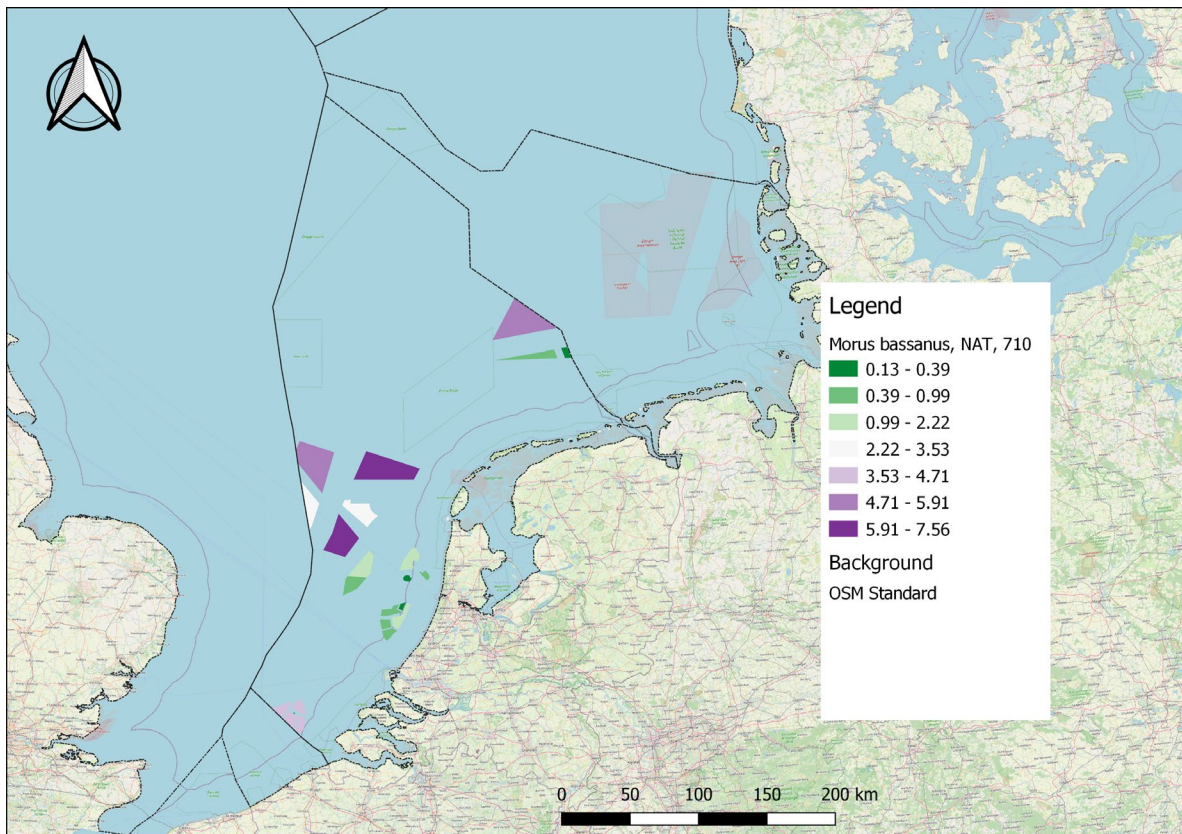
Figure 4-12. *Northern gannet (Morus bassanus, Euring 710) total annual habitat loss casualties per OWF included in the national scenarios.*
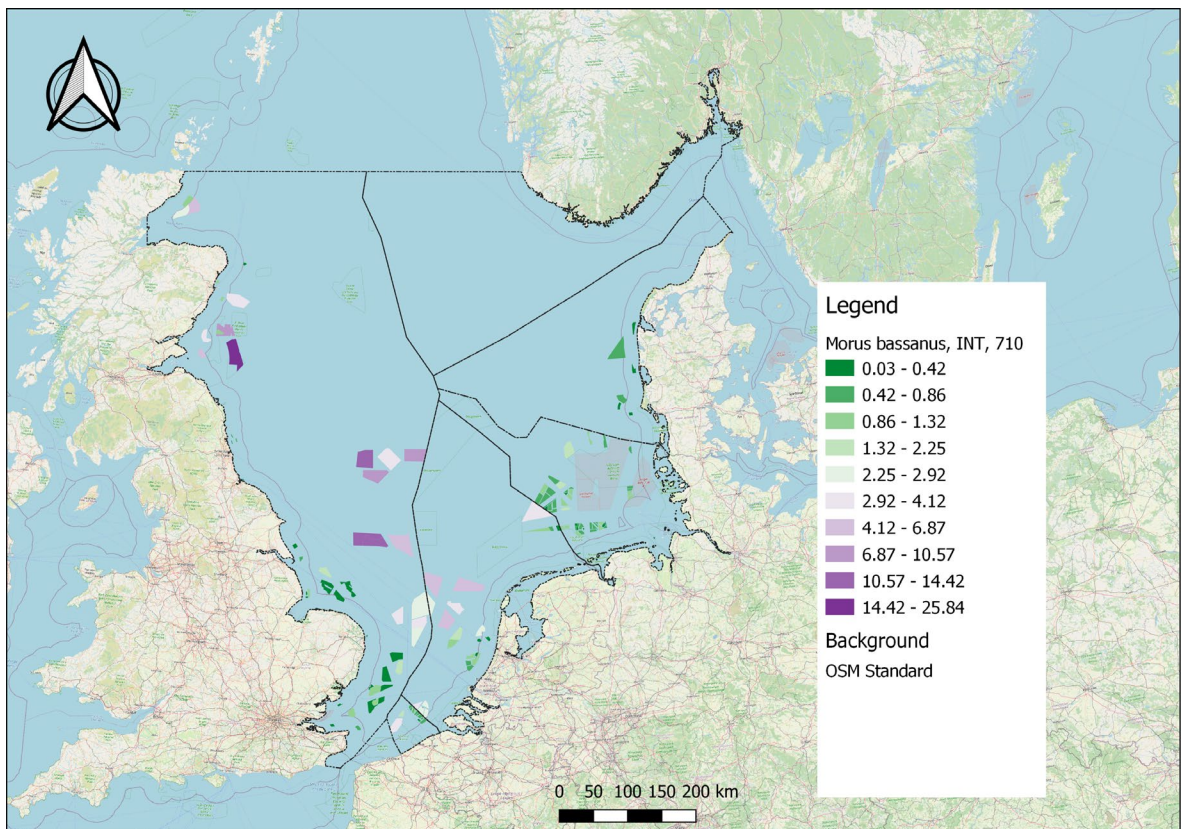
Figure 4-13. *Northern gannet (Morus bassanus, Euring 710) total annual habitat loss casualties per OWF included in the international scenario.*

For the northern gannet, most casualties are predicted in the Dutch northern OWF areas further away from the coast (**Figure 4-12**). The international map shows a slightly different picture with many casualties predicted in OWFs towards the central North Sea, but also near the Scottish coast (**Figure 4-13**). Bird density maps of each bimonthly period and of the annual averages can be found in separate documents (Electronic appendices E3 and E4; respectively E3_DensityMaps_19species_NATINT_period.pdf and E4_DensityMaps_19species_NATINT_yearly.pdf). The numbers of northern gannet casualties from both habitat loss and collision risk are presented in Table 19. There are on average between 204 and 332 casualties per bimonthly period from both habitat loss (this study) and collisions (Potiek *et al.*, 2021b) for the national scenarios. For habitat loss alone, this ranges from 7 to 11. Most casualties are predicted in the 'Rekenvariant III' scenario. The average estimate for the international scenario is 1209 casualties per two months, of which 97% are collision victims. The number of casualties from habitat loss per bimonthly period for the northern gannet is shown for each Dutch OWF area in Annex 4, Table 44.

The estimated maximum abundance used for the national scenarios equals 31,859 individuals, which leads to an estimated mortality rate in between 3.7% ('Basic 2030') and 6.1% ('Rekenvariant III') per year, considering both habitat loss and collision risk (Table 19). For the international scenario a maximum abundance of 162,868 individuals is used, which results in an estimated mortality of 4.4% per year.

Table 19. Overall, juvenile (S0), immature (S1, S2, S3) and adult (SA) mortality (Mort) and survival values for the northern gannet derived from mean numbers of casualties per bimonthly period and max abundance due to habitat loss (this study) and collision mortality (taken from Potiek et al., 2021b). Mortality source' shows the source of the mortality that is considered (HabLoss: Habitat loss, Collisions: collision mortality and Total: both habitat loss and collision mortality together).

Scenario	Mortality source	Mean casualties	Max abundance	Mort	Mort S0	Mort S1	Mort S2	Mort S3	Mort SA	Survival S0	Survival S1	Survival S2	Survival S3	Survival SA
null	null									0.48100	0.81600	0.88400	0.88700	0.91800
Basic_2030	Collisions	198	31,859	0.03657	0.01432	0.01372	0.02743	0.02713	0.03570	0.47411	0.80481	0.85975	0.86294	0.88523
Basic_2030	HabLoss	7	31,859	0.00116	0.00046	0.00044	0.00087	0.00086	0.00114	0.48078	0.81564	0.88323	0.88623	0.91696
Basic_2030	Total	204	31,859	0.03770	0.01477	0.01414	0.02828	0.02796	0.03680	0.47390	0.80446	0.85900	0.86220	0.88422
Rekenvariant I	Collisions	282	31,859	0.05189	0.02033	0.01946	0.03892	0.03849	0.05065	0.47122	0.80012	0.84959	0.85286	0.87150
Rekenvariant I	HabLoss	9	31,859	0.00169	0.00066	0.00063	0.00127	0.00125	0.00165	0.48068	0.81548	0.88288	0.88589	0.91649
Rekenvariant I	Total	291	31,859	0.05351	0.02096	0.02007	0.04013	0.03969	0.05223	0.47092	0.79963	0.84852	0.85180	0.87006
Rekenvariant II	Collisions	296	31,859	0.05432	0.02128	0.02037	0.04074	0.04029	0.05302	0.47077	0.79938	0.84798	0.85126	0.86933
Rekenvariant II	HabLoss	10	31,859	0.00179	0.00070	0.00067	0.00134	0.00133	0.00175	0.48066	0.81545	0.88281	0.88582	0.91640
Rekenvariant II	Total	305	31,859	0.05603	0.02195	0.02101	0.04202	0.04156	0.05469	0.47044	0.79885	0.84685	0.85014	0.86780
Rekenvariant III	Collisions	321	31,859	0.05893	0.02308	0.02210	0.04420	0.04370	0.05751	0.46990	0.79797	0.84493	0.84823	0.86520
Rekenvariant III	HabLoss	11	31,859	0.00197	0.00077	0.00074	0.00148	0.00146	0.00193	0.48063	0.81540	0.88269	0.88570	0.91623
Rekenvariant III	Total	332	31,859	0.06080	0.02381	0.02280	0.04560	0.04510	0.05935	0.46955	0.79739	0.84369	0.84700	0.86352
International	Collisions	1167	162,868	0.04223	0.01654	0.01583	0.03167	0.03132	0.04121	0.47304	0.80308	0.85600	0.85922	0.88017
International	HabLoss	42	162,868	0.00154	0.00060	0.00058	0.00115	0.00114	0.00150	0.48071	0.81553	0.88298	0.88599	0.91662
International	Total	1209	162,868	0.04371	0.01712	0.01639	0.03278	0.03242	0.04266	0.47277	0.80262	0.85502	0.85825	0.87884

Table 20: Overall, juvenile (S0), immature (S1, S2, S3) and adult (SA) mortality (Mort) and survival values for the northern gannet gannet derived from the northern gannet IBM for a maximum travel length of 1 grid cell per time step.

Scenario	Mortality source	Avoidance	Mort	Mort S0	Mort S1	Mort S2	Mort S3	Mort SA	Survival S0	Survival S1	Survival S2	Survival S3	Survival SA
null	Habitat loss		0.00000	0.00000	0.00000	0.00000	0.00000	0.00000	0.48100	0.81600	0.88400	0.88700	0.91800
Rekenvariant III	Habitat loss	0.8	0.00234	0.00092	0.00088	0.00176	0.00174	0.00229	0.48056	0.81528	0.88245	0.88546	0.91590
Rekenvariant III	Habitat loss	1.0	0.00284	0.00111	0.00107	0.00213	0.00211	0.00278	0.48046	0.81513	0.88211	0.88513	0.91545
International	Habitat loss	0.8	0.00795	0.00311	0.00298	0.00596	0.00590	0.00776	0.47950	0.81357	0.87873	0.88177	0.91088
International	Habitat loss	1.0	0.01072	0.00420	0.00402	0.00804	0.00795	0.01046	0.47898	0.81272	0.87689	0.87995	0.90840

4.5.1.1 Individual-based model mortality estimates

The individual-based model for the northern gannet predicted that the median of the annual OWF-induced mortality due to habitat loss was highest (1.07%) for the 'international' scenario with 100% avoidance and lowest (0.234%) for the 'national rekenvariant III' scenario with 80% avoidance (Table 20). These mortality estimates are all higher than those based on the bird density method (Table 19), which equalled 0.154% for the international scenario and 0.197% for the national rekenvariant III scenario.

4.5.2 Northern gannet population level effects
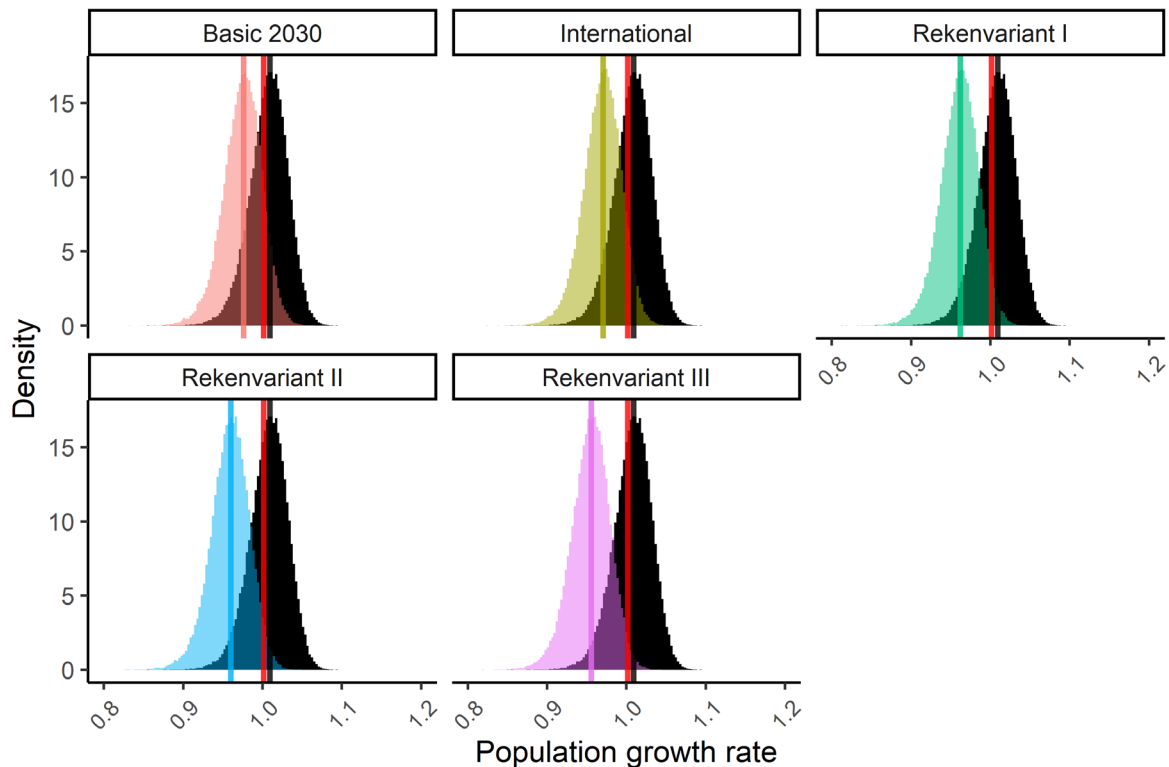
Figure 4-14. *Distribution of population growth rates of the northern gannet for the different scenarios, considering the effects of both habitat loss and collision mortality. Vertical lines indicate the median population growth rates of the ALI threshold (red), the null scenario (black) and each scenario (colours). The distributions for each scenario (in colours) overlay the distribution of the null scenario (in black).*

The estimated mortality from habitat loss and collisions due to OWFs leads to a violation of the ALI set for the northern gannet for all scenarios (Table 21; **Figure 4-14.**). The population abundance threshold for the northern gannet is defined as a 30% smaller population abundance over 3 generations, approximately 46.9 years, compared to a population with no OWFs. The probability that an OWF impact leads to population abundances lower than the population abundance threshold equals 57.2% for the 'Basic 2030' scenario, 62.0% for the 'Rekenvariant III' scenario and 59.3% for the 'International' scenario. The acceptable probability is defined at 50% (Table 9), and the scenario that considers only the OWFs that are already planned thus also exceeds the ALI. With only casualties from habitat loss, violation of the ALI does not occur for any scenario. Considering collision victims alone would already lead to the violation of the ALI for all scenarios.

The OWF-related mortality due to habitat loss as estimated by the IBM did not lead to violation of the ALI for any of the scenarios considered (Table 22 and **Figure 4-15**). Life-stage specific mortality and survival values for the different scenarios are shown in Annex 2. In Annex 2, we present additional results for a maximum travel length between 1 and 8 grid cells per timestep. For a maximum travel length of 8 grid cells per time step, the ALI was violated for the international scenario but not for any of the national scenarios. We find that the response of the OWF-related bimonthly survival to

maximum travel length varies between bimonthly periods. While survival decreases at high maximum travel length in one period, survival first decreases and then increases with increasing maximum travel length in other periods (Annex 2; **Figure 2.**). We were unable to tease out the cause of the different responses of the model estimates to the maximum travel length between bimonthly periods. Without a thorough understanding of the observed results, we cannot be completely confident that the IBM gives reliable estimates of the mortality that is caused by OWF-induced habitat loss. We have identified a probable cause for the high mortality with large maximum travel length, but could not fix it within the constraints of the current project. This error manifests itself only at large maximum travel length, and does not affect the results at smaller values. However, maximum travel length of 8 grid cells is probably a more realistic value for the northern gannet than a maximum travel length of 1 grid cell, and it is therefore important that the issue is resolved in the future.
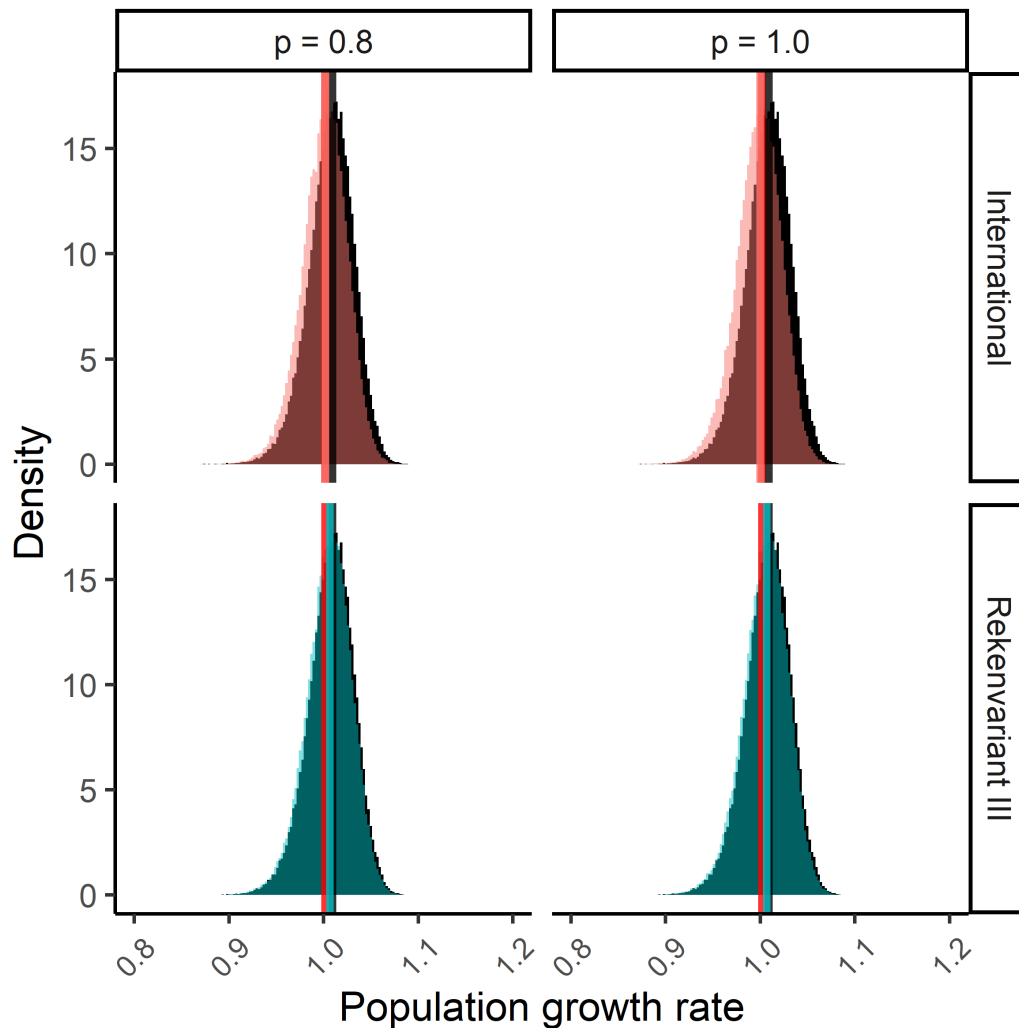
Figure 4-15. *Distribution of northern gannet population growth rates for the different scenarios. Vertical lines indicate the median population growth rate of the ALI threshold (red), the null scenario (black) and each OWF-scenario (colours). Estimates of mortality rates are derived from IBM simulations.*

Table 21. Population growth rates and ALI statistics for the northern gannet. 'Source' shows the source of the OWF effect that is considered (Habitat loss, collision mortality and Total: both habitat loss and collision mortality together). Median and 5% and 95% quantiles of the population growth rate ('Lambda') distributions are reported. 'P impact' represents the fractions of the Lambda distributions that are below the threshold of a 30% smaller population abundance compared to the median lambda of the null scenario after 3 generations, which occurs for a Lambda of 1.002. 'P causality' is the probability that the violation of the population abundance threshold results from the OWF impact. 'ALI 0.5' shows whether P causality exceeds 0.5, the ALI threshold (see Table 9).

Scenario	Source	Lambda median	q05	q95	P impact	P causality	ALI 0.5
Null	Null	1.009	0.966	1.045	0.3731		
Basic 2030	Collisions	0.977	0.934	1.013	0.8619	0.567	TRUE
Basic 2030	Habitat loss	1.008	0.965	1.044	0.3901	0.043	FALSE
Basic 2030	Total	0.976	0.933	1.012	0.8721	0.572	TRUE
Rekenvariant I	Collisions	0.964	0.921	1.000	0.9573	0.610	TRUE
Rekenvariant I	Habitat loss	1.008	0.965	1.043	0.3985	0.064	FALSE
Rekenvariant I	Total	0.962	0.920	0.998	0.9638	0.613	TRUE
Rekenvariant II	Collisions	0.961	0.919	0.998	0.9660	0.614	TRUE
Rekenvariant II	Habitat loss	1.008	0.964	1.043	0.3988	0.064	FALSE
Rekenvariant II	Total	0.960	0.917	0.996	0.9694	0.615	TRUE
Rekenvariant III	Collisions	0.957	0.915	0.994	0.9782	0.619	TRUE
Rekenvariant III	Habitat loss	1.007	0.964	1.043	0.4021	0.072	FALSE
Rekenvariant III	Total	0.956	0.913	0.992	0.9819	0.620	TRUE
International	Collisions	0.972	0.930	1.008	0.9052	0.588	TRUE
International	Habitat loss	1.008	0.965	1.043	0.3958	0.057	FALSE
International	Total	0.971	0.928	1.007	0.9169	0.593	TRUE

Table 22: Population growth rates and ALI statistics for the northern gannet based on annual OWF-induced mortality from habitat loss for the northern gannet as predicted by the IBM. Column 'mortality' shows the median annual mortality per OWF scenario and avoidance parameter. For the population growth rate ('Lambda'), median, 5% and 95% quantiles of the distributions are reported. 'P impact' represents the fractions of the Lambda distributions that are below the threshold of a 30% smaller population abundance compared to the median lambda of the null scenario after 3 generations, which occurs for a Lambda of 1.001. 'P causality' is the probability that the violation of the population abundance threshold results from the OWF impact. 'ALI 0.5' shows whether P causality exceeds 0.5, the ALI threshold (see Table 8). In the IBM, a maximum travel length of 1 grid cell per time step was used.

Scenario	Avoidance	Mortality	Lambda median	q05	q95	P impact	P causality	ALI 0.5
ALI_thres			1.001	0.959	1.037	0.5000	0.251	FALSE
NULL		0.000	1.009	0.966	1.045	0.3745	0.000	FALSE
Rekenvariant III	0.8	0.00234	1.007	0.964	1.042	0.4128	0.093	FALSE
Rekenvariant III	1.0	0.00284	1.007	0.964	1.042	0.4148	0.097	FALSE
International	0.8	0.00795	1.002	0.959	1.038	0.4901	0.236	FALSE
International	1.0	0.0107	0.999	0.956	1.036	0.5344	0.299	FALSE

4.6 Great cormorant (*Phalacrocorax carbo*)

4.6.1 Great cormorant habitat loss casualties and mortality
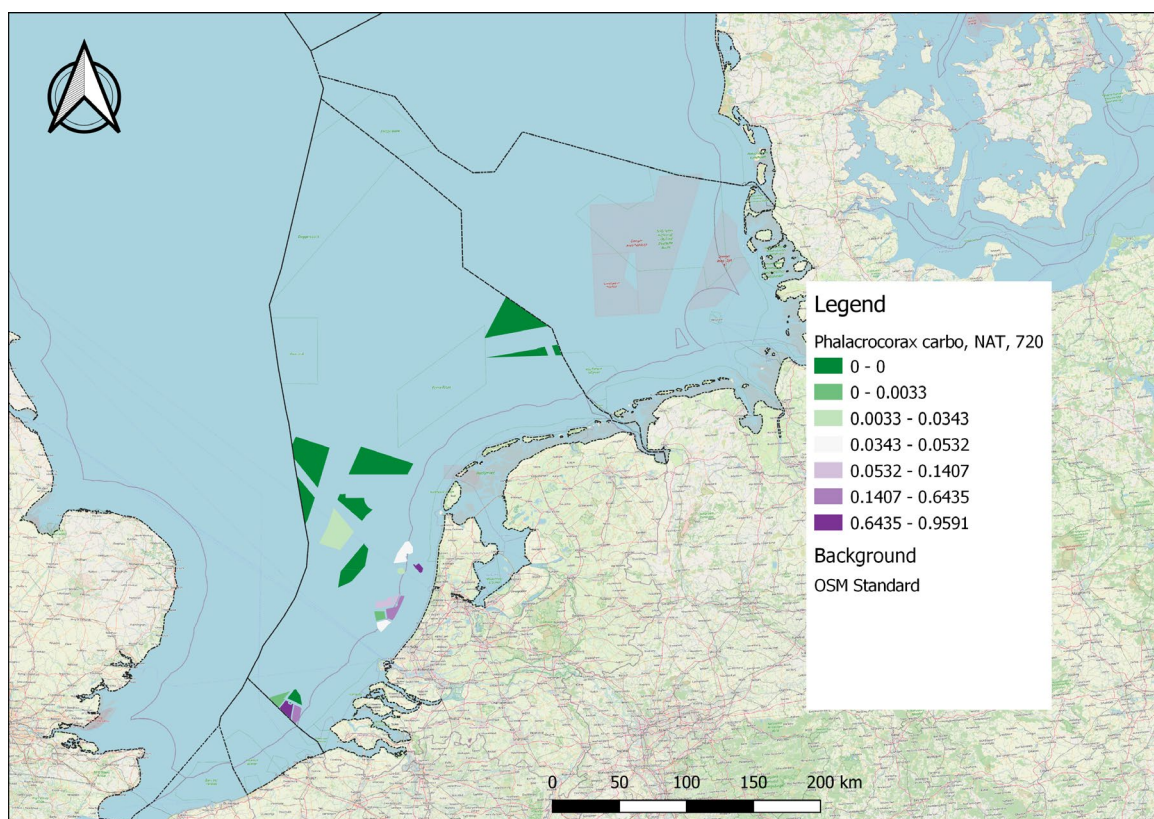
Figure 4-16. *Great cormorant (Phalacrocorax carbo, Euring 720) total annual habitat loss casualties per OWF included in the national scenarios.*
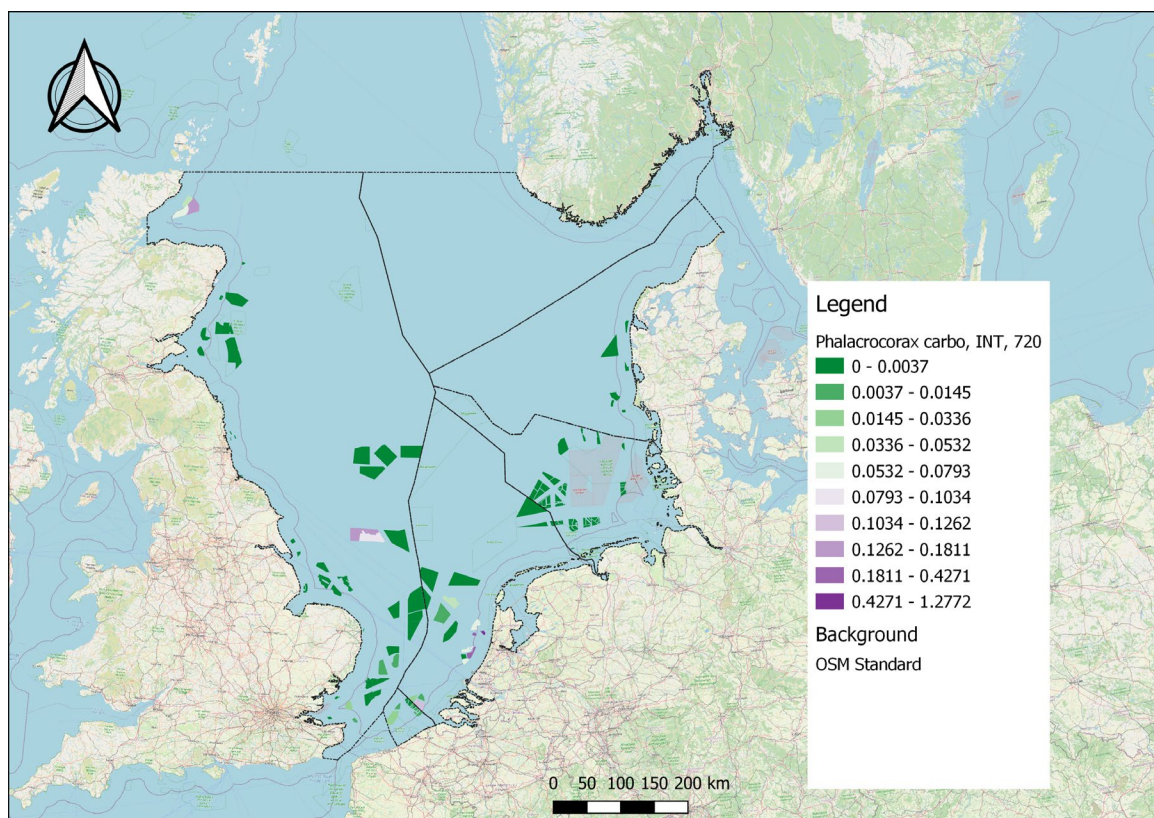
Figure 4-17. *Great cormorant (Phalacrocorax carbo, Euring 720) total annual habitat loss casualties per OWF included in the international scenario.*

For the great cormorant, predicted casualties are overall very low. Most Dutch casualties are predicted in the Dutch OWF areas along the coast (**Figure 4-16**). In an international context, the spatial pattern is similar (**Figure 4-17**), with few victims in most areas and slightly more predicted victims in small areas along the Scottish coast, one area central to the UK EEZ and along the Dutch coast. Note that these are based on very low numbers of birds, where relatively small differences may appear large due to the discrete colour scales. Besides, densities of cormorant are generally highest close to the coast where no wind farms are planned. Bird density maps of each bimonthly period and of the annual averages can be found in separate documents (Electronic appendices E3 and E4; respectively E3_DensityMaps_19species_NATINT_period.pdf and E4_DensityMaps_19species_NATINT_yearly.pdf). Note however, that most offshore wind farms are beyond the normal (pre-OWF) range of cormorant, but that these birds are known to adapt to OWFs. Future distribution patterns of this species will therefore probably shift seaward.

The estimated mean number of great cormorant casualties per bimonthly period is around 1 individual for all scenarios (Table 23). Note that there is no difference in the number of casualties between the national scenarios. Thus, the effect of the new national OWF areas on habitat loss seems negligible as the mean number of casualties does not increase for the scenarios with new OWF areas compared to the scenario with the OWFs that are already planned. With the maximum estimated abundances, the estimated numbers of casualties correspond to a mortality rate of 0.12% and 0.09% per year for the national and international scenarios, respectively (Table 23). The number of casualties per bimonthly period for the great cormorant is shown for each Dutch OWF area in Annex 4, Table 44.

Table 23. Mortality for the great cormorant derived from mean numbers of casualties per bimonthly period and maximum abundance.

Scenario	Mean casualties	Max abundance	mort
Basic 2030	1	2621	0.0012462
Rekenvariant II	1	2621	0.0012462
Rekenvariant III	1	2621	0.0012462
Rekenvariant I	1	2621	0.0012462
International	1	3822	0.0009098

4.7 Common eider (*Somateria mollissima*)

4.7.1 Common eider habitat loss casualties and mortality

Figure 4-18. *Common eider (Somateria mollissima, Euring 2060) total annual habitat loss casualties per OWF included in the national scenarios.*
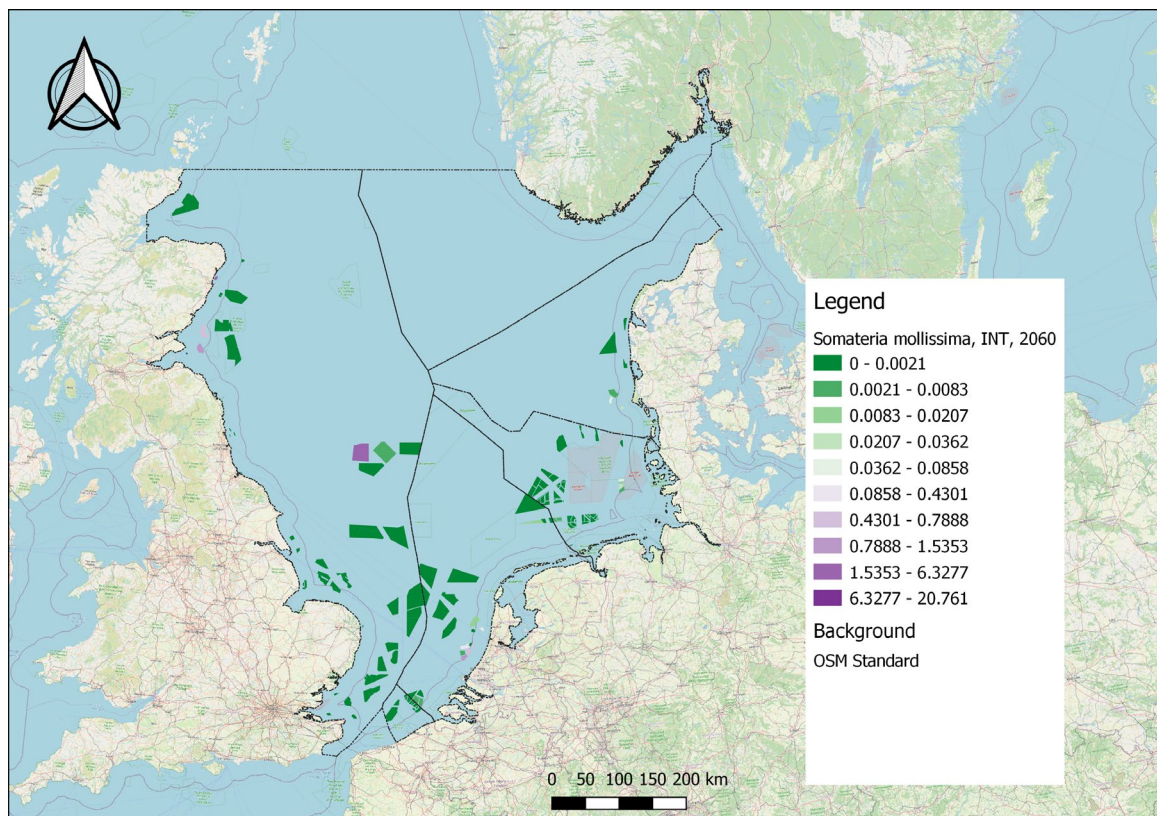
Figure 4-19. *Common eider (Somateria mollissima, Euring 2060) total annual habitat loss casualties per OWF included in the international scenario.*

For the common eider, predicted casualties are overall very low. Most Dutch casualties are predicted in the Dutch OWF areas along the coast (**Figure 4-18**). In an international context, the spatial pattern is similar (**Figure 4-19**), with few victims in most areas and slightly more predicted victims in small areas along the southern Scottish coast, one area central to the UK EEZ and along the German and Dutch coasts. Note that these are based on very low numbers of birds, where relatively small differences may appear large due to the discrete colour scales. Besides, densities of common eider are generally highest close to the coast where no wind farms are planned. Bird density maps of each bimonthly period and of the annual averages can be found in separate documents (Electronic appendices E3 and E4; respectively E3_DensityMaps_19species_NATINT_period.pdf and E4_DensityMaps_19species_NATINT_yearly.pdf).

The estimated mean number of common eider casualties per bimonthly period is around 0.7 individuals for the national scenarios and 5.7 for the international scenario (Table 24). Note that there is no difference in the number of casualties between the national scenarios. Thus, the effect of the new national OWF areas on habitat loss seems negligible as the mean number of casualties does not increase for the scenarios with new OWF areas compared to the scenario with the OWFs that are already planned. With the maximum estimated abundance the estimated number of casualties results in an mortality rate for the national scenarios of 0.019% per year (Table 24). For the international scenario the estimated mortality is 0.03% per year. The number of casualties per bimonthly period for the common eider are shown for each Dutch OWF area in Annex 4, Table 44.

Table 24. Mortality for the common eider derived from mean numbers of casualties per bimonthly period and maximum abundance.

Scenario	Mean casualties	Max abundance	mort
Basic 2030	1	22,134	0.0001958
Rekenvariant II	1	22,134	0.0001958
Rekenvariant III	1	22,134	0.0001958
Rekenvariant I	1	22,134	0.0001958
International	6	96,653	0.0003546

4.8 Common scoter (*Melanitta nigra*)

4.8.1 Common scoter habitat loss casualties and mortality
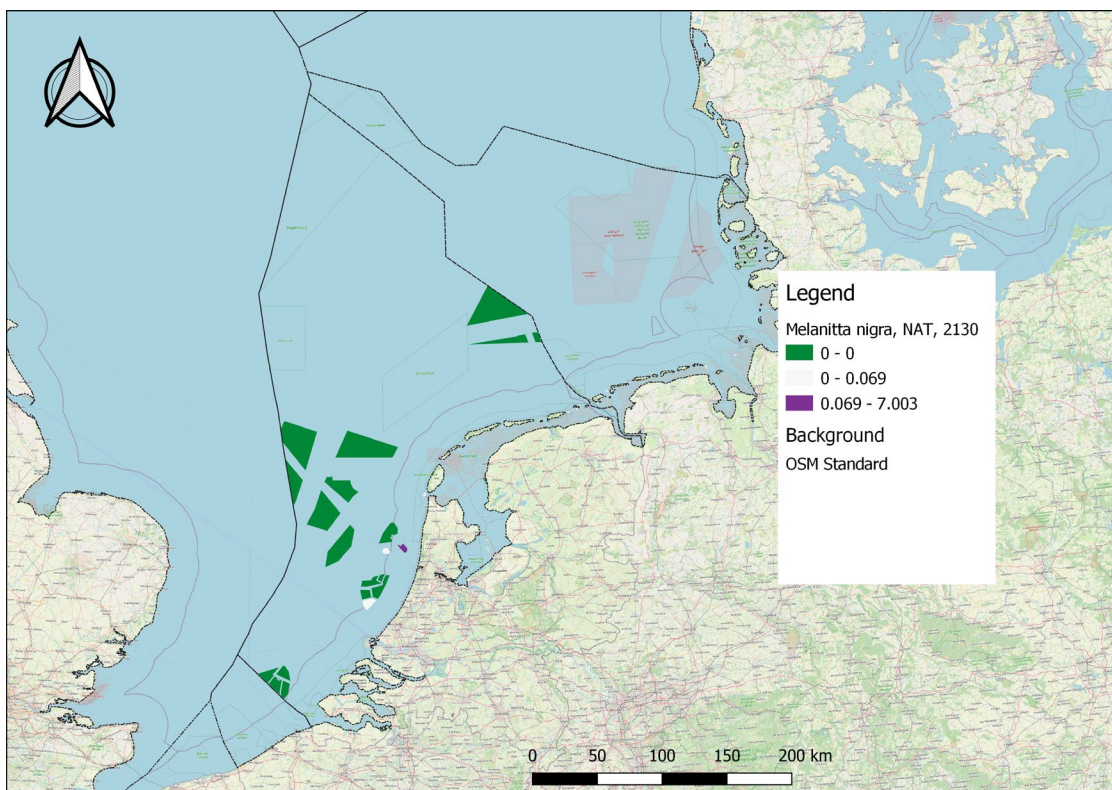
Figure 4-20. *Common scoter (Melanitta nigra, Euring 2130) total annual habitat loss casualties per OWF included in the national scenarios.*
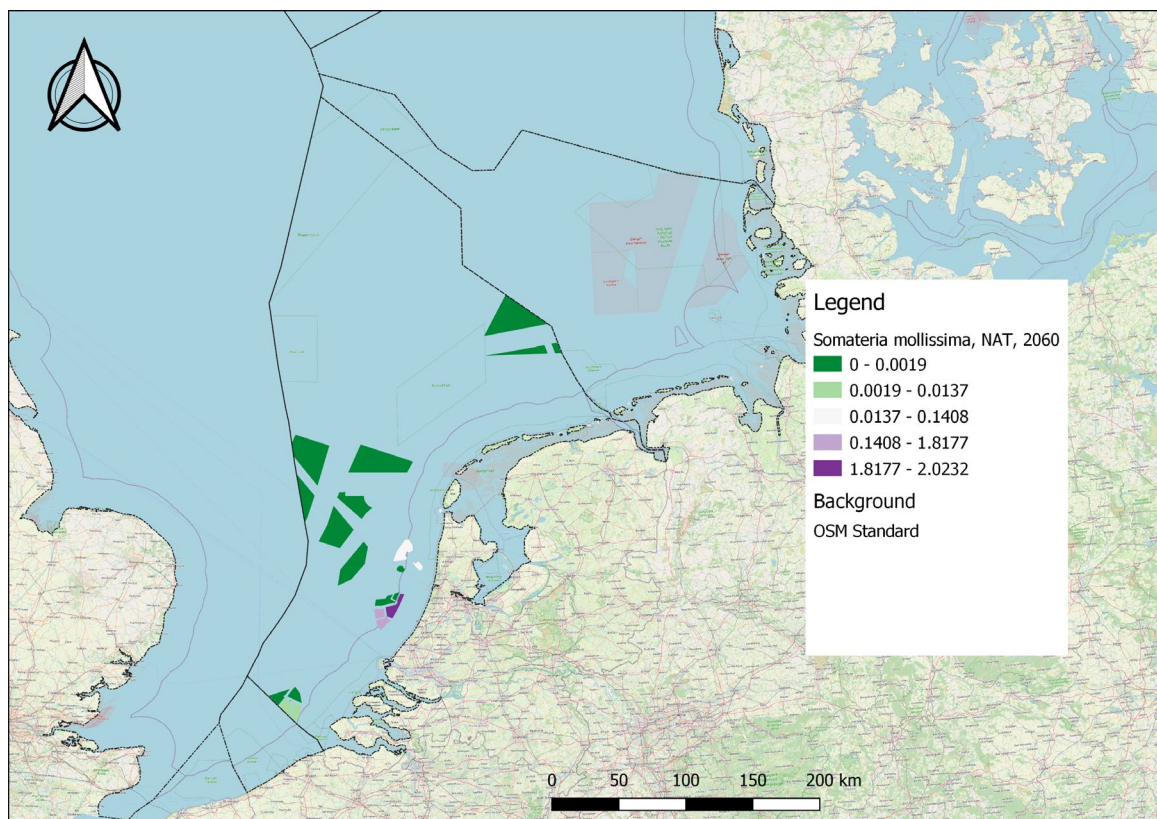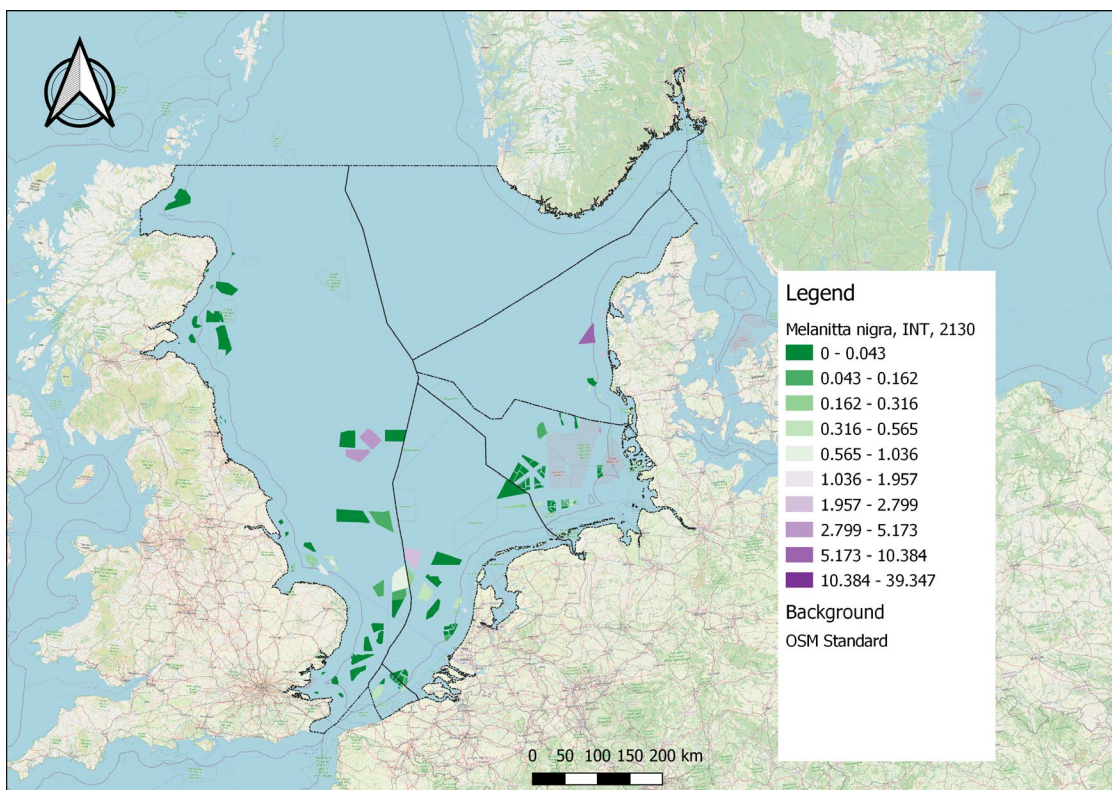

Figure 4-21. *Common scoter (Melanitta nigra, Euring 2130) total annual habitat loss casualties per OWF included in the international scenario.*

For the common scoter, predicted casualties are overall very low. Most Dutch casualties are predicted in some Dutch OWF areas along the coast (**Figure 4-20**). In an international context, the spatial pattern is slightly different (**Figure 4-21**), few victims are predicted in most areas and some areas have more predicted victims, mostly central to the North Sea and at one spot along the Danish coast. Note that these are based on very low numbers of birds, where relatively small differences may appear large due to the discrete colour scales. Besides, densities of common scoters are generally highest close to the coast where no wind farms are planned. Bird density maps of each bimonthly period and of the annual averages can be found in separate documents (Electronic appendices E3 and E4; respectively E3_DensityMaps_19species_NATINT_period.pdf and E4_DensityMaps_19species_NATINT_yearly.pdf).

The estimated mean number of common scoter casualties per bimonthly period is around 2 individuals for the national scenarios and 15 for the international scenario (Table 25). Note that there is no difference in the number of casualties between the national scenarios. Thus, the effect of the new national OWF areas on habitat loss seems negligible as the mean number of casualties does not increase for the scenarios with new OWF areas compared to the scenario with the OWFs that are already planned. With the maximum estimated abundance (Table 25), the estimated number of casualties results in an mortality rate for the national scenarios of 0.014% per year (Table 25). For the international scenario the estimated addition mortality is 0.015% per year. The number of casualties per bimonthly period for the common scoter are shown for each Dutch OWF area in Annex 4, Table 44.

Table 25. Mortality for the common scoter derived from mean numbers of casualties per bimonthly period and maximum abundance.

Scenario	Mean casualties	Max abundance	mort
Basic 2030	2	51,166	0.0001382
Rekenvariant II	2	51,166	0.0001382
Rekenvariant III	2	51,166	0.0001382
Rekenvariant I	2	51,166	0.0001382
International	15	598,905	0.0001456

4.9 Sandwich tern (*Thalasseus sandvicensis*)

4.9.1 Sandwich tern habitat loss casualties and mortality
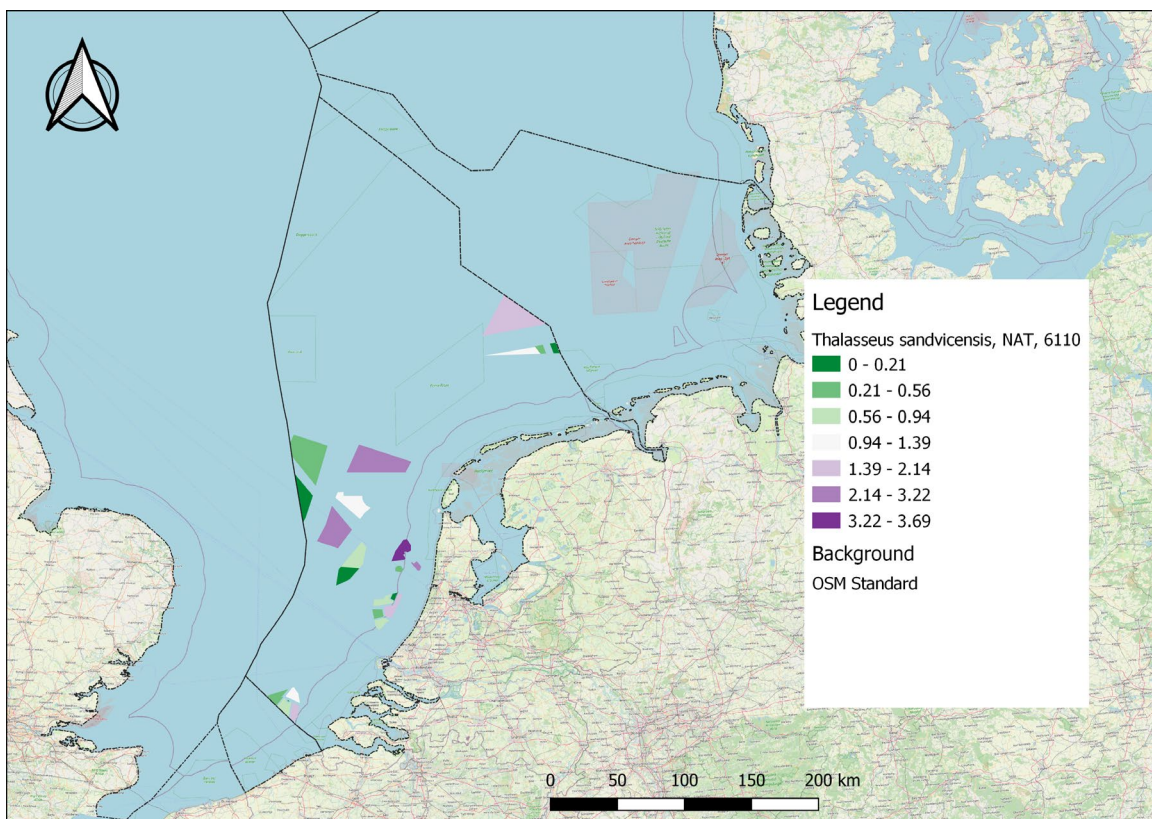
Figure 4-22. *Sandwich tern (Thalasseus sandvicensis, Euring 6110) total annual habitat loss casualties per OWF included in the national scenarios.*
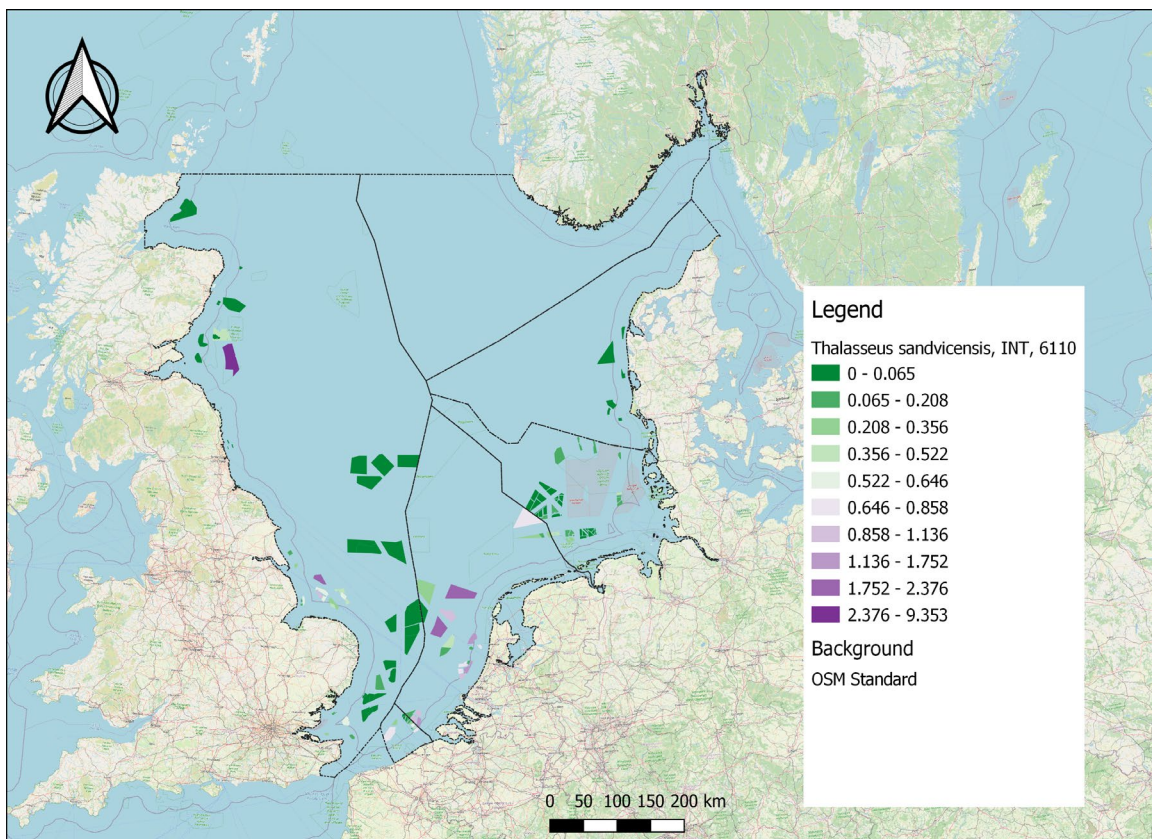
Figure 4-23. *Sandwich tern (Thalasseus sandvicensis, Euring 6110) total annual habitat loss casualties per OWF included in the international scenario.*

For the sandwich tern, most Dutch casualties are predicted in the Dutch OWF areas along the coast (**Figure 4-22**), but also in some of the areas further from the coast, such as "IJmuiden Ver" (OWF – bw6), "Zoekgebied 5 Oost" (OWF - 263o) and "Hollandse Kust Noord" (OWF - 15). The international map shows a similar pattern, with few casualties predicted in international waters except for some areas along the UK and Belgian coasts (**Figure 4-23**). Bird density maps of each bimonthly period and of the annual averages can be found in separate documents (Electronic appendices E3 and E4; respectively E3_DensityMaps_19species_NATINT_period.pdf and E4_DensityMaps_19species_NATINT_yearly.pdf).

The number of sandwich tern casualties from both habitat loss (this study) and collision risk (Potiek *et al.*, 2021b) are presented in Table 26. There are on average in between 9 and 12 casualties per bimonthly period from both habitat loss and collisions for the national scenarios. The average estimate for the international scenario is 19 casualties per two months, of which 58% are collision victims. The number of casualties from habitat loss per bimonthly period for the sandwich tern are shown for each Dutch OWF area in Annex 4, Table 44.

The estimated maximum abundance used for the national scenarios equals 22,603 individuals, which leads to an estimated mortality rate in between 0.23% ('Basic 2030') and 0.30% ('Rekenvariant III') per year, for both habitat loss and collision risk (Table 26). The international scenario uses a maximum abundance of 25,882 individuals, which results in an estimated mortality of 0.43% per year. From Table 26 it can be seen that the OWF-induced mortality is only applied to the adult life stages A_{34} and A_B, which share survival parameter S_A. Survival of the immature life stages (age 0 – 2) is unaffected by OWF-induced mortality in the geographical context of the southern North Sea.

Table 26. Juvenile (S0), immature (S12) and adult (SA) mortality (mort) and survival values for the sandwich tern derived from mean numbers of casualties per bimonthly period and max abundance due to habitat loss (this study) and collision mortality (taken from Potiek et al., 2021b). Mortality source' shows the source of the mortality that is considered (Habitat loss, collision and total (both habitat loss and collision mortality together) mortality). Note that the S0 and S12 survival do not change and were therefore not included in the table.

Scenario	Mortality source	Mean casualties	Max abundance	Mort	Mort S0	Mort S12	Mort SA	Survival SA
null	null							0.94200
Basic 2030	Collisions	6	22,603	0.00142	0	0	0.00142	0.94066
Basic 2030	Habitat loss	4	22,603	0.00091	0	0	0.00091	0.94114
Basic 2030	Total	9	22,603	0.00233	0	0	0.00233	0.93981
Rekenvariant I	Collisions	7	22,603	0.00176	0	0	0.00176	0.94035
Rekenvariant I	Habitat loss	5	22,603	0.00119	0	0	0.00119	0.94088
Rekenvariant I	Total	12	22,603	0.00294	0	0	0.00294	0.93923
Rekenvariant II	Collisions	7	22,603	0.00176	0	0	0.00176	0.94035
Rekenvariant II	Habitat loss	5	22,603	0.00119	0	0	0.00119	0.94088
Rekenvariant II	Total	12	22,603	0.00294	0	0	0.00294	0.93923
Rekenvariant III	Collisions	7	22,603	0.00183	0	0	0.00183	0.94028
Rekenvariant III	Habitat loss	5	22,603	0.00122	0	0	0.00122	0.94086
Rekenvariant III	Total	12	22,603	0.00304	0	0	0.00304	0.93914
International	Collisions	11	25,882	0.00249	0	0	0.00249	0.93965
International	Habitat loss	8	25,882	0.00178	0	0	0.00178	0.94032
International	Total	19	25,882	0.00427	0	0	0.00427	0.93797

4.9.2 Sandwich tern population level effects
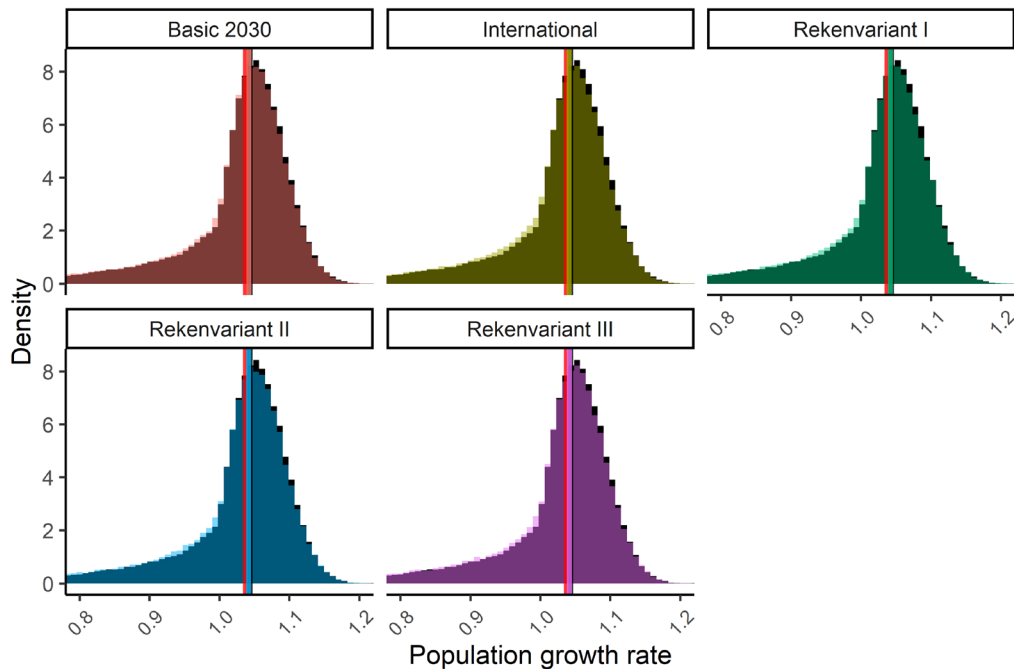
Figure 4-24. *Distribution of population growth rate of the sandwich tern for the different scenarios. Vertical lines indicate the median population growth rates of the ALI threshold (red), the null scenario (black) and each scenario(colours). The distributions for each scenario (in colours) overlay the distribution of the null scenario (in black).*

The estimated mortality from habitat loss and collision mortality due to OWFs does not lead to a violation of the ALI set for the sandwich tern. Median population growth rates estimated for the national scenarios range between 1.041 and 1.042 (Table *27*). Population growth rates estimated for all scenarios are similar to the null scenario (**Figure 4-24**). The probability that a violation of the population abundance threshold results from an OWF-induced impact ranges between 3.5 to 4.2% for the national scenarios and equals 5.4% for the international scenario (Table *27*).

Table 27. Population growth rates and ALI statistics for the sandwich tern. 'Source' shows the source of the OWP effect that is considered (Habitat loss, collision mortality and Total (the joint effect of habitat loss and collision mortality)). Median and 5% and 95% quantiles of the population growth rate ('Lambda') distributions are reported. 'P impact' represents the fractions of the Lambda distributions that are below the threshold of a 30% smaller population abundance compared to the median lambda of the null scenario after 3 generations, which occurs for a Lambda of 1.037. 'P causality' is the probability that the violation of the population abundance threshold results from the OWF impact. 'ALI 0.5' shows whether P causality exceeds 0.5, the ALI threshold (see Table 9).

Scenario	Source	Lambda median	q05	q95	P impact	P causality	ALI 0.5
null	null	1.044	0.805	1.118	0.4443		
Basic 2030	Collisions	1.042	0.801	1.117	0.4570	0.028	FALSE
Basic 2030	Habitat loss	1.043	0.803	1.118	0.4513	0.016	FALSE
Basic 2030	Total	1.042	0.804	1.117	0.4604	0.035	FALSE
Rekenvariant I	Collisions	1.042	0.808	1.118	0.4558	0.025	FALSE
Rekenvariant I	Habitat loss	1.043	0.804	1.118	0.4515	0.016	FALSE
Rekenvariant I	Total	1.042	0.805	1.117	0.4610	0.036	FALSE
Rekenvariant II	Collisions	1.042	0.802	1.117	0.4565	0.027	FALSE
Rekenvariant II	Habitat loss	1.043	0.803	1.118	0.4521	0.017	FALSE
Rekenvariant II	Total	1.041	0.800	1.117	0.4624	0.039	FALSE
Rekenvariant III	Collisions	1.042	0.803	1.118	0.4545	0.022	FALSE
Rekenvariant III	Habitat loss	1.043	0.804	1.118	0.4531	0.019	FALSE
Rekenvariant III	Total	1.041	0.801	1.117	0.4639	0.042	FALSE
International	Collisions	1.042	0.802	1.117	0.4595	0.033	FALSE
International	Habitat loss	1.042	0.803	1.118	0.4561	0.026	FALSE
International	Total	1.041	0.800	1.117	0.4699	0.054	FALSE

4.10 Common guillemot (*Uria aalge*)

4.10.1 Common guillemot habitat loss casualties and mortality

Figure 4-25. *Common guillemot (Uria aalge, Euring 6340) total annual habitat loss casualties per OWF included in the national scenarios.*

Figure 4-26. *Common guillemot (Uria aalge, Euring 6340) total annual habitat loss casualties per OWF included in the international scenario.*

For the common guillemot, most Dutch casualties are predicted in the OWF areas far from the coast (Figure 4-25). The international map shows most casualties in OWF areas inside the UK EEZ (Figure 4-26). Bird density maps of each bimonthly period and of the annual averages can be found in separate documents (Electronic appendices E3 and E4; respectively E3_DensityMaps_19species_NATINT_period.pdf and E4_DensityMaps_19species_NATINT_yearly.pdf).

The estimated mean number of common guillemot casualties per bimonthly period for the national scenarios varies between 99 and 237 and is highest for the 'Rekenvariant III' scenario (Table 28). Using a maximum estimated abundance of 227,587 individuals this corresponds to an annual mortality of 0.26% - 0.62% (Table 28). For the international scenario there are on average 2359 casualties per bimonthly period, corresponding to an annual mortality of 0.84%. The number of casualties per bimonthly period for the common guillemot is shown for each Dutch OWF area in Annex 4, Table 44.

Table 28. Juvenile (S0), Immature (S1, S2) and adult (SA) mortality (mort) and survival values for the common guillemot derived from mean numbers of casualties per bimonthly period and max abundance

Scenario	Mean casualties	Max abundance	Mort	Mort S0	Mort S1	Mort S2	Mort SA	Survival S0	Survival S1	Survival S2	Survival SA
								0.60800	0.77400	0.85800	0.94900
Basic 2030	99	227,587	0.00258	0.00258	0.00258	0.00258	0.00258	0.60643	0.77200	0.85578	0.94655
Rekenvariant I	171	227,587	0.00448	0.00448	0.00448	0.00448	0.00448	0.60527	0.77053	0.85415	0.94474
Rekenvariant II	186	227,587	0.00488	0.00488	0.00488	0.00488	0.00488	0.60503	0.77022	0.85381	0.94436
Rekenvariant III	237	227,587	0.00622	0.00622	0.00622	0.00622	0.00622	0.60422	0.76919	0.85267	0.94310
International	2359	1,677,205	0.00841	0.00841	0.00841	0.00841	0.00841	0.60289	0.76749	0.85079	0.94102

4.10.2   Common guillemot population-level effects

The estimated mortality from habitat loss due to OWFs does not lead to a violation of the ALI set for the common guillemot. Median population growth rates estimated for the national scenarios range between 1.037 and 1.041 (Table *29*). Population growth rates estimated for all scenarios are slightly different from the null scenario (**Figure 4-27**). The probability that a violation of the population abundance threshold results from an OWF-induced impact ranges between 6.0% to 12.7% for the national scenarios and equals 16.6% for the international scenario (Table *29*).

Table 29. *Population growth rates and ALI statistics for the common guillemot. Median and 5% and 95% quantiles of the population growth rate ('Lambda') distributions are reported. 'P impact' represents the fractions of the Lambda distributions that are below the threshold of a 30% smaller population abundance compared to the median lambda of the null scenario after 3 generations, which occurs for a Lambda of 1.038. 'P causality' is the probability that the violation of the population abundance threshold results from the OWF impact. 'ALI 0.5' shows whether P causality exceeds 0.5, the ALI threshold (see Table 9).*

| Scenario	Lambda median	Lambda q05	Lambda q95	P impact	P causality	ALI 0.5
Null	1.044	0.947	1.099	0.4398		
Basic 2030	1.041	0.946	1.096	0.4677	0.060	FALSE
Rekenvariant I	1.039	0.944	1.095	0.4882	0.099	FALSE
Rekenvariant II	1.038	0.943	1.094	0.4936	0.109	FALSE
Rekenvariant III	1.037	0.943	1.093	0.5037	0.127	FALSE
International	1.035	0.940	1.091	0.5276	0.166	FALSE
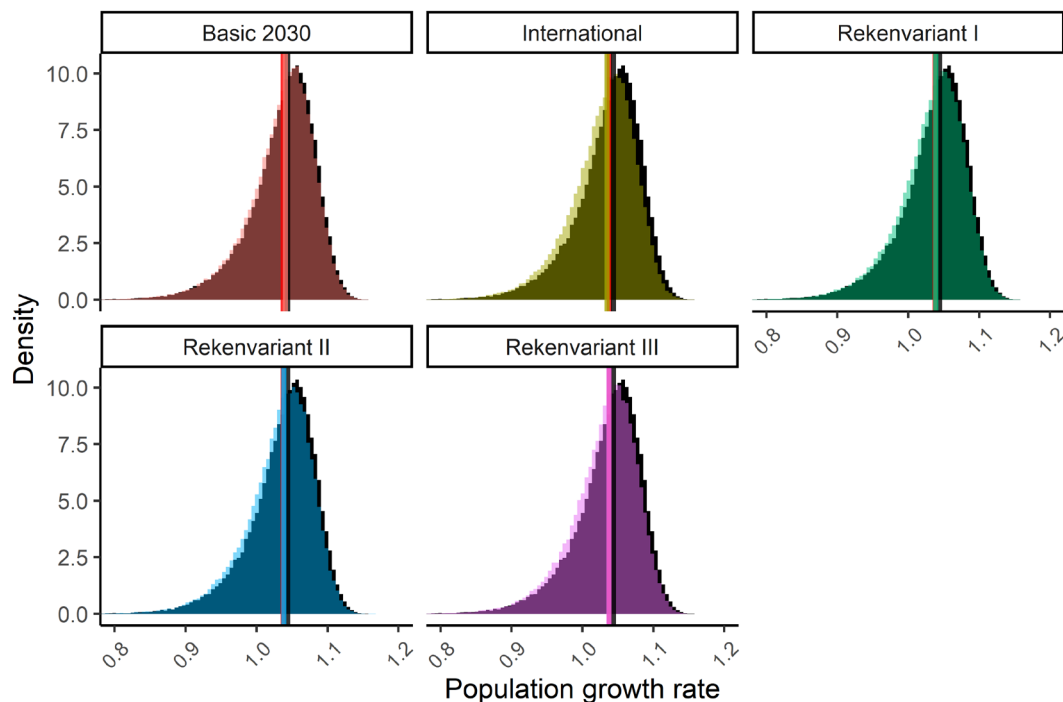
Figure 4-27. *Distribution of population growth rates of the common guillemot for the different scenarios. Vertical lines indicate the median population growth rates of the ALI threshold (red), the null scenario (black) and each scenario(colours). The distributions for each scenario (in colours) overlay the distribution of the null scenario (in black).*

4.11 Razorbill (*Alca torda*)

4.11.1 Razorbill habitat loss casualties and mortality
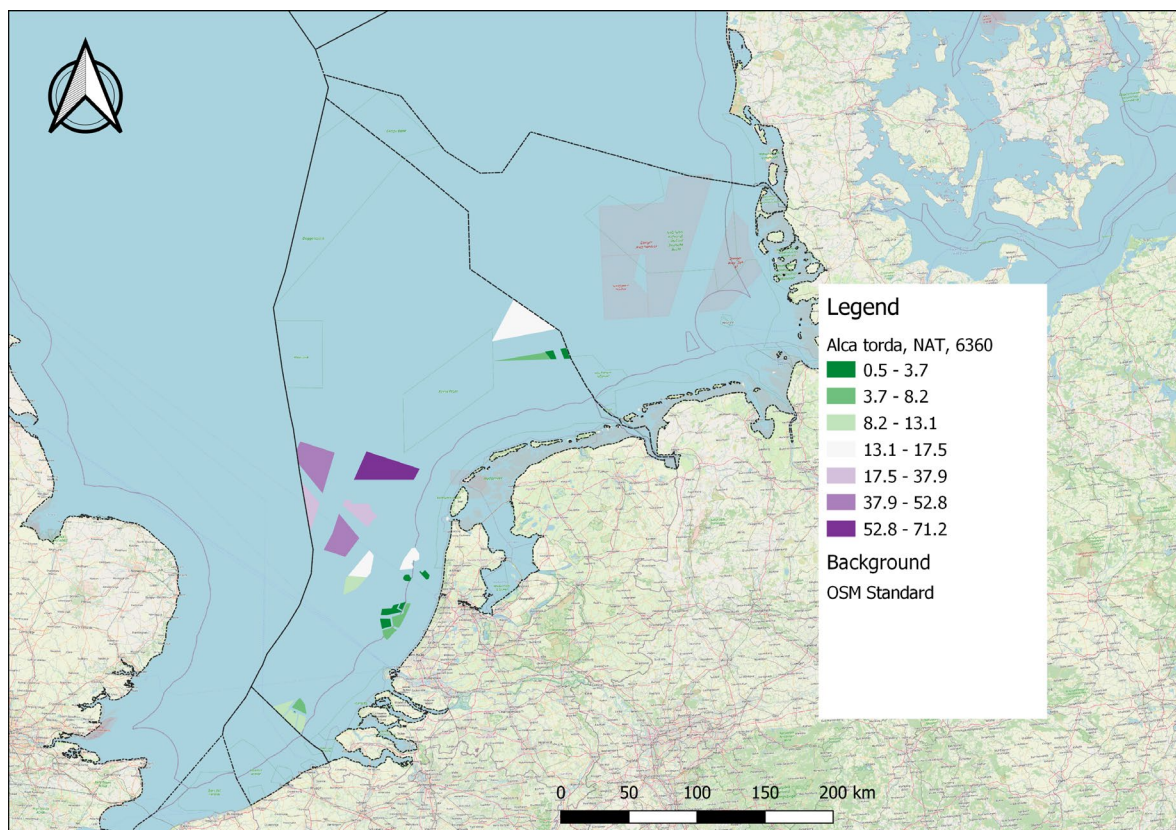
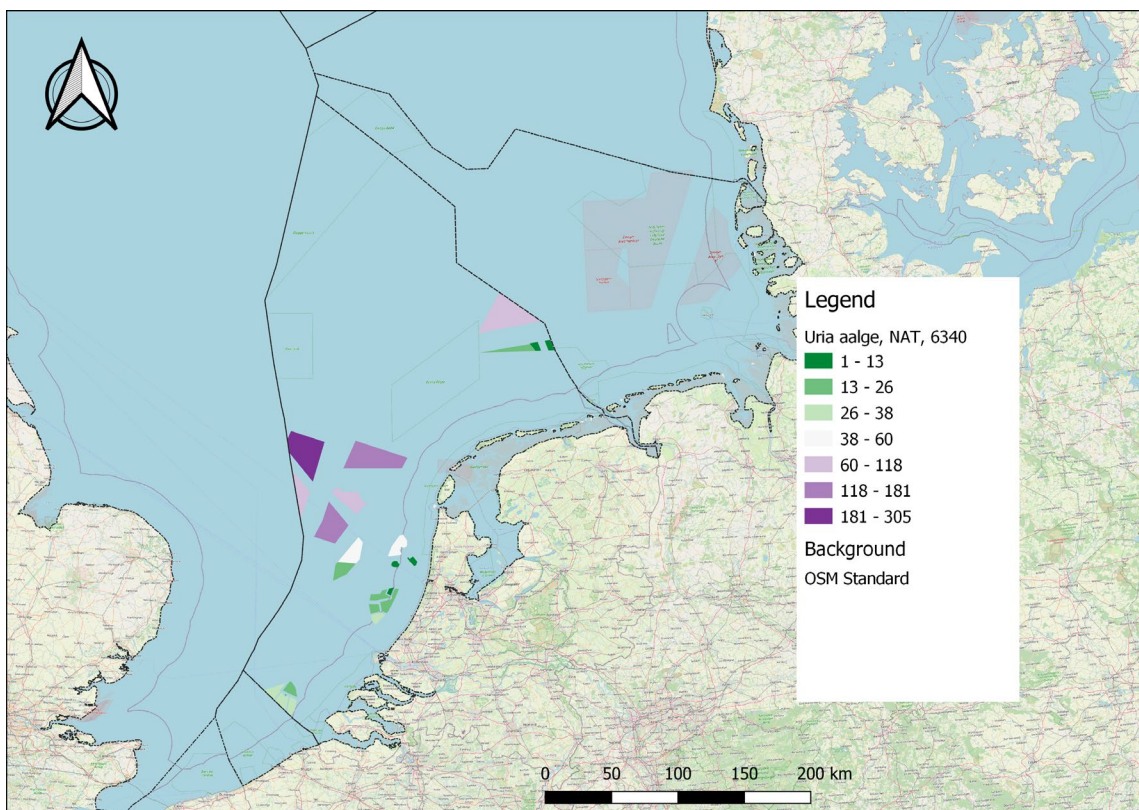**Figure 4-28.** *Razorbill (Alca torda, Euring 6360) total annual habitat loss casualties per OWF included in the national scenarios.*
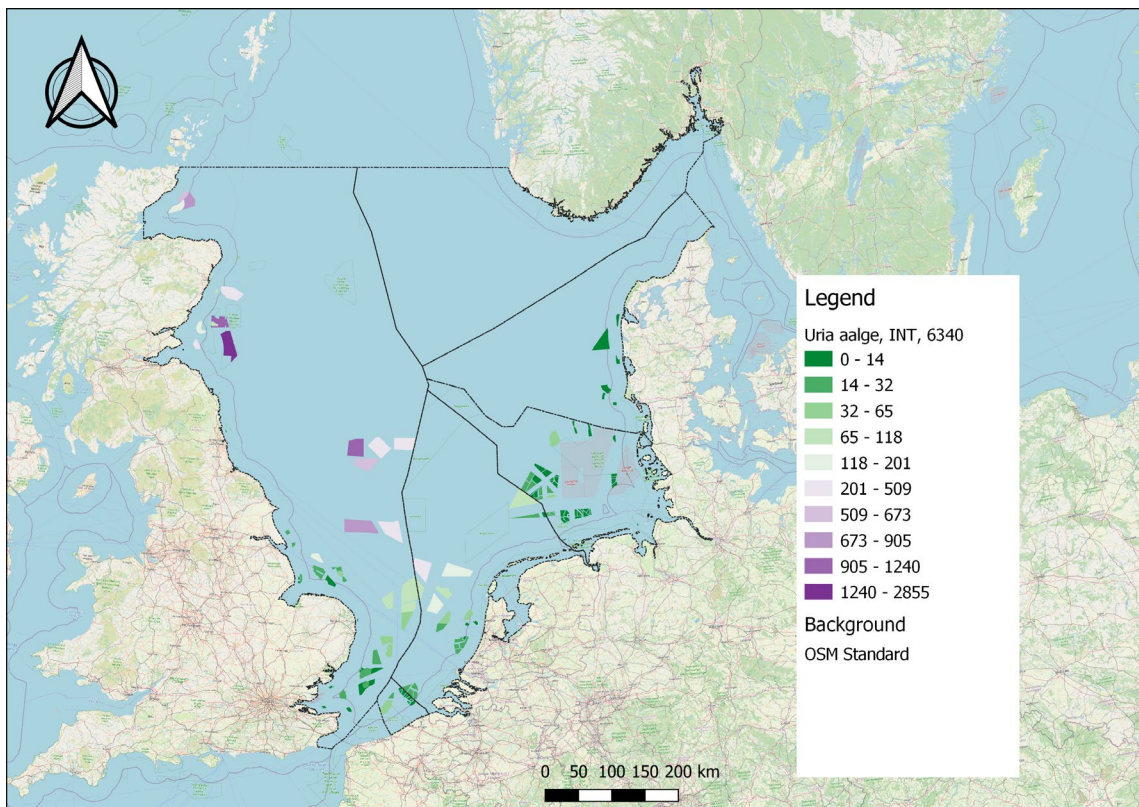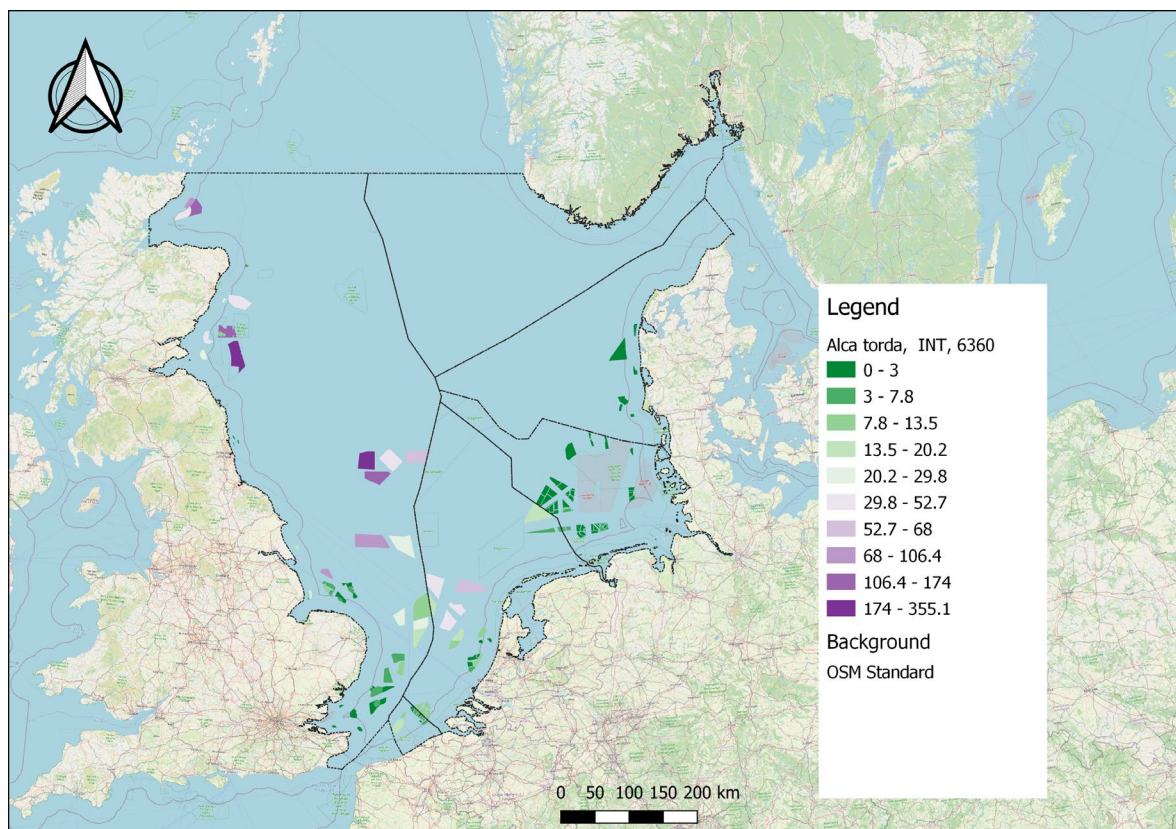

Figure 4-29. *Razorbill (Alca torda, Euring 6360) total annual habitat loss casualties per OWF included in of the international scenario.*

For the razorbill, most Dutch casualties are predicted in the OWF areas far from the coast (**Figure 4-28**). The international map shows most casualties in OWF areas inside the UK EEZ but inside the Dutch OWF areas in the central North Sea medium to high numbers of razorbill casualties are also predicted (**Figure 4-29**). Bird density maps of each bimonthly period and of the annual averages can be found in separate documents (Electronic appendices E3 and E4; respectively E3_DensityMaps_19species_NATINT_period.pdf and E4_DensityMaps_19species_NATINT_yearly.pdf).

The estimated mean number of razorbill casualties per bimonthly period for the national scenarios varies between 28 and 62 and is highest for the 'Rekenvariant III' scenario (Table 30). Using a maximum estimated abundance of 61,669 individuals this corresponds to an annual mortality of 0.27% - 0.60% (Table 30). For the international scenario there are on average 435 casualties per two month period, on an estimated maximum abundance of 227,439 individuals. This corresponds to an annual mortality of 1.1%. The number of casualties per bimonthly period for the razorbill are shown for each Dutch OWF area in Annex 4, Table 44.

Table 30. Immature (S01) and adult (SA) mortality (mort) and survival values for the razorbill derived from mean numbers of casualties per bimonthly period and max abundance.

Scenario	Mean casualties	Max abundance	Mort	Mort S01	Mort SA	Survival S01	Survival SA
null						0.64300	0.90900
Basic 2030	28	61,669	0.00267	0.00267	0.00267	0.64128	0.90657
Rekenvariant I	51	61,669	0.00487	0.00487	0.00487	0.63987	0.90457
Rekenvariant II	55	61,669	0.00524	0.00524	0.00524	0.63963	0.90423
Rekenvariant III	62	61,669	0.00602	0.00602	0.00602	0.63913	0.90353
International	435	227,439	0.01142	0.01142	0.01142	0.63566	0.89862

4.11.2   Razorbill population level effects

The estimated mortality from habitat loss due to OWFs does not lead to a violation of the ALI set for the razorbill. Median population growth rates estimated for the national scenarios range between 1.00 and 1.003 (Table 31) and equals 0.994 for the international scenario. The probability that a violation of the population abundance threshold results from an OWF-induced impact ranges between 3.6% - 7.6% for the national scenarios and equals 14.1% for the international scenario (Table 31). Population growth rates estimated for all scenarios are slightly different from the null scenario (**Figure 4-30**).

Table 31. Population growth rates and ALI statistics for the razorbill. Median and 5% and 95% quantiles of the population growth rate ('Lambda') distributions are reported. 'P impact' represents the fractions of the Lambda distributions that are below the threshold of a 30% smaller population abundance compared to the median lambda of the null scenario after 3 generations, which occurs for a Lambda of 0.998. 'P causality' is the probability that the violation of the population abundance threshold results from the OWF impact. 'ALI 0.5' shows whether P causality exceeds 0.5, the ALI threshold (see Table 9).

Scenario	Lambda median	Lambda q05	Lambda q95	P impact	P causality	ALI 0.5
null	1.006	0.855	1.081	0.4518		
Basic 2030	1.003	0.855	1.080	0.4687	0.036	FALSE
Rekenvariant I	1.000	0.852	1.078	0.4852	0.069	FALSE
Rekenvariant II	1.000	0.853	1.077	0.4871	0.072	FALSE
Rekenvariant III	1.000	0.851	1.077	0.4892	0.076	FALSE
International	0.994	0.846	1.073	0.5261	0.141	FALSE
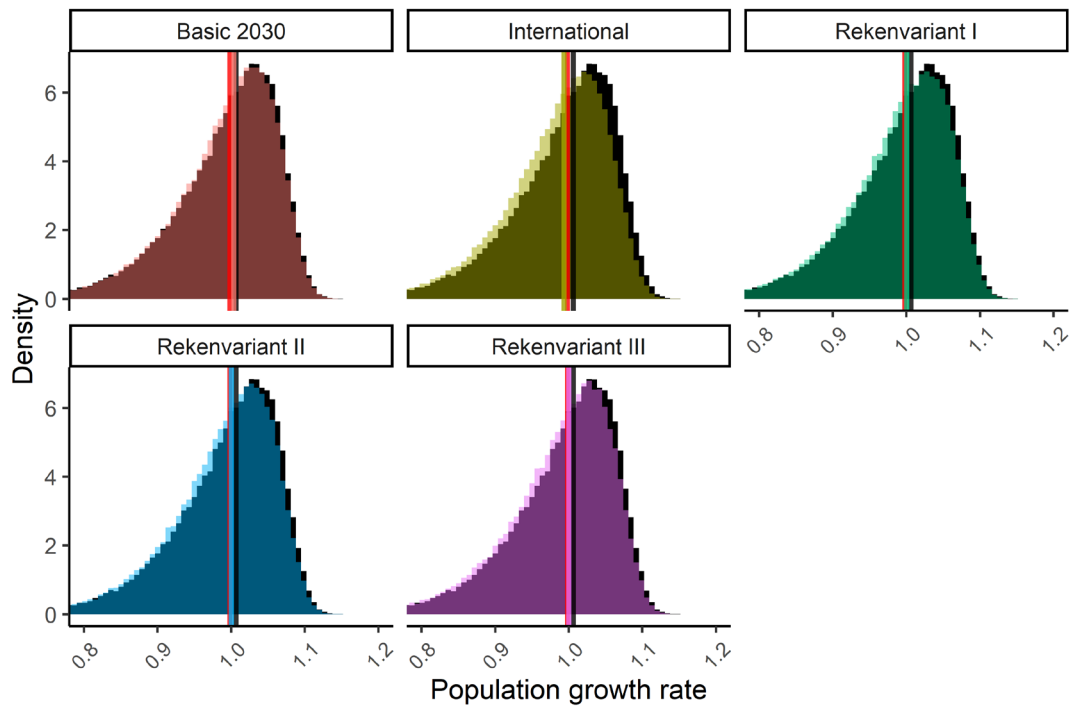
Figure 4-30. *Distributions of population growth rates of the razorbill for the different scenarios. Vertical lines indicate the median population growth rates of the ALI threshold (red), the null scenario (black) and each scenario(colours). The distributions for each scenario (in colours) overlay the distribution of the null scenario (in black).*

4.12 Atlantic puffin (*Fratercula arctica*)

4.12.1 Atlantic puffin habitat loss casualties and mortality
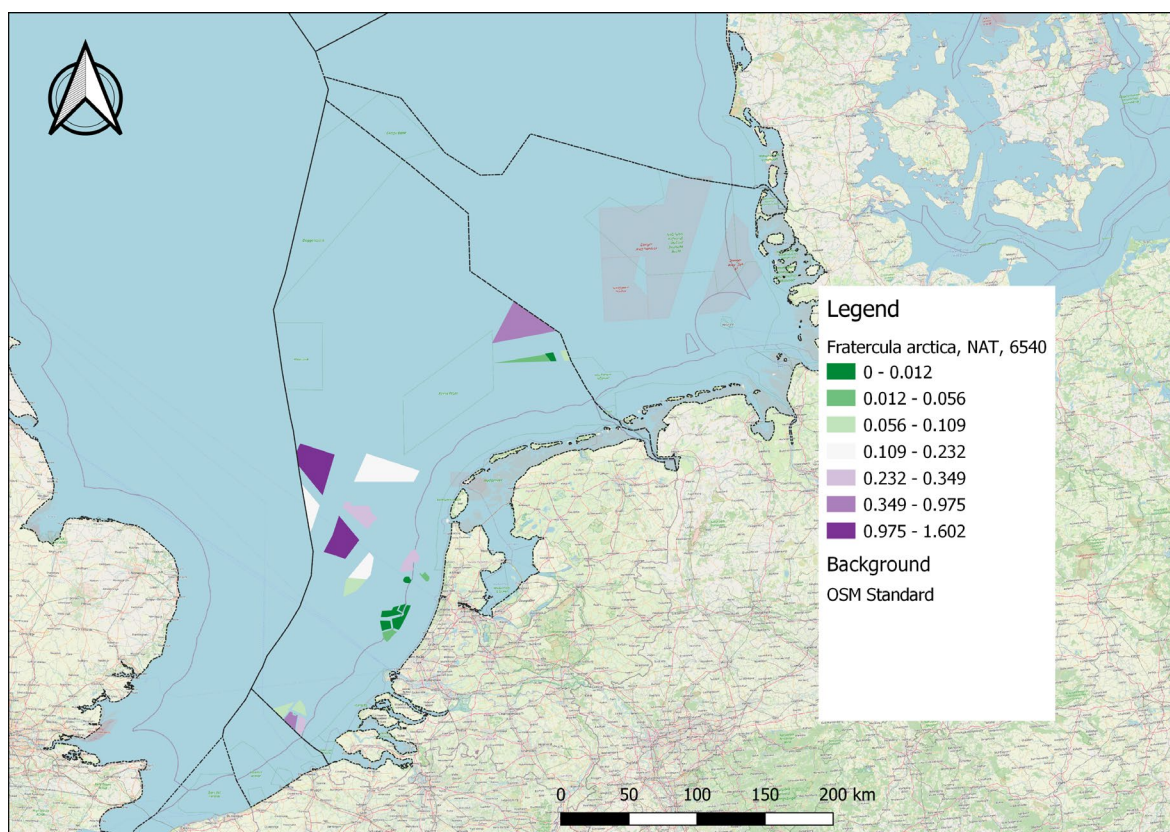
Figure 4-31. *Atlantic puffin (Fratercula arctica, Euring 6540) total annual habitat loss casualties per OWF included in the national scenarios.*
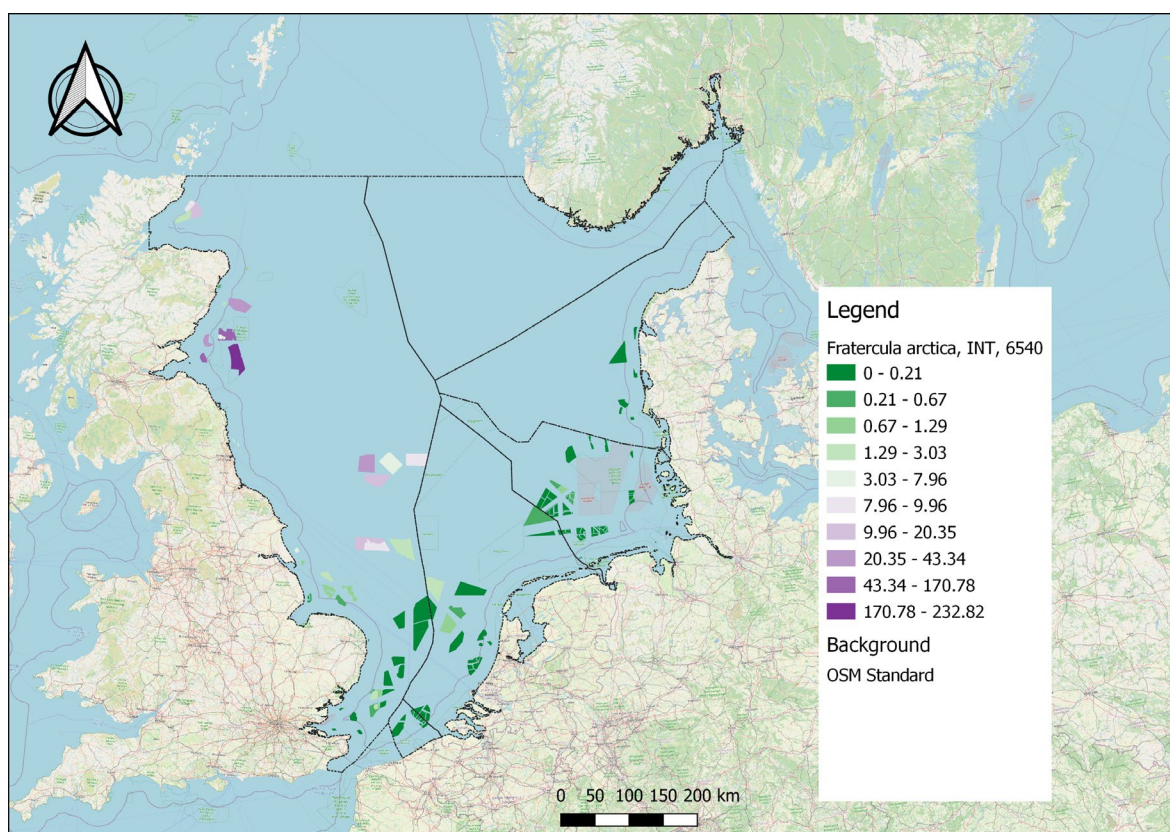
Figure 4-32. *Atlantic puffin (Fratercula arctica, Euring 6540) total annual habitat loss casualties per OWF included in the international scenario.*

For the Atlantic puffin, most Dutch casualties are predicted in the areas further away from the coast (Figure 4-31). The international map predicts few casualties in Dutch OWF areas and most in the OWF areas along the Scottish coast (Figure 4-32). Bird density maps of each bimonthly period and of the annual averages can be found in separate documents (Electronic appendices E3 and E4; respectively E3_DensityMaps_19species_NATINT_period.pdf and E4_DensityMaps_19species_NATINT_yearly.pdf).

The estimated mean number of Atlantic puffin casualties per bimonthly period for the national scenarios varies between 1 and 2 and is highest for the 'Rekenvariant III' scenario (Table 32). Using a maximum estimated abundance of 2,215 individuals this corresponds to an annual mortality between 0.14% - 0.30% (Table 32). For the international scenario there are on average 118 casualties per two month period, on an estimated maximum abundance of 231,775 individuals. This corresponds to an annual mortality of 0.31%. The number of casualties per bimonthly period for the Atlantic puffin are shown for each Dutch OWF area in Annex 4, Table 44.

Table 32. Immature (S03) and adult (S4, S5 and SA) mortality (mort) and survival values for the Atlantic puffin derived from mean numbers of casualties per bimonthly period and max abundance.

Scenario	Mean casualties	Max abundance	Mort	Mort S03	Mort S4	Mort S5	mort SA	Survival S03	Survival S4	Survival S5	Survival SA
null								0.71000	0.78000	0.80000	0.93000
Basic 2030	1	2215	0.00144	0.00144	0.00144	0.00144	0.00144	0.70898	0.77888	0.79885	0.92866
Rekenvariant I	1	2215	0.00217	0.00217	0.00217	0.00217	0.00217	0.70846	0.77831	0.79826	0.92798
Rekenvariant II	1	2215	0.00228	0.00228	0.00228	0.00228	0.00228	0.70838	0.77822	0.79818	0.92788
Rekenvariant III	2	2215	0.00299	0.00299	0.00299	0.00299	0.00299	0.70788	0.77767	0.79761	0.92722
International	118	231,775	0.00305	0.00305	0.00305	0.00305	0.00305	0.70783	0.77762	0.79756	0.92716

4.12.2　Atlantic puffin population level effects

The estimated mortality from habitat loss due to OWFs does not lead to a violation of the ALI set for the Atlantic puffin. Median population growth rates estimated for the national scenarios range between 0.998 and 1.000 (Table 33) and equals 0.998 for the international scenario. The probability that a violation of the population abundance threshold results from an OWF-induced impact ranges between 2.9% - 6.0% for the national scenarios and equals 6.1% for the international scenario (Table 33). Population growth rates estimated for all scenarios are similar to the null scenario (**Figure 4-33**).

Table 33. Population growth rates and ALI statistics for the Atlantic puffin. Median and 5% and 95% quantiles of the population growth rate ('Lambda') distributions are reported. 'P impact' represents the fractions of the Lambda distributions that are below the threshold of a 15% smaller population abundance compared to the median lambda of the null scenario after 3 generations, which occurs for a Lambda of 0.998. 'P causality' is the probability that the violation of the population abundance threshold results from the OWF impact. 'ALI 0.1' shows whether P causality exceeds 0.1, the ALI threshold (see Table 9).

| scenario	Lambda median	Lambda q05	Lambda q95	P impact	P causality	ALI 0.1
Null	1.002	0.892	1.072	0.4735		
Basic 2030	1.000	0.892	1.071	0.4876	0.029	FALSE
Rekenvariant I	0.999	0.890	1.070	0.4971	0.047	FALSE
Rekenvariant II	0.999	0.890	1.070	0.4974	0.048	FALSE
Rekenvariant III	0.998	0.889	1.069	0.5037	0.060	FALSE
International	0.998	0.890	1.069	0.5045	0.061	FALSE
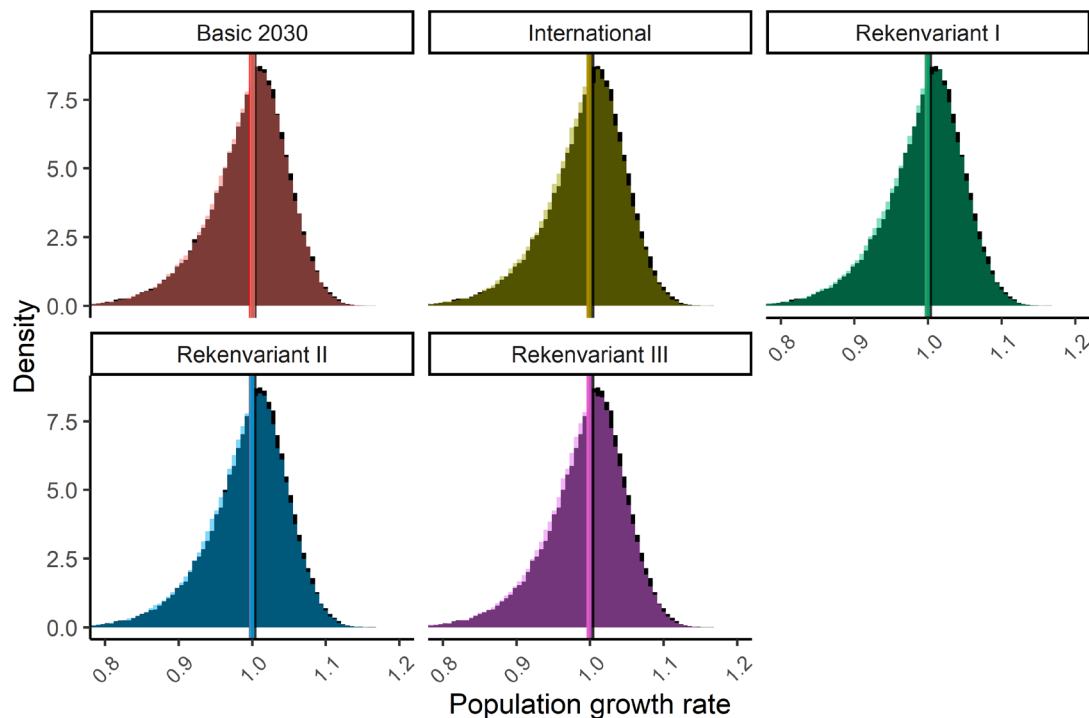
Figure 4-33. *Distributions of population growth rates of the Atlantic puffin for the different scenarios. Vertical lines indicate the median population growth rates of the ALI threshold (red), the null scenario (black) and each scenario(colours). The distributions for each scenario (in colours) overlay the distribution of the null scenario (in black).*

5 Knowledge gaps

In this section knowledge gaps in the KEC assessment framework are discussed. We discuss knowledge gaps in relation to available bird observation data, as well as knowledge gaps related to the statistical and dynamical modelling techniques that have been used in the assessment.

5.1 Bird data

5.1.1 Bird observation data

In the current day and age, seabirds at-sea studies are increasingly performed by private companies, particularly in the realm of offshore wind studies abroad. Much of the collected material is considered confidential, or privately owned, and not forwarded to the ESAS database. There is therefore, presumably, a large body of collected data missing, particularly from the UK and Germany, but possibly also from Denmark and Norway. It is advised that the Dutch government reaches an agreement with other North Sea countries to lift such data bans and make it mandatory for all parties involved to share these data.

Counting seabirds at sea is possibly already hampered by existing offshore wind farms. These alter seabird distribution patterns and make on-site surveys more difficult, unless dedicated OWF surveys are conducted. These, in turn, might go at the expense of surveys in non-OWF areas, making comparisons between wind farm sites and "open sea" more difficult. With more wind farms planned, this problem will only increase. One solution to get access to all parts of the North Sea is to switch to digital aerial surveys, from much greater altitudes (flying well above turbine tip heights). However, this is still costly and being developed, for instance by working on artificial intelligence solutions to deal with the large data-streams generated by such surveys. Future survey designs should probably also be reconsidered, accommodating needs to compare different areas at sea with more power, e.g., coastal versus offshore, Natura 2000, or shipping lanes or OWFs versus other parts.

The ESAS database contains relatively few recent data for waters outside the Dutch Continental Shelf, with even some areas with no data at all. Moreover, many at-sea projects now focus on relative small sections of the North Sea, most notably offshore wind farm sites. Large-scale aerial surveys may fill in this gap (particularly MWTL in The Netherlands), but aerial surveys cannot record bird behaviour, or actual habitat use, at sea. A good overview of how seabirds use the North Sea at large is increasingly difficult to present, while questions like: "would an OWF be better placed here or there?" are asked with ever increasing frequency. It would therefore be good to put seabirds observers on already on-going, North-Sea wide surveys, such as the International Bottom Trawl (IBTS) surveys, conducted by the joint fisheries research institutes around the North Sea. This can be done at relatively low cost, as the ships needed for this work are already sailing. Working from ships has the added advantage that data on e.g., hydrography or prey (fish) abundance can be collected in concert with the seabirds data, in addition to the remote, aerial survey data.

Another set of observational data can be collected from within OWFs (Leopold & Verdaat 2018). Survey data, either from ship or aircraft, shed little light on what birds actually do inside an OWF. Do they just swim, float, or fly through or do they actually seek out OWFs as a foraging or resting habitat? This difference is very important for discussions on presumed habitat loss (further discussed in 5.2.2). On-site data could also be useful in the consideration of the effect of the size of OWFs, the OWFs that are being built today and that will materialize in the near future are an order of magnitude larger than the OWFs in

which most seabird studies have been conducted. Study results from first and second generation, small OWFs are not necessarily representative for new, much larger wind farms at sea. In the "old" OWFs, birds could always see the periphery (the way out) of the wind farm. This is not the case in e.g., Borssele OWF, or in new OWFs in Germany and the UK and the question arises if birds are willing to use the full footprint of such large sites, rather than just the edges. On the other hand, seabirds are adaptable and will probably learn (habituate) to exploit OWFs. It is therefore advisable to perform on-site monitoring studies of seabird behaviour to see how this process of learning will play out, across different species of seabird and marine mammals.

5.1.2   GPS tracking data

One of the largest unknowns in OWF effect assessments is the effect that the presence of OWFs exerts on the behaviour of the birds(Leopold & Verdaat 2018). The level of displacement of birds due to the presence of OWFs is unclear. Very few studies compare local bird densities in OWF areas before construction to the densities after construction. This results in uncertain estimates of the extent of habitat loss due to OWFs (van Kooten *et al*., 2019) as well as the level of macro-avoidance, a parameter that is important for collision risk models (Potiek *et al*., 2021b, van Bemmelen *et al*., 2021). In addition, the habituation of birds to the presence of OWFs is uncertain. It has been suggested that habituation over time may lessen the effects of habitat loss.

Measuring devices, such as GPS trackers, track the whereabouts, flight tracks, including altitudes, and in some cases, behaviour of birds (Gyimesi *et al*., 2017, Potiek & Duijns 2021)*.* One advantage of such research is that the usage of various areas at sea can be linked to particular breeding colonies: some colonies are probably more at risk from OWF development than others. Another advantage is that birds are monitored during the night and during adverse weather: conditions in which visual or digital at-sea surveys are difficult or impossible. Tracking studies are typically conducted at the national level, from breeding sites, but some examples exist of studies of birds caught at sea and subsequently tracked for common scoters (RWS/NIOZ, unpublished) and red-throated divers (Dorsch *et al*., 2019, Heinänen *et al*., 2020). An obvious candidate for such a study would be the great cormorant, as this species has colonized OWFs recently for roosting and feeding. Much could be gained from tracking studies of this species, either conducted from the shore (nearest colonies) or by catching birds in the OWFs. As yet, we do not know if a large part of the population goes to OWFs to feed and rest, or that the birds found in OWFs are specialists. Neither do we know how these birds fare in the OWFs; what they eat here, how they navigate through the air space within an OWF and how they commute between OWFs and between OWFs and the coast. Additionally, it would be useful to study cormorant diets within OWFs, something that can easily be done by collecting regurgitated pellets on site.

Currently, three species of breeding birds are already followed by GPS trackers in OWF-related studies in the Netherlands: lesser black-backed gulls and herring gulls (NIOZ and UvA, INBO and Bureau Waardenburg) and sandwich terns (Bureau Waardenburg and Wageningen Marine Research). From several breeding colonies in the UK, tagging studies are/were performed on: northern gannet, common guillemot, razorbill, kittiwake and shag (Grecian et al. 2018, Carroll et al. 2019, Searle et al. 2019). All these studies were conducted from shore, from breeding colonies. This has the disadvantage that study birds may not go to OWFs at all, as most are specialized on particular feeding modes and feeding habitats. More "bang for the buck" could be achieved by catching birds, e.g., gulls, in OWFs as this would increase the probability of tracking OWF specialists (Rippen *et al*., 2017). Diet studies should always accompany tracking studies, to increase our knowledge on what birds actually do in and around OWFs.

Radar studies can also track bird movements during darkness and poor visibility and have the advantage that bird movement can be tracked in the OWFs themselves, although a drawback of this method is that radar cannot distinguish species, only different sizes of birds . There has been much debate on the possibility to detect actual collisions with radar. Radars cannot detect birds very close to turbine blades. This has led to the development of integrated radar and digital camera systems (Skov, 2019) and of

alternative technical solutions such as heat camera's (Horn *et al*., 2008). Existing systems have been reviewed by Collier (2012), Dirksen (2017), Mollis *et al.* (2019) and Lagerveld *et al.* (2020). It might be useful to implement such monitoring devices in OWFs to monitor bird collisions and possibly also bird behavior in OWFs.

5.2 Methodology

5.2.1 Methods for density map estimation

The current methodology to create the seabird density maps in the assessment framework relies on a GIS-algorithm referred to as Inverse Distance Weighted interpolation with nearest neighbour. It was originally selected (Leopold *et al.*, 2014) for being an exact, deterministic method; the results follow the data where data is available. As a deterministic method, it does not yield results on confidence (nor its counterpart uncertainty). Density maps based on somewhat more advanced statistical methods are probably more suitable for the creation of bird density maps. These statistical methods ideally allow for the correction of spatial correlation in the data and may predict bird densities in areas that are not covered by surveys based on informative covariates such as water depth and distance to coast. In addition, these models can provide measures of confidence, which would allow for the calculation of uncertainty ranges around the estimates. However, also for these methods a higher spatial-temporal coverage of international counting data would be desirable (see 5.1.1). With the current interpolation method, offending peak observations (>10 birds/km^2; see methods section) for seabird species that are moderately attracted or strongly attracted to fishing vessels are spread out over square areas in space. As a result, for some seabird species, square patterns become visible in the map at some places and sometimes at unrealistic parts of the map. It is recommendable to create bird density maps for the next KEC round based on more sophisticated spatial statistical analyses, which allow for a substantiated spatial redistribution of peak observations.

The international and national scenarios are currently based on different density maps. For the national scenarios, density maps are made only based on MWTL data, in the period 2000 - 2020, while for the international scenarios, density maps are made based on ESAS and MWTL data together, in the period 1991-2020. We calculated casualties from habitat loss based on both density maps for all wind farm areas, and it seems that these numbers correspond fairly well (results not shown). It seems somewhat peculiar to calculate the international casualty numbers based on different density maps than the national casualty numbers. The rationale behind this choice was, that the data collection procedure in bird observations has improved substantially in the last twenty years. Where the MWTL database gives sufficient data to exclude these years from the dataset, the data for the international waters (ESAS + MWTL) do not. The national density maps do thus currently give a better, more actual representation of the actual bird densities. It is advisable to create the future KEC calculations based on a single set of (international) maps. It needs to be investigated whether it would be an option to create international density maps based on the more limited period (2000-2020) such as currently already used for the national density maps. Choosing for a single set of international maps per species would also have the side effect that the population sizes are defined at one level. It needs to be discussed whether this is desirable for policy means, perhaps it is more desirable to define effects of wind farm deployment at the "Dutch population level". Although it must be noted, that a "Dutch population" of North Sea seabirds, is nonsense from an ecological perspective, unless a very large proportion of the birds found in the Dutch EEZ breeds in The Netherlands (e.g., lesser black-backed gull, sandwich tern).

For a more mechanistic underpinning of effects of habitat displacement, habitat suitability models could be an informative tool to explore the potential habitat use of seabirds at the North Sea. For example, Mercker *et al.* (2021b, 2021a) have devised a method based on regression techniques and GAM to calculate seabird distributions at the North Sea with human activities (i.e. shipping, fishery and OWF) and a method to wipe-away human activities and arrive at a (hypothetical) distribution without those

influences. Waggitt *et al.* (2020) present seabird distribution maps based on habitat models for the North-East Atlantic. At least ten of the species covered in Waggit *et al.* (2020) are also included in this or the collision study (Potiek *et al.*, 2021b): i.e. puffin, kittiwake, herring gull, lesser black-backed gull, guillemot, cormorant, northern fulmar, great skua, gannet and razorbill. Their approach includes environmental variables and hereby aims to explain bird distributions based on these variables. Also more in-depth knowledge regarding seabird foraging may be useful in identifying essential seabird habitats. Cox *et al.* (2018) attempt to link bio-physical processes and marine mammal and seabird foraging. Such studies can be used to inform habitat suitability models on what physical processes and/or ecological aspects should be included in the preparation of e.g. seabird distribution maps.

5.2.2 Habitat displacement casualties

The calculation of the number of casualties from habitat displacement currently occurs through multiplication of bird density at OWF sites with a species-specific RDRS (relative displacement risk score) value. The RDRS was pioneered by Garthe & Hüppop (2004), refined for seabirds in the UK by Bradbury *et al.* (2014) and adapted to the international North Sea for the second KEC assessment by Leopold *et al.* (2014). Since its first publication in 2014, the factors from Bradbury *et al.* (2014) and those used in KEC3 may have become outdated. For instance, Peschko *et al.* (2020, 2021) conducted detailed studies of changes in behaviour and use of an area with OWF including seasonal differences for guillemot, kittiwake and northern gannet. Moreover, the RDRS scores were calculated based on IUCN population status and estimates of adult survival (Leopold *et al.*, 2014), which are also incorporated in the ALI thresholds (Table 9; Potiek *et al.*, 2021a). As such, these factors, that are meant to represent the conservation status of the species (Bradbury et al. 2014), are doubly represented in the calculations. It would be recommendable to replace the mortality calculation based on RDRS values by a method that includes the avoidance rates used in the collision rate assessments, such that it connects the two methods for the species that are both under investigation for the effects of habitat loss and collision mortality (northern gannet and sandwich tern). Perhaps, it would be feasible to replace the current method by a mortality rate based on expert elicitation. However, a more mechanistic underpinning of the habitat displacement casualties estimation would be advisable. Simple IBMs or a quantitative estimate of the loss in habitat quality and food quantity based on bird density maps or habitat suitability maps could be a way forward to make estimates of displacement casualties based more on ecological processes (see for example section 5.2.4). In order to estimate the severity of habitat loss from offshore wind farms, it is pertinent to determine the dependency of seabirds on availability of food resources (Cury *et al.*, 2011). Regardless, a transparent method should be chosen that allows for a better integration between the habitat displacement and collision mortality methods.

5.2.3 Population models

The matrix population models used in this assessment are density-independent population models, which means that the population growth rate as calculated by these models does not depend on the size of the population. This contrasts with the idea that density-dependent processes are important in determining the dynamics of real-world populations, including seabird populations (Horswill & Robinson 2015, Horswill *et al.*, 2017). Density-dependence can occur in two forms: compensatory and depensatory. In the first case, density dependence acts to compensate for additional losses of individuals (mortality) or reductions in productivity. A compensatory response might occur in a different demographic parameter than the one that induced the response. For example, an increased loss of breeding pairs might increase the recruitment rate of individuals from the non-breeding part of the population. In the case of depensatory density dependence, the effect on a demographic parameter is aggravated, instead of compensated. For example, the loss of individuals from a breeding colony might increase vulnerability to nest predation for the remaining individuals and thus decrease breeding success.

Density dependence can act in multiple, interconnected ways to regulate population size and the form and strength of density dependence are often poorly understood and highly context-dependent (Horswill

& Robinson 2015, Horswill *et al*., 2017). Therefore, incorporating density dependence in population models requires detailed understanding on how it operates and there is no recipe for modelling density dependence that fits all species, all colonies, at all times. As a consequence, most impact assessments, like the current one, use density-independent population models. Another argument for the use of density-independent population models is based on the precautionary principle: without density dependence there are no compensatory effects on mortality or reproduction and the observed changes in population growth rates can be regarded as a worst-case scenario. However, this latter argument is only valid in case of compensatory density dependence. If density dependence acts in a depensatory way, the impact on a population can potentially be underestimated. The relevant question for impact assessment is therefore: which species and/or demographic parameters are potentially regulated by depensatory density dependence?

A review on demographic rates and density-dependence in seabirds by Horswill & Robinson (2015) reports 14 empirical examples of depensatory density dependence, all related to productivity rates. In the majority of examples, depensation was related to anti-predator vigilance or colonial defence that increased rates of productivity (Horswill & Robinson 2015). On the other hand, there were also 12 studies that did not find a relationship between productivity and colony size. For the species considered in the current assessment, depensatory density dependence in productivity rates was found for the sandwich tern (Veen, 1977), the common guillemot (Birkhead, 1977, Harris & Wanless, 1988) and the Atlantic puffin (Harris, 1980). For the latter two species, also compensatory density dependence was found in survival, age of recruitment, emigration or immigration, and recruitment from the non-breeding population (guillemot only). For the sandwich tern, no indications of compensatory density dependence were reported by Horswill & Robinson (2015).

Density dependent processes are important drives of the dynamics of seabird populations, but incorporating them into population models requires a thorough understanding of the dynamics of specific colonies (Horswill & Robinson 2015) . Because depensatory density dependence can act destabilizing, it is advisable to explore its potential to increase the estimated OWF impacts. Such an exploration should prioritize high-risk species, which are those with a large number of estimated casualties (northern gannet) and those for which depensatory density dependence has been described earlier (sandwich tern, common guillemot and Atlantic puffin).

5.2.4 Individual based model of the northern gannet

Compared to the original version of the IBM (van Kooten *et al*., 2019), the movement model of birds was updated to allow for greater travel distances during a single time step. We studied the effect of this by looking at the spatial distribution of birds across the grid during a single simulation with maximum travel length of up to 8 grid cells per time step (Table 34). There is relatively little change in the spatial distribution of birds during a simulation. Birds that are in proximity of good habitat areas concentrate at these sites. Birds in poor habitat quality areas that have no clue in which direction habitat quality improves and do not move, get stuck in their location and eventually die. Although modelled birds can travel larger distances compared to the original version by van Kooten *et al.* (2019), they probably can only profit from this if there is a habitat quality gradient that guides them to good quality patches. Thus, the current movement model of the IBM is inconsistent with long-lived migratory seabirds that can travel large distances to find areas with good foraging opportunities. A more realistic representation of the foraging range and movement patterns of seabirds is especially important given the current and future scale of developments in the North Sea. The IBM should therefore be improved by incorporating more realistic flight patterns and, potentially, allow for a bird's memory of good foraging locations. Ideally, decisions on where to forage and for how long should be based on first principles (*e.g.* fitness optimization, or risk aversion) and the resulting flight patterns should be compared with data derived from GPS-tracked animals.

6   Discussion

The estimated effects of habitat loss do not lead to changes of the population dynamics to such an extent that any of the ALIs was exceeded. The exceedance of the ALI for the northern gannet was due to the high estimates of collision casualties. The northern gannet is considered sensitive to displacement from OWF areas as well as to collisions. The methodology used for the estimation of the collision mortality for the northern gannet is currently being reconsidered in an additional study to exclude uncertainties in the outcomes of the assessment. For a further discussion of the collision mortality of the northern gannet, see Potiek *et al.* (2021b). From displacement by OWFs alone, common guillemot and razorbill are the species that suffer most from habitat loss and supposedly have the highest mortality probabilities from habitat loss. The common guillemot and the razorbill were estimated to be most sensitive to the tested wind energy scenarios. For diver sp., while the estimated numbers of casualties are low, the estimated mortality probabilities are similar to the estimates for the common guillemot. Divers are notoriously hard to count at sea due to their shyness, and the density distribution and the total density estimates are therefore both expected to be quite uncertain for this species. For all other species, the estimated mortality rates are about a factor two lower, and these therefore seem to be much less sensitive to the tested scenarios.

The models used to estimate the population-level effects of displacement by OWFs contain a high level of uncertainty. Where the uncertainty in the life history parameters of the population levels is translated in uncertainty ranges around the estimated population growth rates, uncertainties in the density maps and the casualty calculations are not. Yet, also the estimated densities of the birds in the OWF areas, the total population densities of the birds and the RDRS scores of the birds are all highly uncertain and it can be expected that these affect the estimated mortality probabilities quite a lot. It would therefore be recommendable to develop a method in which the uncertainty in the predictions could be indicated per species. Perhaps a quantification of the uncertainty proves impossible, but at least a method that gives a categorical indication of the level of uncertainty per species should be developed. Such an uncertainty index should be based on the quality of the data used for the bird density maps, the certainty of the displacement mortality rate, as well as the quality of the population model parameters. In addition, it would be recommendable to execute a sensitivity analysis of all input to the final population calculations in order to investigate which of the factors have the strongest effect on the final estimates.

The matrix population models used in the current assessment are a well-established framework for modelling population dynamics and are used frequently for conservation issues (Heppell et al. 2000, Caswell 2001). In addition, the population models used are inherently stochastic, because they account for natural variation in demographic parameters (survival, breeding success, age at first reproduction) and use the resulting distributions of population growth rates to calculate the probabilities that the OWF impacts lead to violation of the population abundance thresholds. The uncertainty in the demographic parameters is accounted for through a Monte-Carlo approach, in which all parameters were sampled from their statistical distributions. For some species there are few data on immature / juvenile survival, age at first breeding or incidence of breeding (proportion of floater individuals). Parameter values of these variables are therefore poorly substantiated. It should be stressed that continued monitoring and efforts to collect these basic life history parameters are imperative for making accurate population assessments and, in addition, provide an indispensable way for monitoring the health of natural populations, especially with the advent of rapid environmental changes induced by climate change.

The Individual-Based Model (IBM), which we used as a second method to estimate mortality from habitat loss for the northern gannet, was originally developed by van Kooten *et al.* (2019). They estimated mortality effects of habitat loss for several species of seabirds, including the northern gannet. For this

latter species, van Kooten *et al.* (2019) showed that the mortality as estimated by the IBM exceeded the mortality calculation based on bird densities in OWF areas. This was also the case in the current assessment. For our 'international' scenario, the IBM estimated an annual OWF-induced mortality probability of 0.0107 (Table 20; for a maximum travel length of 1 grid cell per time step and avoidance of 1.0), while the method based on the overlap between OWF areas and the bird distributions estimated an annual OWF-induced mortality probability of 0.00154 (Table 19). The IBM simulations by van Kooten *et al.* (2019) resulted in an even higher OWF-induced mortality estimate of 0.001572. For Dutch OWFs only, the median annual mortality from habitat loss estimated by van Kooten *et al.* (2019) was equal to 0.0. The corresponding estimate in the current assessment equals 0.00284 (Table 34).

It should be noted, that our results are not directly comparable with van Kooten *et al.* (2019) because several aspects of the IBM were changed. We chose to use habitat maps that are derived from bird density maps such that the estimates of the IBM would be comparable to the other method used to calculate habitat loss effects. Van Kooten *et al.* (2019), on the other hand, used habitat maps based on habitat suitability models that include abiotic factors such as depth, sediment type, distance to colony and slope and aspect of the sea floor. Inclusion of multiple abiotic factors into a habitat suitability model can potentially lead to a more homogeneous food landscape, but how this impacts the estimated OWF-induced mortality depends on whether the homogenization leads to an in- or decrease of total habitat quality situated within offshore wind farms. Second, different bird observation data underly the habitat maps, as the databases of bird abundances (ESAS + MWTL) have been updated since the study by van Kooten *et al.* (2019). Third, the OWFs that are included in the current study are different from those used by van Kooten *et al.* (2019), as the development zones 258, 263o, 270, 272 and 274 are only included in the current assessment. Fourth, van Kooten *et al.* (2019) used a grid cell size of 0.01 degree in each direction, which corresponds to approximately 1.1 km in north-south direction and 0.6 km in east-west direction. This is substantially smaller than the grid cell size used here (5km x 5km). This implies that even with a maximum travel length of 1 grid cell per time step, the movement of birds in the IBM of van Kooten *et al.* (2019) is more local than in the current version.

Insights into the robustness of a model can be obtained by performing a sensitivity analysis. Overall, IBMs are parameter rich and computationally intensive. Performing a sensitivity analysis for an individual-based model is therefore generally time-consuming. For the northern gannet IBM used here, and developed by van Kooten *et al.* (2019), a systematic sensitivity analysis is lacking and we do not have a good understanding of the model's robustness. However, we did consider the response of the IBM to changes in the maximum travel length parameter in the current study (Annex 2; **Figure 2.**). We found that the response of the OWF-related bimonthly survival to maximum travel length varies between bimonthly periods. While survival decreases at high maximum travel length in one period, survival first decreases and then increases with increasing maximum travel length in other periods (Annex 2; **Figure 2.**). We were unable to reconcile the different responses of the maximum travel length between bimonthly periods without understanding the cause of the high mortality at high maximum travel length. Without a thorough understanding of why the observed results are obtained, we cannot be completely confident that these results are a reliable indicator of the mortality that is caused by OWF-induced habitat loss. We therefore conclude that the IBM requires further scrutiny, analysis, and refinement before it can be used as a reliable tool for impact assessment.

The international offshore wind farm scenario used in this report is based on the list of OWF areas provided by RWS in march 2021. International planning of wind farm search areas develops rapidly and have probably changed since then. There are several indications that the rate of deployment of international OWFs will be considerably faster than the international scenario anticipates. As a consequence, the casualties estimated for the international scenario may be on the low side. For example, while the Norwegian farms were excluded from our study, Norway has a development zone 'Sørlige Nordsjø II' that is located within the KEC-study area. Norwegian authorities appear to be working towards licensing for this area in Q1 2022 (offshorewind.biz 2021a). It thus seems plausible that around 2030 turbines are operational at this location. In addition, the current international scenario is somewhat conservative for the UK as well, it contains ~34 GW for the UK by 2030 and ~37 GW by 2031. It is more

likely that the UK will deploy 40 GW by 2030 (Reuters, 2021), although some of the 40 GW target could be sited outside the study area (e.g. UK Atlantic south coast, Irish Sea). Moreover, the Danish parliament has recently passed legislation to allow additional offshore wind energy deployment. The additional wind energy island is expected to be in place by 2030 and to be servicing 3 GW power of a total of the 10 GW by that time (offshorewind.biz, 2021b).

The current study is based on the current technological practice regarding the layout of offshore wind farms. Future wind farms may be set up completely differently, depending on the (fast) technological developments in this area. During the consecutive KEC assessments rounds, the turbine size, in MW per turbine, has already increased substantially. Taller wind turbines with longer blades can produce more power. It is expected that the turbine size will increase further over the coming years (Calma, 2022). As a consequence, the spacing of wind turbines will likely be different, large turbines may need to be placed further apart for optimal performance. It is so far unknown how such changes in wind turbine characteristics may affect the collision risks and extent of habitat loss for seabirds.

How different future wind farms may look, is nicely illustrated by the scientific tests that are conducted with vertical axis wind turbines (Hansen *et al.*, 2021). These turbines are thought to have a greater efficiency, but also a smaller footprint and a lower height. The space in between the rows of such turbines would become much smaller, making it harder for birds to pass through the wind farms. Therefore, wind farms made up of such turbines could be differently perceived by seabirds and avoidance rates of these farms could be totally different. Other possible future designs include the Touchwind Mono (Touchwind BV, 2021), which tilts the rotor moving towards horizontal with increasing windspeeds. Since these designs are very different from the current designs it is likely that, if they were to be deployed, the risks of habitat loss and collisions would differ from the current OWFs. Moreover, wind turbines may be altered to decrease bird collision risks (Miao *et al.*, 2019; offshorewind.biz, 2021b). This could potentially increase avoidance of wind farm areas by birds that already tend to avoid areas with wind turbines. It is unclear if and when such changes might be implemented in new offshore wind farms.

Sovacool (2009) attempts to provide a context to bird fatalities from wind energy, by providing similar estimates for nuclear power and fossil fuels, at 0.3, 0.4 and 5.2 fatalities/GWh respectively. The largest component in the estimate for fossil fuel power plants is attributed to rapidly accelerating climate change. For comparison, other sources of land-bird fatalities are also listed. These include building windows; domestic and feral cats; poisoning from pesticides and collision with communication towers (each caused annually more casualties than could be attributed to wind energy, nuclear power or fossil fuel energy production). For seabirds, a similar study could be done, and should include mortality due to rats, domestic cats, mink, fisheries bycatch and oil spills at sea.

Global climate change is expected to strongly affect species distributions in marine ecosystems. It is highly uncertain how global climate change will impact the presence of seabirds in the North Sea in the coming years (Burthe *et al.*, 2014). While seabird distributions may shift, they may also suffer due to change in abundance of their prey species (Piatt *et al.*, 2020). Recent marine heat waves have been linked to extreme mortality events of *Uria aalge* in the North Pacific (Piatt *et al.,* 2020) and may have already become the "new normal" (Tanaka & van Houtan 2022). As such, seabird distributions, but also life history parameters, may change drastically under the influence of climate change. It is thus highly unpredictable how seabird population dynamics and distributions at the North Sea will develop in the near future. The current estimates of the effects of offshore wind farms on seabirds are based on the assumption that the seabird distributions and life history parameters will remain as they are. The estimates in this study give the best estimate possible based on the species distribution data and assessment framework available to us at the current moment, and are based on the assumption that seabird distributions will not drastically change in the next 30 years.

7 Quality Assurance

Wageningen Marine Research utilises an ISO 9001:2015 certified quality management system. The organisation has been certified since 27 February 2001. The certification was issued by DNV.

References

Ashcroft, R. E. 1979. Survival rates and breeding biology of puffins on Skomer island, Wales. Ornis Scandinavica 10:100.

Baptist, H. J. M., and P. A. Wolf. 1993. Atlas van de vogels van het Nederlands Continentaal Plat. Ministerie van Verkeer en Waterstaat, Directoraat-Generaal Rijkswaterstaat, Dienst Getijdewateren, 's-Gravenhage.

Beijersbergen, R. B. A. 2001. Grote sterns op de Hooge platen. De Levende Natuur 102:98–99.

van Bemmelen, R. S. A., F. H. Soudijn, D. Benden, A. Potiek, C. Chen, N. T. Hintzen, T. Wilkes, T. Van Kooten, and A. Gyimesi. 2021. Individual-based model lesser black- backed gulls in the Netherlands. Report number 21-168, Bureau Waardenburg, Culemborg.

Birkhead, T. R. 1977. The effect of habitat and density on breeding success in the common guillemot (*Uria aalge*). The Journal of Animal Ecology 46:751.

Booth, C. J. 1999. Breeding success of red-throated divers on Orkney mainland, 1973-1998. Scottish Birds 20:94–97.

Bradbury, G., M. Trinder, B. Furness, A. N. Banks, R. W. G. Caldow, and D. Hume. 2014. Mapping seabird sensitivity to offshore wind farms. PLoS ONE 9:e106366.

Breton, A. R., A. W. Diamond, and S. W. Kress. 2006. Encounter, survival, and movement probabilities from an Atlantic Puffin (*Fratercula arctica*) metapopulation. Ecological Monographs 76:133–149.

Buckland, S. T., and B. J. Turnock. 1992. A robust line transect method. Biometrics 48:901–909.

Burthe, S., S. Wanless, M. Newell, A. Butler, and F. Daunt. 2014. Assessing the vulnerability of the marine bird community in the western North Sea to climate change and other anthropogenic impacts. Marine Ecology Progress Series 507:277–295.

Calma, J. 2022, February 3. Offshore wind projects are outpacing the ships that build them. https://www.theverge.com/2022/2/3/22916065/offshore-wind-energy-demand-installation-vessels-supply.

Camphuysen, C. J., A. D. Fox, M. F. Leopold, and I. Krag Petersen. 2004. Towards standardised seabirds at sea census techniques in connection with environmental impact assessments for offshore wind farms in the U.K. Environmental Research Institute. COWRIE – BAM- 02-2002.

Carroll, M. J., E. D. Wakefield, E. S. Scragg, E. Owen, S. Pinder, M. Bolton, J. J. Waggitt, and P. G. H. Evans. 2019. Matches and mismatches between seabird distributions estimated from at-sea surveys and concurrent individual-level tracking. Frontiers in Ecology and Evolution 7.

Caswell, H. 2001. Matrix population models: Construction analysis and interpretation. 2nd edition. Sinauer Associates, Sunderland.

Collier, M. P., S. Dirksen, and K. L. Krijgsveld. 2012. A review of methods to monitor collisions or micro-avoidance of birds with offshore wind turbines - Part 2: Feasibility study of systems to monitor collisions. Strategic Ornithological Support Services Project SOSS-03A:30.

Cox, S. L., C. B. Embling, P. J. Hosegood, S. C. Votier, and S. N. Ingram. 2018. Oceanographic drivers of marine mammal and seabird habitat-use across shelf-seas: A guide to key features and recommendations for future research and conservation management. Estuarine, Coastal and Shelf Science 212:294–310.

Crouse, D. T., L. B. Crowder, and H. Caswell. 1987. A stage-based population model for loggerhead sea turtles and implications for conservation. Ecology 68:1412–1423.

Cury, P., I. L. Boyd, S. Bonhommeau, T. Anker-Nilssen, R. J. Crawford, R. W. Furness, J. A. Mills, E. J. Murphy, H. Osterblom, M. Paleczny, J. F. Piatt, J.-P. Roux, L. Shannon, and W. J. Sydeman. 2011. Global seabird response to forage fish depletion – One-third for the birds. Science 334:1703–1706.

Deakin, Z., K. Hamer, R. Sherley, S. Bearhop, T. Bodey, B. Clark, W. Grecian, M. Gummery, J. Lane, G. Morgan, L. Morgan, R. Phillips, E. Wakefield, and S. Votier. 2019. Sex differences in migration

and demography of a wide-ranging seabird, the northern gannet. Marine Ecology Progress Series 622:191–201.

Derks, P., and K. De Kraker. 2005. De ontwikkeling van de kolonie grote sterns in het Grevelingenmeer in vergelijking met de rest van Nederland, België en aangrenzend Noord-Frankrijk. Nieuwsbrief Nederlandse Zeevogelgroep 6:2–4.

Dierschke, V., R. W. Furness, and S. Garthe. 2016. Seabirds and offshore wind farms in European waters: Avoidance and attraction. Biological Conservation 202:59–68.

Dirksen, S. 2017. Review of methods and techniques for field validation of collision rates and avoidance amongst birds and bats at offshore wind turbines. Sjoerd Dirksen Ecology report number SjDE 17-01:47.

Dorsch, M., C. Burger, A. Schubert, G. Nehls, B. Kleinschmidt, P. Quillfeldt, S. Heinänen, R. Žydelis, and J. Morkūnas. 2019. DIVER – German tracking study of seabirds in areas of planned Offshore Wind Farms at the example of divers. Pages 1–285 FKZ 0325747A/B.

Drewitt, A. L., and R. H. W. Langston. 2006. Assessing the impacts of wind farms on birds: Impacts of wind farms on birds. Ibis 148:29–42.

Eklöf, K., and P. Koskimies. 2018. Kaakkurien kanssa 42 vuotta – Miten kaakkurit liikkuvat ja kuinka pesinnät onnistuvat? Linnut-vuosikirja 2017:118-121.

Eriksson, M. O. G. 2012. Projekt Lom 2011. Vår Fågelvärld Supplement 52:45–55.

Fayet, A. L., R. Freeman, T. Anker-Nilssen, A. Diamond, K. E. Erikstad, D. Fifield, M. G. Fitzsimmons, E. S. Hansen, M. P. Harris, M. Jessopp, A.-L. Kouwenberg, S. Kress, S. Mowat, C. M. Perrins, A. Petersen, I. K. Petersen, T. K. Reiertsen, G. J. Robertson, P. Shannon, I. A. Sigurðsson, A. Shoji, S. Wanless, and T. Guilford. 2017. Ocean-wide Drivers of Migration Strategies and Their Influence on Population Breeding Performance in a Declining Seabird. Current Biology 27:3871-3878.e3.

Fijn, R. C., R. S. A. van Bemmelen, J. W. de Jong, F. A. Arts, D. Beuker, E. L. Bravo Rebolledo, B. W. R. Engels, M. Hoekstein, R.-J. Jonkvorst, S. Lilipaly, M. Sluijter, K. D. Van Straalen, and P. A. Wolf. 2019. Verspreiding en abundantie van zeevogels en zeezoogdieren op het Nederlands Continentaal Plat in 2018-2019. RWS-Centrale Informatievoorziening BM 19.23. Bureau Waardenburg Rapportnr. 19-258. Bureau Waardenburg & Deltamilieu Projecten, Culemborg.

Fijn, R. C., R. S. A. van Bemmelen, J. W. de Jong, F. A. Arts, D. Beuker, E. L. Bravo Rebolledo, B. W. R. Engels, M. Hoekstein, R.-J. Jonkvorst, S. Lilipaly, M. Sluijter, K. D. Van Straalen, and P. A. Wolf. 2020. Verspreiding en abundantie van zeevogels en zeezoogdieren op het Nederlands Continentaal Plat in 2019-2020. RWS-Centrale Informatievoorziening BM 20.22. Bureau Waardenburg Rapportnr. 20-324. Bureau Waardenburg & Deltamilieu Projecten, Culemborg.

Garthe, S., and O. Hüppop. 2004. Scaling possible adverse effects of marine wind farms on seabirds: Developing and applying a vulnerability index. Journal of Applied Ecology 41:724–734.

Gomersall, C. H. 1986. Breeding performance of the red-throated diver *Gavia stellata* in Shetland. Ecography 9:277–284.

Grecian, W. J., J. V. Lane, T. Michelot, H. M. Wade, and K. C. Hamer. 2018. Understanding the ontogeny of foraging behaviour: insights from combining marine predator bio-logging with satellite-derived oceanography in hidden Markov models. Journal of The Royal Society Interface 15:20180084.

Grosbois, V., and P. M. Thompson. 2005. North Atlantic climate variation influences survival in adult fulmars. Oikos 109:273–290.

Gyimesi, A., T. J. Evans, J. F. Linnebjerg, J. W. De, J. M. P. Collier, and R. C. Fijn. 2017. Review and analysis of tracking data to delineate flight characteristics and migration routes of birds over the Southern North Sea. Bureau Waardenburg BV, rapport nr. 16-139.

Hansen, J. T., M. Mahak, and I. Tzanakis. 2021. Numerical modelling and optimization of vertical axis wind turbine pairs: A scale up approach. Renewable Energy 171:1371–1381.

Harris, M. P. 1980. Breeding performance of puffins *Fratercula arctica* in relation to nest density, laying date and year. Ibis 122:193–209.

Harris, M. P., T. Anker-Nilssen, R. H. McCleery, K. E. Erikstad, D. N. Shaw, and V. Grosbois. 2005. Effect of wintering area and climate on the survival of adult Atlantic puffins Fratercula arctica in the eastern Atlantic. Mar Ecol Prog Ser 297:283–296.

Harris, M. P., F. Daunt, M. I. Bogdanova, J. J. Lahoz-Monfort, M. A. Newell, R. A. Phillips, and S. Wanless. 2013. Inter-year differences in survival of Atlantic puffins *Fratercula arctica* are not associated with winter distribution. Marine Biology 160:2877–2889.

Harris, M. P., M. Frederiksen, and S. Wanless. 2007. Within- and between-year variation in the juvenile survival of Common Guillemots *Uria aalge*. Ibis 149:472–481.

Harris, M. P., M. Heubeck, M. I. Bogdanova, M. A. Newell, S. Wanless, and F. Daunt. 2020. The importance of observer effort on the accuracy of breeding success estimates in the Common Guillemot *Uria aalge*. Bird Study 67:93–103.

Harris, M. P., and S. Wanless. 1989. The breeding biology of Razorbills *Alca torda* on the Isle of May. Bird Study 36:105–114.

Harris, M. P., and S. Wanless. 2011. The Puffin. T. & A.D. Poyser, London.

Harris, M., and S. Wanless. 1988. The breeding biology of Guillemots *Uria aalge* on the Isle of May over a six year period. Ibis 130:172–192.

Heinänen, S., R. Žydelis, B. Kleinschmidt, M. Dorsch, C. Burger, J. Morkūnas, P. Quillfeldt, and G. Nehls. 2020. Satellite telemetry and digital aerial surveys show strong displacement of red-throated divers (*Gavia stellata*) from offshore wind farms. Marine Environmental Research 160.

Hemmingsson, E., and M. O. G. Eriksson. 2002. Ringing of red-throated diver *Gavia stellata* and black-throated diver *Gavia arctica* in Sweden. Newsletter Diver/Loon Specialist Group, Wetlands International 4:8–13.

Heppell, S. S., D. T. Crouse, and L. B. Crowder. 2000. Using matrix models to focus research and management efforts in conservation. Pages 148–168 Quantitative Methods for Conservation Biology. Springer-Verlag, New York.

Hin, V. 2021. KEC4popmodels: Matrix population models to assess mortality effects of Offshore Wind Parks on seabird Populations. Rpackage, Wageningen Marine Research.

Horn, J. W., E. B. Arnett, and T. H. Kunz. 2008. Behavioral responses of bats to operating wind turbines. Journal of Wildlife Management 72:123–132.

Horswill, C., S. H. O'Brien, and R. A. Robinson. 2017. Density dependence and marine bird populations: are wind farm assessments precautionary? Journal of Applied Ecology 54:1406–1414.

Horswill, C., and R. A. Robinson. 2015. Review of seabird demographic rates and density dependence. JNCC Report No. 552, Peterborough.

Jenouvrier, S., C. Barbraud, and H. Weimerskirch. 2003. Effects of climate variability on the temporal population dynamics of southern fulmars: *Climate variability and fulmar population dynamics*. Journal of Animal Ecology 72:576–587.

van der Jeugd, H., B. J. Ens, M. Versluijs, and H. Schekkerman. 2014. Geïntegreerde monitoring van vogels van de Nederlandse waddenzee. Sovon Vogelonderzoek Nederland, Nijmegen.

Kahle, D., and H. Wickham. 2013. ggmap: Spatial Visualization with ggplot2. The R Journal 5:144–161.

Koffijberg, K., J. S. M. Cremer, P. De Boer, J. Nienhuis, H. Schekkerman, and J. Postma. 2017. Broedsucces van kustbroedvogels in de Waddenzee. Resultaten 2015-2016 en trends in broedsucces in 2005-2016. Wageningen / Nijmegen.

van Kooten, T., F. Soudijn, I. Tulp, C. Chen, D. Benden, and M. Leopold. 2019. The consequences of seabird habitat loss from offshore wind turbines, version 2 : Displacement and population level effects in 5 selected species. Wageningen Marine Research, IJmuiden.

Lagerveld, S., C. A. Noort, L. Meesters, L. Bach, P. Bach, and S. Geelhoed. 2020. Assessing fatality risk of bats at offshore wind turbines. Wageningen Marine Research report C025/20.

Lane, J. V., R. Jeavons, Z. Deakin, R. B. Sherley, C. J. Pollock, R. J. Wanless, and K. C. Hamer. 2020. Vulnerability of northern gannets to offshore wind farms; seasonal and sex-specific collision risk and demographic consequences. Marine Environmental Research 162:105196.

Lavers, J. L., I. L. Jones, A. W. Diamond, and G. J. Robertson. 2008. Annual survival of North American Razorbills (Alca torda) varies with ocean climate indices. Canadian Journal of Zoology 86:51–61.

Leopold, M. F., M. Boonman, M. P. Collier, N. Davaasuren, R. C. Fijn, A. Gyimesi, J. de Jong, R. H. Jongbloed, B. Jonge Poerink, J. C. Kleyheeg-Hartman, K. L. Krijgsveld, S. Lagerveld, R. Lensink, M. J. M. Poot, van der W. J.T, and M. Scholl. 2014. A first approach to deal with cumulative

effects on birds and bats of offshore wind farms and other human activities in the Southern North Sea. IMARES Report C166/14, IMARES.

Leopold, M. F., and H. J. P. Verdaat. 2018. Pilot field study: observations from a fixed platform on occurrence and behaviour of common guillemots and other seabirds in offshore wind farm Luchterduinen. Wageningen Marine Research report C068/18, Wageningen Marine Research, IJmuiden.

Lewis, S., D. A. Elston, F. Daunt, B. Cheney, and P. M. Thompson. 2009. Effects of extrinsic and intrinsic factors on breeding success in a long lived seabird. Oikos 118:521–528.

Lloyd, C. 1974. Movement and survival of British razorbills. Bird Study 21:102–116.

Lloyd, C. S., and C. M. Perrins. 1977. Survival and age at first breeding in the Razorbill (*Alca torda*). Bird-banding 48:239–252.

Lowther, P. E., A. W. Diamond, S. W. Kress, G. J. Robertson, K. Russell, D. N. Nettleship, G. M. Kirwan, D. Christie, C. Sharpe, E. Garcia, and P. F. D. Boesman. 2020. Atlantic Puffin (*Fratercula arctica*). *in* S. M. Billerman, B. K. Keeney, P. G. Rodewald, and T. S. Schulenberg, editors. Birds of the World. Cornell Lab of Ornithology.

Masden, E. A., D. T. Haydon, A. D. Fox, and R. W. Furness. 2010. Barriers to movement: Modelling energetic costs of avoiding marine wind farms amongst breeding seabirds. Marine Pollution Bulletin 60:1085–1091.

Mavor, R. A., M. Heubeck, S. Schmitt, and M. Parsons. 2008. Seabird numbers and breeding success in Britain and Ireland, 2006. Joint Nature Conservation Committee, Peterborough.

Meade, J., B. J. Hatchwell, J. L. Blanchard, and T. R. Birkhead. 2013. The population increase of common guillemots *Uria aalge* on Skomer Island is explained by intrinsic demographic properties. Journal of Avian Biology 44:055–061.

Mercker, M., V. Dierschke, K. Camphuysen, A. Kreutle, N. Markones, N. Vanermen, and S. Garthe. 2021a. An indicator for assessing the status of marine-bird habitats affected by multiple human activities: A novel statistical approach. Ecological Indicators 130:108036.

Mercker, M., N. Markones, K. Borkenhagen, H. Schwemmer, J. Wahl, and S. Garthe. 2021b. An Integrated Framework to Estimate Seabird Population Numbers and Trends. The Journal of Wildlife Management 85:751–771.

Miao, R., P. N. Ghosh, M. Khanna, W. Wang, and J. Rong. 2019. Effect of wind turbines on bird abundance: A national scale analysis based on fixed effects models. Energy Policy 132:357–366.

Mollis, M., R. Hill, O. Hüppop, L. Bach, T. Coppack, S. Pelletier, T. Dittmann, and A. Schulz. 2019. Measuring bird and bat collision and avoidance, volume 4. Wildlife and wind farms, conflicts and solutions.

Newell, M., M. P. Harris, C. M. Gunn, S. Burthe, S. Wanless, and F. Daunt. 2016. Isle of May seabird studies in 2015. Joint Nature Conservation Committee, Peterborough.

Newell, M., M. P. Harris, A. Skene, S. Wanless, and F. Daunt. 2013. Isle of May seabird studies in 2010. Joint Nature Conservation Committee, Aberdeen.

O'Brien, S. H., A. S. C. P. Cook, and R. A. Robinson. 2017. Implicit assumptions underlying simple harvest models of marine bird populations can mislead environmental management decisions. Journal of Environmental Management 201:163–171.

offshorewind.biz. 2021a, June 14. Oil Giant BP Announces Offshore Wind Bid in Norway. https://www.offshorewind.biz/2021/06/14/oil-giant-bp-announces-offshore-wind-bid-in-norway/.

offshorewind.biz. 2021b, September 3. Danish Parliament Decides on Energy Island Specifics, State to Own 50.1 Pct. https://www.offshorewind.biz/2021/09/03/danish-parliament-decides-on-energy-island-specifics-state-to-own-50-1-pct/.

offshorewind.biz. 2021c, October 11. 4.1 GW Scottish Offshore Wind Project Adapts to Protect Birds. https://www.offshorewind.biz/2021/10/11/4-1-gw-scottish-offshore-wind-project-adapts-to-protect-birds/.

Ollason, J. C., and G. M. Dunnet. 1978. Age, experience and other factors affecting the breeding success of the fulmar, *Fulmarus glacialis*, in Orkney. The Journal of Animal Ecology 47:961.

Peschko, V., B. Mendel, M. Mercker, J. Dierschke, and S. Garthe. 2021. Northern gannets (*Morus bassanus*) are strongly affected by operating offshore wind farms during the breeding season. Journal of Environmental Management 279:111509.

Peschko, V., M. Mercker, and S. Garthe. 2020. Telemetry reveals strong effects of offshore wind farms on behaviour and habitat use of common guillemots (*Uria aalge*) during the breeding season. Marine Biology 2020 167:8 167:1–13.

Piatt, J. F., J. K. Parrish, H. M. Renner, S. K. Schoen, T. T. Jones, M. L. Arimitsu, K. J. Kuletz, B. Bodenstein, M. García-Reyes, R. S. Duerr, R. M. Corcoran, R. S. A. Kaler, G. J. McChesney, R. T. Golightly, H. A. Coletti, R. M. Suryan, H. K. Burgess, J. Lindsey, K. Lindquist, P. M. Warzybok, J. Jahncke, J. Roletto, and W. J. Sydeman. 2020. Extreme mortality and reproductive failure of common murres resulting from the northeast Pacific marine heatwave of 2014-2016. PLOS ONE 15:e0226087.

Potiek, A., M. P. Collier, H. Schekkerman, and R. C. Fijn. 2019. Effects of turbine collision mortality on population dynamics of 13 bird species. Bureau Waardenburg Report 18-342, Bureau Waardenburg, Culemborg.

Potiek, A., and S. Duijns. 2021. Review of tracking devices to study spatio-temporal disturbance of seabirds by offshore wind farms. Bureau Waardenburg Rapportnr. 21-046, Bureau Waardenburg, Culemborg.

Potiek, A., G. IJntema, T. van Kooten, M. F. Leopold, and M. P. Collier. 2021a. Acceptable Levels of Impact from offshore wind farms on the Dutch Continental Shelf for 21 bird species. A novel approach for defining acceptable levels of additional mortality from turbine collisions and avoidance-induced habitat loss. Bureau Waardenburg Report 21-0120, Bureau Waardenburg, Culemborg, The Netherlands.

Potiek, A., J. J. Leemans, R. P. Middelveld, and A. Gyimesi. 2021b. Cumulative impact assessment of collisions with existing and planned offshore wind turbines in the southern North Sea. Analysis of additional mortality using collision rate modelling and impact assessment based on population modelling for development according to roadmap 2030 and 2040. Bureau Waardenburg Report, 21-205, Bureau Waardenburg, Culemborg.

Reed, T. E., M. P. Harris, and S. Wanless. 2015. Skipped breeding in common guillemots in a changing climate: restraint or constraint? Frontiers in Ecology and Evolution 3.

Reuters. 2021. Britain announces biggest auction round in renewable energy scheme. https://www.reuters.com/world/uk/britain-announces-biggest-round-its-renewable-energy-scheme-2021-09-12/.

Reynolds, T. J., M. P. Harris, R. King, R. L. Swann, D. C. Jardine, M. Frederiksen, and S. Wanless. 2011. Among-colony synchrony in the survival of Common Guillemots Uria aalge reflects shared wintering areas:14.

Rippen, A. D., E. van der Zee, and A. Brenninkmeijer. 2017. Quickscan opportunities and constraints catching gulls at sea. A&W-report 2356. Altenburg & Wymenga ecological consultants, Feanwâlden.

van Roomen, M., J. Stahl, H. Schekkerman, C. van Turnhout, and R. Vogel. 2013. Advies ten behoeve van het opstellen van een monitoringplan voor vogels in het Nederlandse Noordzeegebied. Sovon-rapport 2013/22.

Sandvik, H., K. E. Erikstad, R. T. Barrett, and N. G. Yoccoz. 2005. The effect of climate on adult survival in five species of North Atlantic seabirds. Journal of Animal Ecology 74:817–831.

Schekkerman, H., F. Arts, R.-J. Buijs, W. Courtens, T. Van Daele, R. Fijn, A. Van Kleunen, H. Van der Jeugd, M. Roodbergen, E. Stienen, L. De Vries, and B. J. Ens. 2021. Geïntegreerde populatie-analyse van vijf soorten kustbroedvogels in het Zuidwestelijk Deltagebied. Sovon Vogelonderzoek Nederland, Nijmegen.

Schmutz, J. A. 2014. Survival of adult redtThroated loons (*Gavia stellata*) may be linked to marine conditions. Waterbirds 37:118–124.

Searle, K., A. Butler, D. Mobbs, M. Bogdanova, J. Waggitt, P. Evans, M. Rehfisch, R. Buisson, and F. Daunt. 2019. Development of a 'Seabird Sensitivity Mapping Tool for Scotland'. CEH Report, Marine Schotland, Centre for Ecology & Hydrology, ORJIP.

Shaw, D. 2012. Fair isle's seabirds in 2009/2010. Fair Isle Observatory report for 2009-10. Fair Isle Observatory, report for 2009-10, Fair Isle Bird Observatory, Fair Isle, Shetland ZE2 9JU.

Shaw, D. N., C. A. Holt, and H. E. Maggs. 2002. Fair Isle seabird studies 2000. JNCC Report No. 332.

Skov, H. 2019. Automated bird monitoring in offshore wind farms. DHI Blog: Drops of knowledge.

Sovacool, B. K. 2009. Contextualizing avian mortality: A preliminary appraisal of bird and bat fatalities from wind, fossil-fuel, and nuclear electricity. Energy Policy 37:2241–2248.

St. John Glew, K., S. Wanless, M. P. Harris, F. Daunt, K. E. Erikstad, H. Strøm, J. R. Speakman, B. Kürten, and C. N. Trueman. 2019. Sympatric Atlantic puffins and razorbills show contrasting responses to adverse marine conditions during winter foraging within the North Sea. Movement Ecology 7:33.

Stienen, E., and A. Brenninkmeijer. 1992. Ecologisch profiel van de grote stern (*Sterna sandvicensis*). DLO Instituut voor Bos- en Natuuronderzoek, Arnhem.

Stubbings, E. M., B. I. Buche, J. A. Riordan, B. Baker, and M. J. Wood. 2018. Seabird monitoring on Skomer Island in 2018. Joint Nature Conservation Committe, Peterborough.

Tanaka, K. R., and K. S. van Houtan. 2022. The recent normalization of historical marine heat extremes. PLOS Climate 1:e0000007.

Tasker, M. L., P. H. Jones, T. Dixon, and B. F. Blake. 1984. Counting seabirds at sea from ships: A review of methods employed and a suggestion for a standardized approach. The Auk 101:567–577.

Thompson, P. M., and J. C. Ollason. 2001. Lagged effects of ocean climate change on fulmar population dynamics. Nature 413:417–420.

Touchwind BV. 2021. Mono • TouchWind. https://touchwind.org/technology/.

Van Kooten, T., F. Soudijn, I. Tulp, C. Chen, D. Benden, and M. Leopold. 2019. The consequences of seabird habitat loss from offshore wind turbines, version 2 : Displacement and population level effects in 5 selected species. Wageningen Marine Research, IJmuiden.

Veen, J. 1977. Functional and causal aspects of nest distribution in colonies of the sandwich tern (*Sterna s. sandvicencis* Lath.). Behaviour Supplement:1–193.

Waggitt, J. J., P. G. H. Evans, J. Andrade, A. N. Banks, O. Boisseau, M. Bolton, G. Bradbury, T. Brereton, C. J. Camphuysen, J. Durinck, T. Felce, R. C. Fijn, I. Garcia-Baron, S. Garthe, S. C. V. Geelhoed, A. Gilles, M. Goodall, J. Haelters, S. Hamilton, L. Hartny-Mills, N. Hodgins, K. James, M. Jessopp, A. S. Kavanagh, M. Leopold, K. Lohrengel, M. Louzao, N. Markones, J. Martínez-Cedeira, O. Ó Cadhla, S. L. Perry, G. J. Pierce, V. Ridoux, K. P. Robinson, M. B. Santos, C. Saavedra, H. Skov, E. W. M. Stienen, S. Sveegaard, P. Thompson, N. Vanermen, D. Wall, A. Webb, J. Wilson, S. Wanless, and J. G. Hiddink. 2020. Distribution maps of cetacean and seabird populations in the North-East Atlantic. Journal of Applied Ecology 57:253–269.

van der Wal, J. T., M. E. B. van Puijenbroek, and M. F. Leopold. 2018. Cumulatieve effecten van offshore wind parken: habitatverlies zeevogels: update voor vijf zeevogelsoorten tot 2030. Wageningen Marine Research rapport C059/18, Wageningen Marine Research.

Wanless, S., M. Frederiksen, M. P. Harris, and S. N. Freeman. 2006. Survival of Gannets *Morus bassanus* in Britain and Ireland, 1959–2002. Bird Study 53:79–85.

Justification
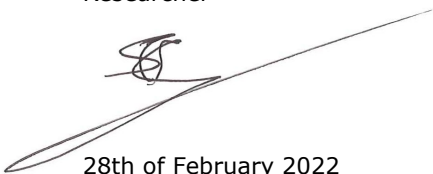
Report C007/22
Project Number: 4315100166

The scientific quality of this report has been peer reviewed by a colleague scientist and a member of the Management Team of Wageningen Marine Research

Approved: Ir. S.C.V. Geelhoed
                   Researcher

Signature:

Date: 28th of February 2022

Approved: Dr. ir. T.P. Bult
                   Director

Signature:

Date: 28th of February 2022

Annex 1 OWFs per scenario

UniekID	OWF name	Country	Expected date	Capacity (MJ)	Basic 2030 Snc	Rekenvariant I scn	Rekenvariant II scn	Rekenvariant III scn	International scn
1	Borssele 2	Netherlands	2020	376.00	x	x	x	x	x
2	Borssele 3	Netherlands	2019	366.00	x	x	x	x	x
3	Borssele 4 – Blauwwind	Netherlands	2019	366.00	x	x	x	x	x
4	Borssele Site V -Two towers	Netherlands	2020	19.00	x	x	x	x	x
5	Egmond aan Zee	Netherlands	2006	108.00	x	x	x	x	x
6	Prinses Amaliawindpark	Netherlands	2006	120.00	x	x	x	x	x
7	Eneco Luchterduinen	Netherlands	2014	129.00	x	x	x	x	x
8	Gemini Zee energie	Netherlands	2015	300.00	x	x	x	x	x
9	Gemini Buitengaats	Netherlands	2015	300.00	x	x	x	x	x
10	Hollandse Kust Zuid Holland IV	Netherlands	2022	385.00	x	x	x	x	x
11	Hollandse Kust Zuid Holland III	Netherlands	2022	385.00	x	x	x	x	x
12	Hollandse Kust Zuid Holland II	Netherlands	2021	385.00	x	x	x	x	x
13	Hollandse Kust Zuid Holland I	Netherlands	2021	385.00	x	x	x	x	x
14	Borssele 1	Netherlands	2020	376.00	x	x	x	x	x
15	Hollandse Kust Noord (Tender 2019)	Netherlands	2022	700.00	x	x	x	x	x
bw4	Ten noorden van de Waddeneilanden – (Tender 2022)	Netherlands	2026	700.00	x	x	x	x	x
bw6	Ijmuiden Ver	Netherlands	2027	4000.00	x	x	x	x	x
bw7	Hollandse Kust West – (Tender 2020/2021)	Netherlands	2024	1400.00	x	x	x	x	x
bw8	Hollandse Kust West zuidelijke punt	Netherlands	2028	700.00		x	x	x	x
258	Zoekgebied 1 Noord	Netherlands	2030	4000.00				x	x
272	Zoekgebied 1 Zuid	Netherlands	2030	2000.00			x	x	x
274	Zoekgebied 2 Noord	Netherlands	2030	4000.00		x	x	x	x
263o	Zoekgebied 5 Oost origineel	Netherlands	2029	4000.00		x	x	x	x
270	Ijmuiden Ver Noord	Netherlands	2028	2000.00		x	x	x	x
BE01	Thornton Bank phase I	Belgium	2008	30.00					x
BE02	Northwind	Belgium	2013	216.00					x
BE03	Belwind	Belgium	2009	165.00					x
BE04	Norther	Belgium	2018	369.60					x
BE05	Rentel	Belgium	2017	309.00					x
BE06	Seamade (SeaStar)	Belgium	2019	252.00					x
BE07	Seamade (Mermaid)	Belgium	2019	235.00					x
BE08	Nobelwind	Belgium	2016	165.00					x
BE09	Thornton Bank phase II	Belgium	2010	184.50					x
BE10	Thornton Bank phase III	Belgium	2011	110.70					x
BE12	Northwester 2	Belgium	2019	219.00					x
BE14	Princess Elisabeth – Noordhinder Noord – 2023 Tender	Belgium	2025	700.00					x
BE15	Princess Elisabeth – Fairybank/Nordhinder Zuid – 2025 Tender	Belgium	2027	1400.00					x
DE39	Albatros	Germany	2019	112.00					x
DE01	Alpha Ventus	Germany	2008	60.00					x
DE05	Amrumbank West	Germany	2013	302.00					x
DE23	BARD Offshore 1	Germany	2010	400.00					x
DE04	Borkum Riffgrund 1	Germany	2013	312.00					x

DE30	Borkum Riffgrund 2	Germany	2018	450.00		x
DE03	Borkum Riffgrund 3	Germany	2023	900.00		x
DE08	Butendiek	Germany	2014	288.00		x
DE02	DanTysk	Germany	2013	288.00		x
DE24	Deutsche Bucht	Germany	2018	252.00		x
DE19	EnBW He Dreiht	Germany	2024	900.00		x
DE09	Global Tech I	Germany	2012	400.00		x
DE13	Gode Wind 1 and 2	Germany	2015	582.00		x
DE0H	Gode Wind 3	Germany	2023	241.75		x
DE11	Hohe See	Germany	2018	497.00		x
DE33	Kaskasi	Germany	2021	342.00		x
DE07	Meerwind Süd/Ost	Germany	2012	288.00		x
DE26	Merkur	Germany	2017	396.00		x
DE3C	N-10.1	Germany	2029	1000.00		x
DE3I	N-10.2	Germany	2029	700.00		x
DE3R	N-13-3	Germany	2030	1000.00		x
DE2Q	N-3.5	Germany	2027	420.00		x
DE2R	N-3.6	Germany	2027	480.00		x
DE2S	N-3.7	Germany	2025	225.00		x
DE2T	N-3.8	Germany	2025	433.00		x
DE2V	N-6.6	Germany	2028	630.00		x
DE2W	N-6.7	Germany	2028	270.00		x
DE2X	N-7.2	Germany	2026	930.00		x
DE2Z	N-8.4	Germany	2026	425.00		x
DE3A	N-9.1	Germany	2028	1000.00		x
DE3B	N-9.2	Germany	2028	1000.00		x
DE3S	N-9.3	Germany	2029	1000.00		x
DE3T	N-9.4	Germany	2029	1000.00		x
DE20	Nordergründe	Germany	2016	110.70		x
DE28	Nordsee One	Germany	2015	332.10		x
DE06	Nordsee Ost	Germany	2012	295.20		x
DE21	Riffgat	Germany	2012	108.00		x
DE12	Sandbank	Germany	2015	288.00		x
DE27	Trianel Windpark Borkum I	Germany	2011	200.00		x
DE0K	Trianel Windpark Borkum II	Germany	2018	203.00		x
DE36	Veja Mate	Germany	2016	402.00		x
DK03	Horns Rev 1	Denmark	2002	160.00		x
DK10	Horns Rev 2	Denmark	2008	209.30		x
DK19	Horns Rev 3	Denmark	2017	406.70		x
DK22	Thor – 2020 Tender	Denmark	2025	1000.00		x
DK48	Vesterhav Nord/Syd	Denmark	2022	344.00		x
UK04	Dudgeon	United Kingdom	2016	402.00		x
UK05	Greater Gabbard	United Kingdom	2009	504.00		x
UK07	Gunfleet Sands	United Kingdom	2008	172.80		x
UK0V	Dogger Bank B	United Kingdom	2023	1200.00		x
UK10	Humber Gateway	United Kingdom	2013	219.00		x
UK11	Inner Dowsing	United Kingdom	2007	97.20		x
UK12	Kentish Flats	United Kingdom	2004	90.00		x
UK13	Lincs	United Kingdom	2011	270.00		x
UK14	London Array	United Kingdom	2011	630.00		x
UK15	Lynn	United Kingdom	2007	97.20		x
UK18	Race Bank	United Kingdom	2016	573.30		x

UK1F	Dogger Bank C	United Kingdom	2024	1200.00		x
UK1G	Sofia	United Kingdom	2024	1400.00		x
UK1K	Hornsea Project Three	United Kingdom	2026	2400.00		x
UK1U	Hornsea Project Two	United Kingdom	2020	1386.00		x
UK23	Scroby Sands	United Kingdom	2003	60.00		x
UK27	Sheringham Shoal	United Kingdom	2009	316.80		x
UK28	Teesside	United Kingdom	2012	62.10		x
UK29	Thanet	United Kingdom	2009	300.00		x
UK2Q	East Anglia Hub – ONE North	United Kingdom	2024	800.00		x
UK30	Triton Knoll	United Kingdom	2020	857.00		x
UK34	Westermost Rough	United Kingdom	2014	210.00		x
UK39	East Anglia Hub – TWO	United Kingdom	2025	900.00		x
UK3F	Scottish Sectoral Marine Plan – E3	United Kingdom	2030	1000.00		x
UK40	Moray East	United Kingdom	2019	950.00		x
UK44	Seagreen	United Kingdom	2021	1140.00		x
UK47	Aberdeen Offshore Wind farm (EOWDC)	United Kingdom	2018	93.20		x
UK4F	Race Bank Extension	United Kingdom	2029	573.00		x
UK4G	Dudgeon Extension	United Kingdom	2028	402.00		x
UK4H	Sheringham Shoal Extension	United Kingdom	2028	317.00		x
UK4I	Five Estuaries	United Kingdom	2030	353.00		x
UK4J	North Falls	United Kingdom	2029	504.00		x
UK4N	Kincardine – Phase 2	United Kingdom	2020	48.00		x
UK4P	Seagreen 1A	United Kingdom	2024	360.00		x
UK53	Beatrice	United Kingdom	2017	588.00		x
UK54	Inch Cape	United Kingdom	2026	1000.00		x
UK56	Neart na Gaoithe	United Kingdom	2020	448.00		x
UK60	Kentish Flats Extension	United Kingdom	2015	49.50		x
UK62	Galloper	United Kingdom	2016	353.00		x
UK64	East Anglia ONE	United Kingdom	2018	714.00		x
UK66	East Anglia Hub – THREE	United Kingdom	2023	1400.00		x
UK67	Norfolk Vanguard	United Kingdom	2025	1800.00		x
UK69	Norfolk Boreas	United Kingdom	2027	1800.00		x
UK70	Blyth Offshore Demonstrator Phase 1	United Kingdom	2017	41.50		x
UK74	Berwick Bank	United Kingdom	2028	2300.00		x
UK76	Hywind Scotland Pilot Park	United Kingdom	2017	30.00		x
UK77	Moray West	United Kingdom	2024	950.00		x
UK79	Blyth Offshore Demonstrator Phase 2	United Kingdom	2024	58.40		x

| UK80 | Dogger Bank A | United Kingdom | 2022 | 1200.00 | | x |
| UK81 | Hornsea Project One | United Kingdom | 2018 | 1218.00 | | x |

Annex 2   Individual based model northern gannet

This annex describes additional analysis of the IBM of the northern gannet. The effect of maximum travel lengths from 1 to 8 grid cells were considered on the estimated survival and metabolic rates estimated during the calibration routines of the model.

Metabolism

Prior to the estimation of the effect of OWFs, the IBM estimates a metabolic rate during a calibration routine for each bimonthly period. The metabolic rate determines the amount of energy that a bird spends each timestep and therefore also determines how long a bird will survive if it is unable to find food. In the IBM, birds that do not find food live longer if they have a low metabolic rate.
The calibrated metabolic rate increased with increasing maximum travel length (1-8) of the birds (**Figure 1**). This is probably due to the fact that agents were able to reach habitats with higher quality with larger step sizes. In addition, there was considerable variation between bimonthly periods; for some periods the calibrated metabolism was higher across all maximum travel lengths. This effect on the calibrated metabolism is due to differences in habitat quality (bird density maps) between different bimonthly periods. Bimonthly periods with higher habitat quality across the entire grid also had a high value for the calibrated metabolic rate.
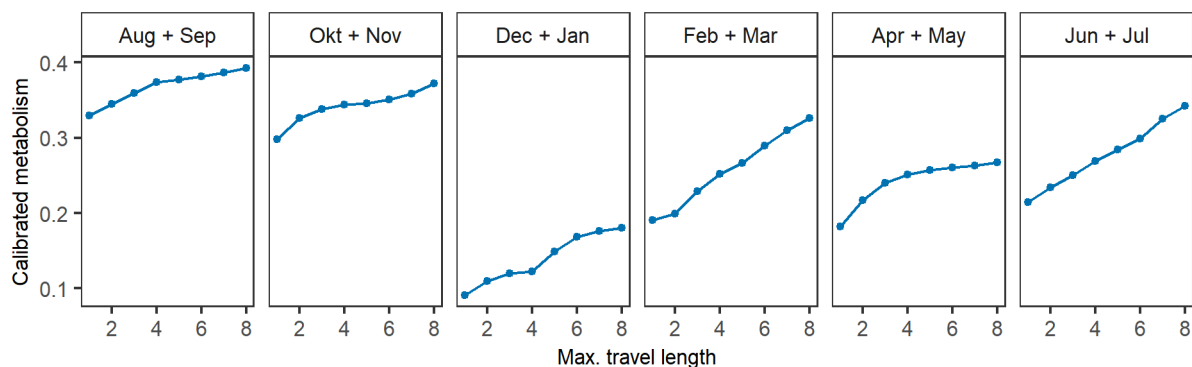
Figure 1. *Calibrated metabolism per maximum travel length and bimonthly period.*

Bimonthly survival

Because OWFs led to a reduction in habitat quality, the bimonthly survival values with OWFs are generally lower than the survival value without OWFs. However, due to the stochastic nature of the IBM, there will be some simulations that predict a higher survival in presence of OWFs. This will occur more frequently if the predicted effect of OWFs on bird survival is small.

There was considerable variation in the bimonthly survival values in presence of OWFs as estimated by the IBM. For the months August until November the OWF-induced reduction in baseline survival was negligible to small. For December – January, the IBM predicted a significant reduction in survival for the international OWF-scenario for maximum travels length of 1, 7 and 8, but this effect was absent for the national '*rekenvariant III*' scenario. A similar result was obtained for the period February – March; OWF-related survival was reduced for low and high maximum travel lengths in the international scenario, but not in the national *rekenvariant III* scenario. Taken together, these results suggest that during the period

December – March, OWF-effects on survival are caused by international OWFs, as opposed to Dutch OWFs.
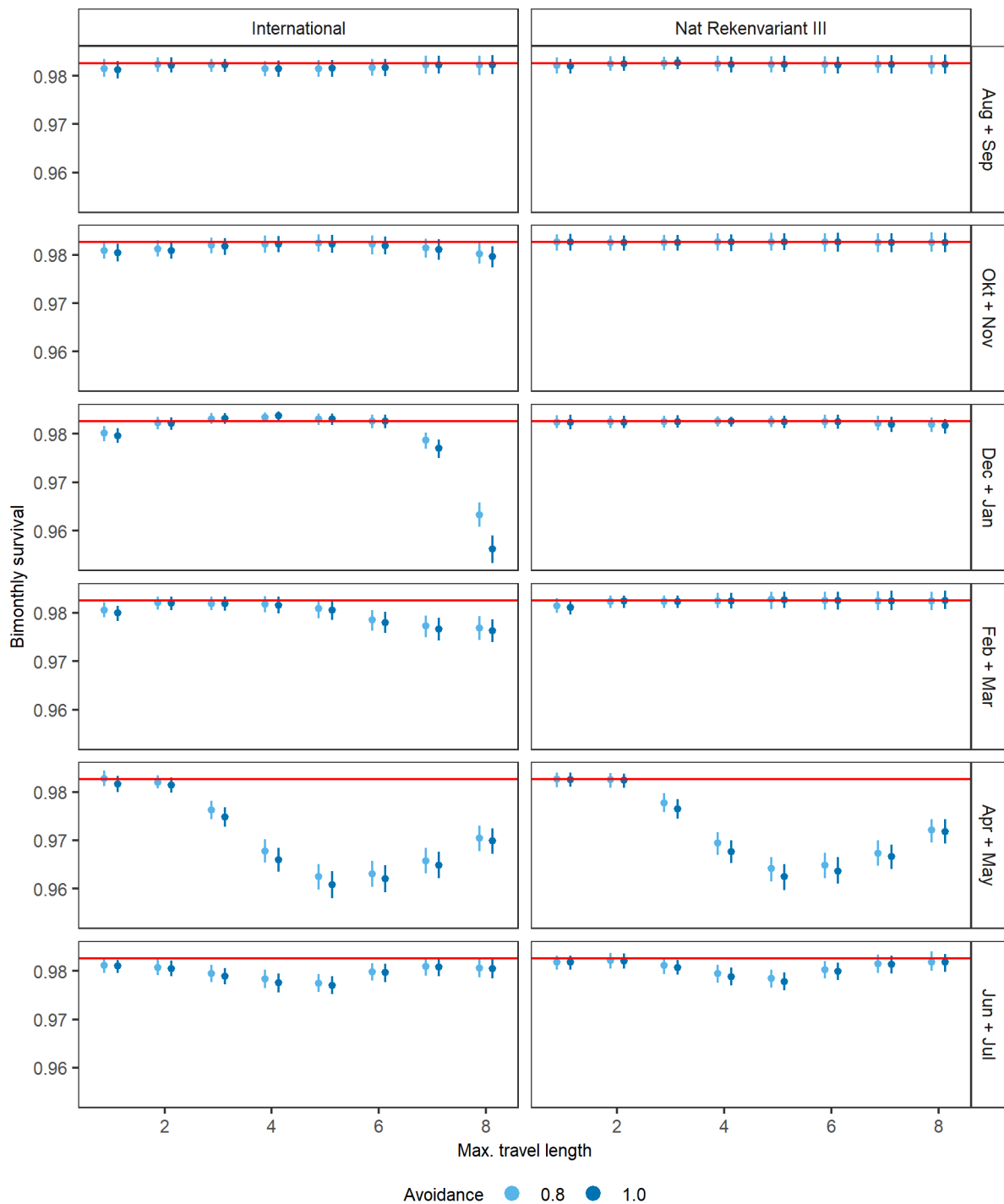
Figure 2. *Survival as estimated by the northern gannet IBM for each combination of bimonthly period, OWF-scenario (international and nat. 'rekenvariant III'), avoidance parameter (0.8 and 1.0) and max. travel length (1 – 8). The red line corresponds to the bimonthly baseline survival value of 0.98259. The blue points show median survival values and line ranges extend towards the 5th and 95th percentiles.*

During the period April – May, the IBM estimated reduced survival for almost all maximum travel lengths (except 1 and 2) for both OWF-scenarios. Although less substantial, a similar pattern was obtained for the period June – July, where both OWF-scenarios led to a comparable reduction in survival that was

especially apparent for intermediate values of the maximum travel length. These results suggest that during the period April – July mainly Dutch OWFs are responsible for the reduction in survival. It should be noted, however, that we cannot conclude that there is no effect of international OWFs on survival during this period, as we have not studied the effect of international OWFs in isolation, but only in combination with Dutch OWFs.

In almost all cases, a complete avoidance ($p = 1.0$) only leads to a slightly lower value of bimonthly survival compared to an avoidance of 0.8. However, during December – January and a maximum travel length of 8 grid cells per time step, the survival in the international scenario for avoidance 1.0 is significantly lower than for an avoidance of 0.8 (line ranges do not overlap). This indicates a high sensitivity of survival to small changes in habitat quality at these particular settings of the model.

Taken together, for some bimonthly periods there is a clear response of the maximum travel length on bimonthly survival, while for other periods there is no response. Initially, one would expect that an increased foraging range would allow birds to profit from foraging sites that are further away. Stated otherwise, with a restricted searching range, birds would have a lower probability of escaping an area of poor habitat quality compared to birds with an extended searching range. Extending the bird's searching area would therefore diminish the estimated effect of habitat loss from OWFs. Also, there is no a priori reason why this would differ between the different bimonthly periods considered.

On the other hand, an indirect consequence of increasing the maximum travel length is that it increases the calibrated metabolic rate (**Figure 1**). So, while birds can access more distant food patches, they also require a higher energy intake to ensure survival. The calibration ensures that these two effects are balanced such that survival remains at a fixed level in OWF-free simulations. The question is whether the increased metabolism can explain the increase in OWF-induced reduction in survival for higher maximum travel lengths. A closer inspection of Figure 1 and Figure 2 reveals that for the period December – January, there is a decelerating increase of metabolism with increasing maximum travel length, while there is an accelerating decrease in survival. This indicates that the sensitivity of habitat-loss from OWFs on bird survival is higher at a higher metabolic rate. Figure 3. illustrates this by showing the bimonthly survival as a function of the calibrated metabolic rate. A slightly higher metabolic rate leads to a much larger effect of OWFs on survival. Also the large difference in survival between the two avoidance values at a maximum travel length of 8 indicates a high sensitivity and a potential lack of model robustness.

It can be hypothesized that the impact of habitat loss by OWFs only becomes apparent at larger maximum travel lengths, because survival of simulated birds with a larger searching area (maximum travel length) is more determined by changes in habitat quality and less by their ability to find food. However, we would expect to see a similar pattern in the other bimonthly periods. In contrast, there is no consistent pattern across the six bimonthly periods and, instead, we find for April – March that OWF-related survival first decreases with maximum travel length, and then increases again. This latter increase cannot be explained if the impact of habitat loss by OWFs only becomes apparent at high maximum travel length. We are therefore unable to reconcile the different responses of the maximum ravel length between bimonthly periods without a better insight into the cause of the high mortality at high maximum travel length.
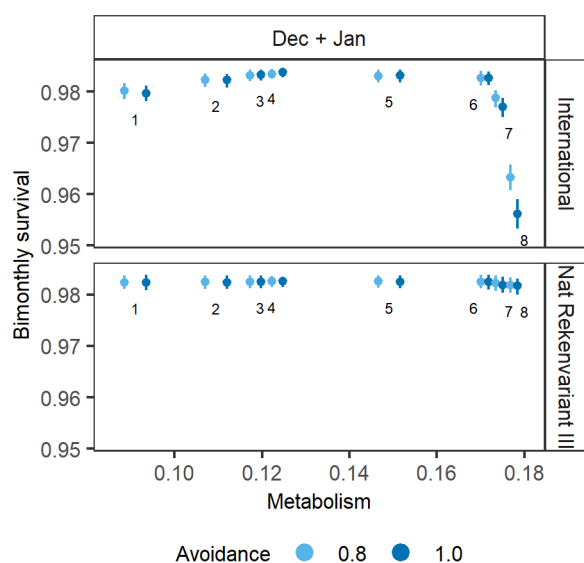
Figure 3. bimonthly survival as estimated by the IBM as a function of the calibrated metabolic rate per OWF-scenario (different rows) and avoidance parameter (colours). Numbers indicate the max. travel length that is associated with each calibrated metabolic rate. Additional horizontal spacing was used to distinguish between different avoidance parameters.

Annual survival and mortality

For the international scenario, annual OWF-related mortality increased with increasing maximum travel length. This reflected the joint effect of maximum travel length on survival for the periods April-May and December–January (**Figure 4**). For the national *rekenvariant III* scenario, the pattern of annual mortality with maximum travel length is mainly driven by the April–May period.
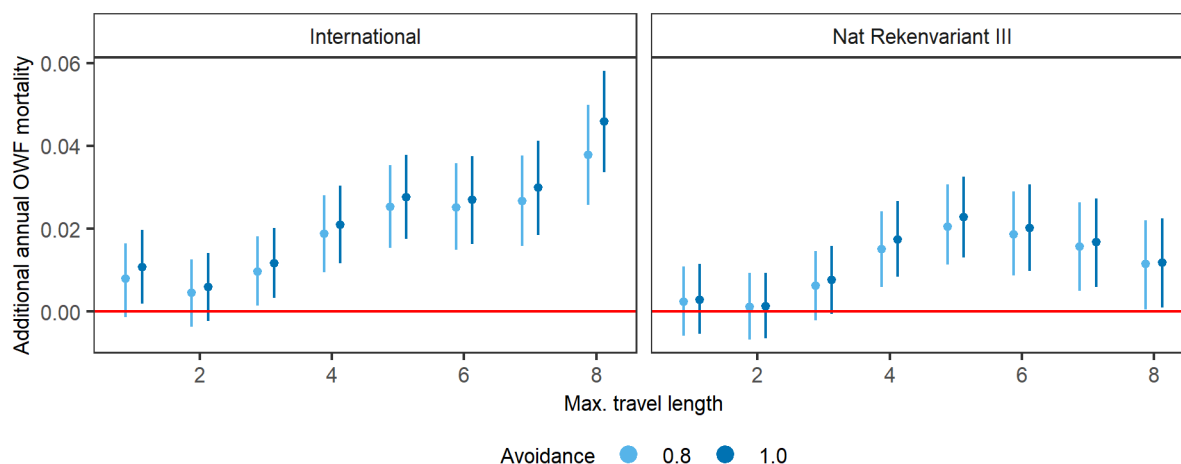
Figure 4. Annual mortality values from OWF-induced habitat loss as estimated by the northern gannet IBM). Blue points show median mortality values and line ranges extend towards the 5th and 95th percentiles. The same data are shown in Table 34.

Population effects and ALI calculations

We used the northern gannet matrix population model to calculate the effect of OWF-induced mortality – as estimated by the IBM – on the population growth rate. This was done only for maximum travel lengths of 1 and 8 grid cells per timestep. We assumed the same life-stage specific vulnerability to OWF-induced mortality as those used for the default mortality calculation. The resulting life-stage specific mortality and survival values are shown in Table 34.

Population growth rates and related ALI statistics are shown in Table 35. The OWF-induced mortality, as estimated by the IBM, leads to a violation of the ALI for the international OWF scenario and a maximum travel length of 8 grid cells per time step. This result is irrespective of the avoidance parameter p or the mortality confidence level used. For the national *rekenvariant III* scenario, the highest probability of impact is 70.2% and the associated probability that this impact is caused by OWF-induced habitat loss equals 46.7%.

Table 34. Annual mortality values per OWF-scenario and maximum travel length. Shown are median mortality values +/- 5th and 95th percentiles. The same data are plotted in **Figure 3***.*

Max. travel length	International avoidance 0.8	International avoidance 1.0	Nat. *rekenvariant III* avoidance 0.8	Nat. *rekenvariant III* avoidance 1.0
1	0.00795 +/- (0; 0.0165)	0.0107 +/- (0.00189; 0.0197)	0.00234 +/- (0; 0.0109)	0.00284 +/- (0; 0.0114)
2	0.00453 +/- (0; 0.0125)	0.0059 +/- (0; 0.0142)	0.00106 +/- (0; 0.00927)	0.00124 +/- (0; 0.00927)
3	0.00964 +/- (0.00144; 0.0181)	0.0116 +/- (0.00327; 0.0202)	0.00627 +/- (0; 0.0146)	0.00764 +/- (0; 0.0159)
4	0.0188 +/- (0.00942; 0.028)	0.0209 +/- (0.0117; 0.0304)	0.015 +/- (0.00587; 0.0242)	0.0174 +/- (0.00842; 0.0267)
5	0.0253 +/- (0.0154; 0.0353)	0.0276 +/- (0.0176; 0.0378)	0.0205 +/- (0.0113; 0.0307)	0.0229 +/- (0.0131; 0.0325)
6	0.0251 +/- (0.0149; 0.0359)	0.027 +/- (0.0163; 0.0375)	0.0187 +/- (0.00873; 0.029)	0.0202 +/- (0.00975; 0.0306)
7	0.0266 +/- (0.0158; 0.0376)	0.0299 +/- (0.0185; 0.0412)	0.0157 +/- (0.00497; 0.0263)	0.0167 +/- (0.00598; 0.0273)
8	0.0379 +/- (0.0258; 0.0498)	0.0458 +/- (0.0337; 0.0581)	0.0115 +/- (0.000536; 0.022)	0.0118 +/- (0.001; 0.0225)
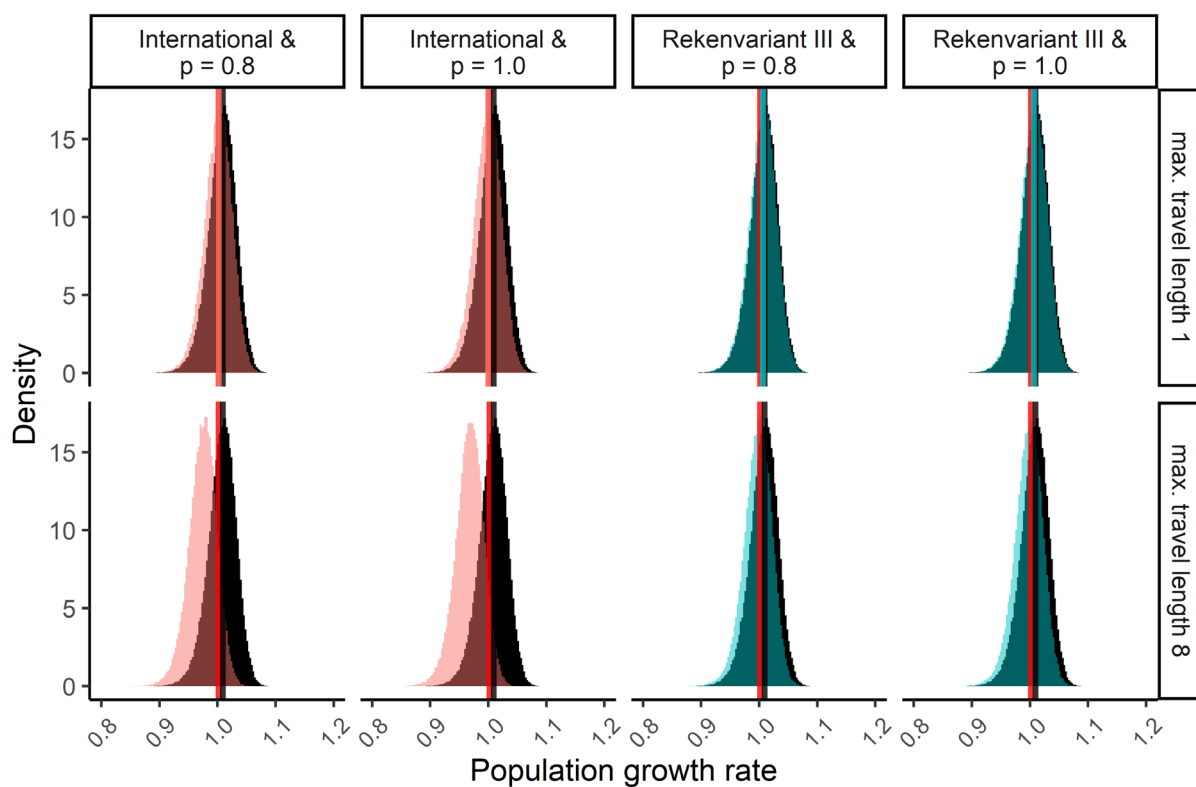
Figure 5. *Distribution of population growth rates of the northern gannet for the different scenarios. Vertical lines indicate the median population growth rates of the ALI threshold (red), the null scenario (black) and each OWF-scenario (colours). Estimates of mortality rates are derived from IBM simulations.*

Table 35. Life-stage specific mortality and survival values as used in the matrix population model for the northern gannet. Mortality estimates are derived from the northern gannet IBM.

Scenario / avoidance	Confidence level	Avoidance	Max. travel length	Mort	Mort S0	Mort S1	Mort S2	Mort S3	Mort SA	Survival S0	Survival S1	Survival S2	Survival S3	Survival SA
NULL				0.00000	0.00000	0.00000	0.00000	0.00000	0.00000	0.48100	0.81600	0.88400	0.88700	0.91800
International	5%	0.8	1	0.01652	0.00647	0.00619	0.01239	0.01225	0.01612	0.47789	0.81095	0.87305	0.87613	0.90320
International	50%	0.8	1	0.00795	0.00311	0.00298	0.00596	0.00590	0.00776	0.47950	0.81357	0.87873	0.88177	0.91088
International	95%	0.8	1	0.00000	0.00000	0.00000	0.00000	0.00000	0.00000	0.48100	0.81600	0.88400	0.88700	0.91800
International	5%	1.0	1	0.01966	0.00770	0.00737	0.01474	0.01458	0.01919	0.47730	0.80998	0.87097	0.87407	0.90039
International	50%	1.0	1	0.01072	0.00420	0.00402	0.00804	0.00795	0.01046	0.47898	0.81272	0.87689	0.87995	0.90840
International	95%	1.0	1	0.00189	0.00074	0.00071	0.00141	0.00140	0.00184	0.48064	0.81542	0.88275	0.88576	0.91631
Rekenvariant III	5%	0.8	1	0.01090	0.00427	0.00409	0.00817	0.00808	0.01064	0.47895	0.81266	0.87677	0.87983	0.90823
Rekenvariant III	50%	0.8	1	0.00234	0.00092	0.00088	0.00176	0.00174	0.00229	0.48056	0.81528	0.88245	0.88546	0.91590
Rekenvariant III	95%	0.8	1	0.00000	0.00000	0.00000	0.00000	0.00000	0.00000	0.48100	0.81600	0.88400	0.88700	0.91800
Rekenvariant III	5%	1.0	1	0.01145	0.00448	0.00429	0.00859	0.00849	0.01117	0.47884	0.81250	0.87641	0.87947	0.90774
Rekenvariant III	50%	1.0	1	0.00284	0.00111	0.00107	0.00213	0.00211	0.00278	0.48046	0.81513	0.88211	0.88513	0.91545
Rekenvariant III	95%	1.0	1	0.00000	0.00000	0.00000	0.00000	0.00000	0.00000	0.48100	0.81600	0.88400	0.88700	0.91800
International	5%	0.8	8	0.04983	0.01952	0.01869	0.03738	0.03696	0.04864	0.47161	0.80075	0.85096	0.85422	0.87335
International	50%	0.8	8	0.03788	0.01484	0.01420	0.02841	0.02809	0.03697	0.47386	0.80441	0.85889	0.86208	0.88406
International	95%	0.8	8	0.02578	0.01010	0.00967	0.01934	0.01912	0.02516	0.47614	0.80811	0.86691	0.87004	0.89490
International	5%	1.0	8	0.05812	0.02276	0.02179	0.04359	0.04311	0.05673	0.47005	0.79822	0.84547	0.84877	0.86593
International	50%	1.0	8	0.04581	0.01794	0.01718	0.03436	0.03397	0.04471	0.47237	0.80198	0.85363	0.85686	0.87696
International	95%	1.0	8	0.03370	0.01320	0.01264	0.02528	0.02500	0.03290	0.47465	0.80569	0.86165	0.86483	0.88780
Rekenvariant III	5%	0.8	8	0.02196	0.00860	0.00823	0.01647	0.01628	0.02143	0.47686	0.80928	0.86944	0.87256	0.89833
Rekenvariant III	50%	0.8	8	0.01148	0.00450	0.00431	0.00861	0.00852	0.01121	0.47884	0.81249	0.87639	0.87945	0.90771
Rekenvariant III	95%	0.8	8	0.00054	0.00021	0.00020	0.00040	0.00040	0.00052	0.48090	0.81584	0.88364	0.88665	0.91752
Rekenvariant III	5%	1.0	8	0.02249	0.00881	0.00843	0.01687	0.01668	0.02195	0.47676	0.80912	0.86909	0.87220	0.89785
Rekenvariant III	50%	1.0	8	0.01176	0.00460	0.00441	0.00882	0.00872	0.01147	0.47879	0.81240	0.87621	0.87927	0.90747
Rekenvariant III	95%	1.0	8	0.00100	0.00039	0.00038	0.00075	0.00074	0.00098	0.48081	0.81569	0.88334	0.88634	0.91710

Table 36. Population growth rates and ALI statistics for the northern gannet, resulting from mortality estimates from the northern gannet IBM. Median, 5% and 95% quantiles of the population growth rate ('Lambda') distribution are reported. 'P impact' represents the fractions of the Lambda distribution that are below the threshold of a 50% smaller population abundance compared to the median lambda of the null scenario after 3 generations, which occurs for a Lambda of 1.009. 'P causality' is the probability that the violation of the population abundance threshold results from the OWF impact. 'ALI 0.5' shows whether P causality exceeds 0.5, the ALI threshold for this species.

Scenario	Confidence level	Avoidance	Max. travel length	Lambda median	q05	q95	P impact	P causality	ALI 0.5
NULL				1.009	0.966	1.045	0.3745	0.000	FALSE
ALI threshold				1.001	0.959	1.037	0.5000	0.251	FALSE
Rekenvariant III	5%	0.8	1	1	0.957	1.035	0.5329	0.297	FALSE
Rekenvariant III	50%	0.8	1	1.007	0.964	1.042	0.4128	0.093	FALSE
Rekenvariant III	95%	0.8	1	1.009	0.966	1.045	0.3777	0.008	FALSE
Rekenvariant III	5%	1.0	1	0.999	0.956	1.035	0.5435	0.311	FALSE
Rekenvariant III	50%	1.0	1	1.007	0.964	1.042	0.4148	0.097	FALSE
Rekenvariant III	95%	1.0	1	1.009	0.966	1.045	0.376	0.004	FALSE
International	5%	0.8	1	0.994	0.952	1.031	0.6196	0.396	FALSE
International	50%	0.8	1	1.002	0.959	1.038	0.4901	0.236	FALSE
International	95%	0.8	1	1.009	0.966	1.045	0.3771	0.007	FALSE
International	5%	1.0	1	0.992	0.949	1.028	0.6672	0.439	FALSE
International	50%	1.0	1	0.999	0.956	1.036	0.5344	0.299	FALSE
International	95%	1.0	1	1.007	0.964	1.043	0.3998	0.063	FALSE
Rekenvariant III	5%	0.8	8	0.99	0.947	1.026	0.694	0.46	FALSE
Rekenvariant III	50%	0.8	8	0.999	0.956	1.035	0.5427	0.31	FALSE
Rekenvariant III	95%	0.8	8	1.008	0.966	1.044	0.3846	0.026	FALSE
Rekenvariant III	5%	1.0	8	0.989	0.946	1.026	0.702	0.467	FALSE
Rekenvariant III	50%	1.0	8	0.999	0.956	1.034	0.5458	0.314	FALSE
Rekenvariant III	95%	1.0	8	1.008	0.965	1.044	0.3865	0.031	FALSE
International	5%	0.8	8	0.965	0.923	1.001	0.9502	0.606	TRUE
International	50%	0.8	8	0.976	0.933	1.012	0.875	0.572	TRUE
International	95%	0.8	8	0.986	0.944	1.023	0.7464	0.498	TRUE
International	5%	1.0	8	0.958	0.916	0.995	0.9762	0.616	TRUE
International	50%	1.0	8	0.969	0.926	1.005	0.9296	0.597	TRUE
International	95%	1.0	8	0.979	0.937	1.016	0.8364	0.552	TRUE

Annex 3 Population models

Diver sp. (*Gavia sp.*)

The matrix model for the diver sp. is based on the red-throated diver *Gavia stellata* and contains three life stages; a juvenile stage J_{01} (age 0 and 1), a pre-breeding adult stage A_2 (age 2) and a breeding adult stage A_B (age 3+). This subdivision was based on the available data on survival, which was estimated for individuals at age 0, age 1 and age 3+. Because reproduction starts at age 3 (Horswill & Robinson, 2015), we include a pre-breeding adult stage for individuals with age 2. Survival and transitions between stages during the non-breeding season are described by the winter transition matrix $\mathbf{A}_{w,Gs}$:

$$
\mathbf{A}_{w,Gs} = \begin{pmatrix} \dfrac{S_J(1-S_J)}{(1-S_J{}^2)} & 0 & 0 \\ \dfrac{S_J{}^2(1-S_J)}{(1-S_J{}^2)} & 0 & 0 \\ 0 & S_A & S_A \end{pmatrix}.
\tag{7}
$$

With annual survival of juveniles S_J, and survival of pre-breeding and breeding adults S_A.
A fraction of the adults produce offspring during the breeding season. Reproduction is modelled by the summer transition matrix $\mathbf{A}_{s,Gs}$:

$$
\mathbf{A}_{s,Gs} = \begin{pmatrix} 1 & 0 & F_A(1-P_F) \\ 0 & 1 & 0 \\ 0 & 0 & 1 \end{pmatrix}.
\tag{8}
$$

Adults produce F_A female offspring (number of fledged *female* chicks per female). The probability that a female skips reproduction during the breeding season equals P_F.
The annual projection matrix is calculated as $\mathbf{A}_{Gs} = \mathbf{A}_{w,Gs} \cdot \mathbf{A}_{s,Gs}$, which results in:

$$
\mathbf{A}_{Gs} = \begin{pmatrix} \dfrac{S_J(1-S_J)}{(1-S_J{}^2)} & 0 & F_A(1-P_F)\,S_J\dfrac{(1-S_J)}{(1-S_J{}^2)} \\ \dfrac{S_J{}^2(1-S_J)}{(1-S_J{}^2)} & 0 & F_A(1-P_F)\,S_J{}^2\dfrac{(1-S_J)}{(1-S_J{}^2)} \\ 0 & S_A & S_A \end{pmatrix}.
\tag{9}
$$

Diver parameter values
Parameter values for the diver are listed in Table 37. The value of F_A is an average from various sources, weighted by the number of years covered and includes data from Finland (Eklöf & Koskimies, 2018), Sweden (Eriksson, 2012) and an overall UK estimate reported by Horswill & Robinson (2015). There is no information on the probability of skipping reproduction (P_F) for the red-throated diver. Based on the range of estimates for other seabirds we adopt a value of 0.05. The standard deviation for P_F is derived from the range rule using the range 0.0 – 0.5. The mean for juvenile survival (S_J) is an average of the values for age 0 (0.6) and age 1 (0.62) as reported by Hemmingsson & Eriksson (2002). The standard deviation was calculated from these two values, which probably results in an underestimate of the true variation in this parameter. Hemmingsson & Eriksson (2002) also report a survival estimate of individuals of age 3 years and older (0.84). This value was combined with the estimate of Schmutz (2014) for adults birds in Alaska, who also reports a the standard deviation for adult survival.

Table 37. Default parameter values for red-throated diver (Gavia stellata).

Symbol	Mean	Unit	SD	Description	Remark	Years of data	Source
F_A	0.381	# / year	0.0905	fledged female offspring	Data from Sweden and UK	52	1, 2, 3, 4, 7
P_F	0.05	-	0.125	skipped breeding probability	SD based on range rule	-	-
S_J	0.61	-	0.0141	annual survival probability age 0-1	Based on two estimates from Sweden	17	5
S_A	0.861	-	0.132	annual survival probability adults age 2+	Based on estimate from Sweden (5) and Alaska (6)	23	5, 6
a_m	3	years	-	age at recruitment			7

[1](Eriksson, 2012), [2](Eklöf & Koskimies, 2018), [3](Gomersall, 1986), [4](Booth, 1999), [5](Hemmingsson & Eriksson 2002), [6](Schmutz, 2014), [7](Horswill & Robinson, 2015)

Northern gannet (*Morus bassanus*)

The matrix model for the northern gannet (*Morus bassanus)* is composed of a juvenile stage: J_0 (age 0), three immature stages: I_1 (age 1), I_2 (age 2) and I_3 (age 3), a pre-breeding adult stage: A_4 (age 4), and a breeding adult stage A_B (age 5+). The juvenile and immature stages have different survival probabilities (S_0, S_1, S_2 and S_3), while the survival probability of pre-breeding adults equals that of breeding adults (S_A). Survival and transitions between stages during the non-breeding season are described by the winter transition matrix $\mathbf{A_{w,Mb}}$:

$$\mathbf{A_{w,Mb}} := \begin{pmatrix} 0 & 0 & 0 & 0 & 0 & 0 \\ S_0 & 0 & 0 & 0 & 0 & 0 \\ 0 & S_1 & 0 & 0 & 0 & 0 \\ 0 & 0 & S_2 & 0 & 0 & 0 \\ 0 & 0 & 0 & S_3 & 0 & 0 \\ 0 & 0 & 0 & 0 & S_A & S_A \end{pmatrix}. \tag{10}$$

Adult females produce offspring during the breeding season. Only part of the females reproduce and parameter P_F equals the probability of not reproducing. Because maximal clutch size of northern gannets is 1 egg (Wanless *et al.*, 2006), the breeding success parameter F_A describes the number of fledged chicks of both sexes per female individual. Reproduction is modelled by the summer transition matrix $\mathbf{A_{s,Mb}}$:

$$\mathbf{A_{s,Mb}} := \begin{pmatrix} 1 & 0 & 0 & 0 & 0 & \frac{F_A}{2}(1-P_F) \\ 0 & 1 & 0 & 0 & 0 & 0 \\ 0 & 0 & 1 & 0 & 0 & 0 \\ 0 & 0 & 0 & 1 & 0 & 0 \\ 0 & 0 & 0 & 0 & 1 & 0 \\ 0 & 0 & 0 & 0 & 0 & 1 \end{pmatrix}. \tag{11}$$

The annual projection matrix is calculated as $\mathbf{A}_{Mb} = \mathbf{A}_{w,Mb} \cdot \mathbf{A}_{s,Mb}$

$$\mathbf{A}_{Mb} = \begin{pmatrix} 0 & 0 & 0 & 0 & 0 & 0 \\ S_0 & 0 & 0 & 0 & 0 & \frac{F_A}{2}(1-P_F)S_0 \\ 0 & S_1 & 0 & 0 & 0 & 0 \\ 0 & 0 & S_2 & 0 & 0 & 0 \\ 0 & 0 & 0 & S_3 & 0 & 0 \\ 0 & 0 & 0 & 0 & S_A & S_A \end{pmatrix}. \tag{12}$$

The reproduction term $(S_0 \frac{F_A}{2}(1-P_F))$ correctly appears in the second row of $\mathbf{A}_{Mb}$, because population census occurs just after the yearling individuals have turned 1 year old.

Northern gannet parameter values

There are a number of reports of life-history parameters for this species. Horswill & Robinson (2015) report a UK-wide average for the breeding parameter F_A, which was adopted here (Table 38). Because there are no data on probability of skipping reproduction, we adopted the same value for P_F as for the

red-throated diver (Table 37). Annual survival probabilities for the juvenile and immature stages were taken from Wanless *et al.* (2006), who report values derived from colonies at Bass Rock, Hermaness, Ailsa Craig and Great Saltee (UK and Ireland). For these colonies, Wanless *et al.* (2006) also report a value for adult survival, which was complemented with a more recent estimate from Bass Rock (Lane *et al.*, 2020) and an adult survival estimate from Grassholm, Wales (Deakin *et al.*, 2019).

Table 38. Northern gannet life-history parameters

Symbol	Mean	SD	Unit	Description	Remark	Years of data	Source
F_A	0.7	0.082	# / year	Fledged number of offspring per female	National average UK	>90	1
P_F	0.05	0.125	-	Skipped breeding probability	SD based on range rule		
S_0	0.481	0.0853	-	Annual survival probability age 0		43	2
S_1	0.816	0.0393	-	Annual survival probability age 1		43	2
S_2	0.884	0.0293	-	Annual survival probability age 2		43	2
S_3	0.887	0.0301	-	Annual survival probability age 3		43	2
S_A	0.918	0.0199	-	Adult annual survival probability		101	2, 3, 4
a_{Gm}	5		Years	Age at recruitment			1

[1](Horswill & Robinson, 2015); [2](Wanless *et al.*, 2006); [3] (Lane *et al.*, 2020); [4](Deakin *et al.*, 2019)

Sandwich tern (*Thalasseus sandvicensis*)

The matrix model for the sandwich tern (*Thalasseus sandvicensis*) is composed of a juvenile stage J_0 (age 0), an immature stage J_{12} (age 1 and 2), a young adult stage A_{34} (age 3 and 4) and an old adult stage A_B (age 5+). Immature individuals of age one and two years old are grouped into a single stage, because estimated mortality rates are identical for these ages. Recruitment in the sandwich tern occurs at age 3 (Van der Jeugd *et al.*, 2014). Because adults aged 3 and 4 years have a significantly lower breeding success than older individuals (Veen 1977), we define an additional adult class for these ages. Survival and transitions between stages during the non-breeding season are described by the winter transition matrix $\mathbf{A_{w,Ts}}$:

$$\mathbf{A_{w,Ts}} = \begin{pmatrix} 0 & 0 & 0 & 0 \\ S_0 & \dfrac{S_{12}(1-S_{12})}{(1-S_{12}{}^2)} & 0 & 0 \\ 0 & \dfrac{S_{12}{}^2(1-S_{12})}{(1-S_{12}{}^2)} & \dfrac{S_A(1-S_A)}{(1-S_A{}^2)} & 0 \\ 0 & 0 & \dfrac{S_A{}^2(1-S_A)}{1-S_A{}^2} & S_A \end{pmatrix}. \tag{13}$$

With survival of juveniles S_0, survival of immatures S_{12} and survival of adults S_A.
Part of the females produce offspring during the breeding season. Reproduction is modelled by the summer transition matrix $\mathbf{A_{s,Ts}}$:

$$\mathbf{A_{s,Ts}} = \begin{pmatrix} 1 & 0 & 0.3F_A(1-P_F) & F_A(1-P_F) \\ 0 & 1 & 0 & 0 \\ 0 & 0 & 1 & 0 \\ 0 & 0 & 0 & 1 \end{pmatrix}. \tag{14}$$

Sandwich terns brood size varies between 1-2 eggs per brood. The breeding success parameter F_A therefore represents number of *female* offspring per year. Breeding success of young females equals 0.3 times the breeding success of older females (Veen, 1977). Note that this parameter is hard coded

and hence does not vary between different stochastic realization of the summer transition matrix. The probability that an adult female skips reproduction equals P_F for both young and old females. The annual projection matrix is calculated as $\mathbf{A}_{Ts} = \mathbf{A}_{w,Ts} \cdot \mathbf{A}_{s,Ts}$, with

$$\mathbf{A}_{Ts} = \begin{pmatrix} 0 & 0 & 0 & 0 \\ S_0 & S_{12}\dfrac{(1-S_{12})}{(1-S_{12}{}^2)} & 0.3F_A(1-P_F)S_0 & F_A(1-P_F)S_0 \\ 0 & \dfrac{S_{12}{}^2(1-S_{12})}{(1-S_{12}{}^2)} & \dfrac{S_A(1-S_A)}{(1-S_A{}^2)} & 0 \\ 0 & 0 & \dfrac{S_A{}^2(1-S_A)}{(1-S_A{}^2)} & S_A \end{pmatrix}. \tag{15}$$

Sandwich tern parameter values

The parameter values for the sandwich tern (Table 39) are based on studies of sandwich tern colonies in the Netherlands. The value for the breeding success parameter (F_A) is based on 82 years of data in total, from 7 different studies (Table 39). There is no information on the probability of skipping reproduction for the sandwich tern. Van Kooten *et al.* (2019) used values for P_F of 0.05, 0.1 and 0.2 and here we adopt their median value of 0.1. The standard deviation for P_F is derived from the range rule by assuming a range of 0 to 0.5 for this parameter. The incidence of skipped breeding is equal for both adult stages. Survival probabilities are based on studies of Van der Jeugd *et al.* (2014) and recent data from Schekkerman *et al.* (2021).

Table 39. Default parameter values sandwich tern

Symbol	Mean	SD	Unit	Description	Remark	Years of data	Source
F_A	0.325	0.160	# / year	Fledged female offspring		82	1-7
P_F	0.1	0.125	-	Skipped breeding probability, all adult stages			
S_0	0.508	0.0917	-	Annual survival probability juveniles, age 0		51	7
S_{12}	0.777	0.0518	-	Annual survival probability immatures, age 1 and 2		51	1, 7
S_A	0.942	0.108	-	Annual survival probability adults, age 3+		51	1, 7
a_{Tm}	3	-	Years	Age at maturation			7

[1](Schekkerman *et al.*, 2021) [2](Derks & De Kraker, 2005); [3](Koffijberg *et al.*, 2017); [4](Beijersbergen, 2001) [5](Veen, 1977) [6](Stienen & Brenninkmeijer 1992) ; [7](Van der Jeugd *et al.*, 2014).

Razorbill (*Alca torda*)

The matrix model for the razorbill (*Alca torda*) is composed of a juvenile stage J_{01} (age 0 and 1), a pre-breeding adult stage A_{234} (age 2 to 4) and a breeding adult stage A_B (age 5+). Both pre-breeding and breeding adults have the same survival probability S_A, which differs from the survival of juveniles S_{01}. Survival and transitions between stages during the non-breeding season are described by winter transition matrix $\mathbf{A}_{w,At}$:

$$\mathbf{A}_{w,At} = \begin{pmatrix} \dfrac{S_{01}(1-S_{01})}{(1-S_{01}{}^2)} & 0 & 0 \\ \dfrac{S_{01}{}^2(1-S_{01})}{(1-S_{01}{}^2)} & S_A\dfrac{(1-S_A{}^2)}{(1-S_A{}^3)} & 0 \\ 0 & S_A{}^3\dfrac{(1-S_A)}{(1-S_A{}^3)} & S_A \end{pmatrix}. \tag{16}$$

A fraction P_F of the breeding adult females skip reproduction each year. Females that do reproduce lay one egg and produce F_A chicks each year. Reproduction during the breeding season is modelled by the summer transition matrix $\mathbf{A}_{s,At}$:

$$\mathbf{A_{s,At}} = \begin{pmatrix} 1 & 0 & \dfrac{F_A}{2}(1-P_F) \\ 0 & 1 & 0 \\ 0 & 0 & 1 \end{pmatrix}. \tag{17}$$

The annual projection matrix is calculated as $\mathbf{A_{At}} = \mathbf{A_{w,At}} \cdot \mathbf{A_{s,At}}$, which leads to

$$\mathbf{A_{At}} = \begin{pmatrix} \dfrac{S_{01}(1-S_{01})}{(1-S_{01}{}^2)} & 0 & \dfrac{F_A}{2}(1-P_F)\dfrac{S_{01}(1-S_{01})}{(1-S_{01}{}^2)} \\ \dfrac{S_{01}{}^2(1-S_{01})}{(1-S_{01}{}^2)} & S_A\dfrac{(1-S_A{}^2)}{(1-S_A{}^3)} & \dfrac{F_A}{2}(1-P_F)\dfrac{S_{01}{}^2(1-S_{01})}{(1-S_{01}{}^2)} \\ 0 & S_A{}^3\dfrac{(1-S_A)}{(1-S_A{}^3)} & S_A \end{pmatrix}. \tag{18}$$

Razorbill parameter values

Parameter values for the razorbill (Table 40) were taken from various studies on colonies in the UK and Ireland. The mean value of the breeding success parameter F_A is based on 85 years of data from 7 different colonies. Horswill & Robinson (2015) report an estimate of only 3% for the incidence of missed breeding from a study by Harris & Wanless (1989). We used this value as mean for parameter P_F, because it is based on species-specific observations. We calculated the SD for this parameter from the range rule using a range of 0 – 0.5.

Values of immature survival S_{01} are based on colonies at Skokholm, Wales (Lloyd & Perrins, 1977) and in the Britain and Irish Sea (Lloyd, 1974). Values for adult survival are based on 4 colonies around the UK, and 1 colony at Hornøya, Norway (Sandvik *et al.*, 2005).

Table 40. Default parameter values razorbill

Symbol	Mean	SD	unit	Description	Remark	Years of data	Source
F_A	0.550	0.138	# / year	Fledged chicks per year		85	1 – 4
P_F	0.03	0.125	-	Skipped breeding probability, all adult stages	SD based on range rule with range 0 – 0.5.	-	5
S_{01}	0.643	0.048	-	Annual survival probability age 0 and 1		21	6,7
S_A	0.909	0.0678	-	Adult annual survival probability		97	4,7-10
a_{Rm}	5	-	Years	Age at recruitment			

[1](Mavor *et al.*, 2008); [2](Shaw, 2012); [3](Newell *et al.*, 2013); [4](Stubbings *et al.*, 2018); [5](Harris & Wanless, 1989); [6](Lloyd, 1974); [7](Lloyd & Perrins, 1977), [8](Sandvik *et al.*, 2005); [9](St. John Glew *et al.*, 2019); [10](Lavers *et al.*, 2008).

Common guillemot (*Uria aalge*)

The matrix model for the common guillemot (*Uria aalge*) is composed of three juvenile life stages; J_0 (age 0), J_1 (age 1) and J_2 (age 2), a pre-breeding adult life stage (age 3-5) and a breeding adult life stage A_B (age 6+). Each juvenile life stage has its own survival parameter, S_0, S_1 and S_2. Pre-breeding and breeding adult have survival probability S_A. Survival and transitions between stages during the non-breeding season are described by winter transition matrix $\mathbf{A_{w,Ua}}$:

$$\mathbf{A_{w,Ua}} = \begin{pmatrix} 0 & 0 & 0 & 0 & 0 \\ S_0 & 0 & 0 & 0 & 0 \\ 0 & S_1 & 0 & 0 & 0 \\ 0 & 0 & S_2 & \dfrac{S_A(1-S_A{}^2)}{(1-S_A{}^3)} & 0 \\ 0 & 0 & 0 & \dfrac{S_A{}^3(1-S_A)}{(1-S_A{}^3)} & S_A \end{pmatrix}. \tag{19}$$

A fraction P_F of the breeding adult females skip reproduction each year. Because the maximum clutch size is one egg, the breeding success parameter F_A represents the number of fledged chicks per breeding female. Reproduction during the breeding season is modelled by the summer transition matrix $\mathbf{A}_{s,Ua}$:

$$\mathbf{A}_{s,Ua} = \begin{pmatrix} 1 & 0 & 0 & 0 & \frac{F_A}{2}(1-P_F) \\ 0 & 1 & 0 & 0 & 0 \\ 0 & 0 & 1 & 0 & 0 \\ 0 & 0 & 0 & 1 & 0 \\ 0 & 0 & 0 & 0 & 1 \end{pmatrix}. \tag{20}$$

The annual projection matrix is calculated as $\mathbf{A}_{Ua} = \mathbf{A}_{w,Ua} \cdot \mathbf{A}_{s,Ua}$, which leads to

$$\mathbf{A}_{Ua} = \begin{pmatrix} 0 & 0 & 0 & 0 & 0 \\ S_0 & 0 & 0 & 0 & \frac{F_A}{2}(1-P_F)S_0 \\ 0 & S_1 & 0 & 0 & 0 \\ 0 & 0 & S_2 & \frac{S_A\left(1-S_A{}^2\right)}{\left(1-S_A{}^3\right)} & 0 \\ 0 & 0 & 0 & \frac{S_A{}^3(1-S_A)}{\left(1-S_A{}^3\right)} & S_A \end{pmatrix}. \tag{21}$$

Common guillemot parameter values

Parameter values for the common guillemot are reported in Table 41. There are numerous studies that report life-history parameters for this species. Mean and standard deviation for breeding success parameter F_A were obtained from five studies covered a total of 194 years of data. The mean and standard deviation for P_F are based on a single study of birds from the Isle of May, Scotland covering 33 years (Reed *et al.*, 2015). Survival probabilities were derived from birds at Skomer, Wales and the Isle of May and Canna Isles, Scotland. Sandvik *et al.* (2005) also report values for adult survival from birds at Hornøya, Norway.

Table 41. Default parameter values common guillemot

Symbol	Mean	SD	Unit	Description	Remark	Years of data	source
F_A	0.664	0.149	# / year	fledged offspring	area specific estimates (UK), available	194	1 – 5
P_F	0.07	0.03	-	skipped breeding probability	SD based on range rule using range 0.02-0.14	33	6
S_0	0.608	0.132	-	annual survival probability age 0		68	7,10
S_1	0.774	0.112	-	annual survival probability age 1		64	7,8,10
S_2	0.858	0.0736	-	annual survival probability age 2		64	7,8,10
S_A	0.949	0.0447	-	annual survival probability adults age 3+			7-10
a_{UM}	6	-	Years	age at recruitment			1

[1] (Mavor *et al.*, 2008); [2](Newell *et al.*, 2013); [3](Harris *et al.*, 2020); [4](Shaw, 2012) [5] (Meade *et al.*, 2013) [6](Reed *et al.*, 2015); [7](Reynolds *et al.*, 2011); [8] (Harris *et al.*, 2007); [9] (Sandvik *et al.*, 2005 p. 200); [10](Meade *et al.*, 2013)

Northern fulmar (*Fulmarus glacialis*)

The matrix model for the northern fulmar (*Fulmarus glacialis*) is composed of a juvenile stage J, a pre-breeding adult stage A_{PB} and a breeding adult life stage A_B. The ages that correspond to each life

stage depend on the duration (in years) of the juvenile and pre-breeding adult life stages, which are parameters in northern fulmar matrix model. Survival rates of juveniles (S_J) differ from survival of pre-breeding and breeding adults (S_A). Survival and transitions between stages during the non-breeding season are described by winter transition matrix $\mathbf{A_{w,Fg}}$:

$$
\mathbf{A_{w,Fg}} = \begin{pmatrix} \dfrac{S_J\left(1 - S_J^{N_J-1}\right)}{\left(1 - S_J^{N_J}\right)} & 0 & 0 \\ \dfrac{S_J^{N_J}(1 - S_J)}{\left(1 - S_J^{N_J}\right)} & S_A\dfrac{\left(1 - S_A^{N_{PB}-1}\right)}{\left(1 - S_A^{N_{PB}}\right)} & 0 \\ 0 & S_A^{N_{PB}}\dfrac{(1 - S_A)}{\left(1 - S_A^{N_{PB}}\right)} & S_A \end{pmatrix}. \tag{16}
$$

Here, N_J represents the number of juvenile age classes and N_{PB} is the number of pre-breeding age classes. Note that these parameters can only take whole numbers (integer values).

A fraction P_F of the breeding adult females skip reproduction each year. Because females only lay a single egg, the breeding success parameter F_A represents the number of fledged chicks per breeding female per year. Reproduction during the breeding season is modelled by the summer transition matrix $\mathbf{A_{s,Fg}}$:

$$
\mathbf{A_{s,Fg}} = \begin{pmatrix} 1 & 0 & \dfrac{F_A}{2}(1 - P_F) \\ 0 & 1 & 0 \\ 0 & 0 & 1 \end{pmatrix}. \tag{17}
$$

The annual projection matrix is calculated as $\mathbf{A_{Fg}} = \mathbf{A_{w,Fg}} \cdot \mathbf{A_{s,Fg}}$, which leads to

$$
\mathbf{A_{Fg}} = \begin{pmatrix} \dfrac{S_J\left(1 - S_J^{N_J-1}\right)}{\left(1 - S_J^{N_J}\right)} & 0 & \dfrac{F_A}{2}(1 - P_F)\dfrac{S_J\left(1 - S_J^{N_J-1}\right)}{\left(1 - S_J^{N_J}\right)} \\ \dfrac{S_J^{N_J}(1 - S_J)}{\left(1 - S_J^{N_J}\right)} & S_A\dfrac{\left(1 - S_A^{N_{PB}-1}\right)}{\left(1 - S_A^{N_{PB}}\right)} & \dfrac{F_A}{2}(1 - P_F)\dfrac{S_J^{N_J}(1 - S_J)}{\left(1 - S_J^{N_J}\right)} \\ 0 & S_A^{N_{PB}}\dfrac{(1 - S_A)}{\left(1 - S_A^{N_{PB}}\right)} & S_A \end{pmatrix}. \tag{16}
$$

Northern fulmar parameter values

Parameter values for the northern fulmar are reported in Table 42. Mean and standard deviation for breeding success parameter F_A were obtained from five studies of four different Island around the UK that covered 108 years of data in total. The mean and standard deviation for P_F are based on a single study of birds from Eynhallow, Orkney Islands, Scotland covering 36 years (Thompson & Ollason, 2001). Juvenile survival was calculated from survival across the immature years of the southern fulmar at Île des Pétrels, Antarctica. Jenouvrier *et al.* (2003) report a survival probability across age 0 to 11 of 0.26, which corresponds to an annual survival of 0.884. Female age at first breeding is at least 10 years (Ollason & Dunnet 1978) and we assumed that during six of those years individuals experience juvenile mortality rates, while the remaining four years they experience adult mortality rates. Like the matrix models for the other species, we do not consider variation in the length of the juvenile and the pre-breeding adult stage.

Table 42. Default parameter values northern fulmar

Symbol	Mean	SD	Unit	Description	Remark	Years of data	source
F_A	0.42	0.13	# / year	fledged offspring		108	1 – 5
P_F	0.304	0.113	-	skipped breeding probability		36	6
S_J	0.884	0.054	-	annual survival probability juveniles	Southern fulmar	39	7
S_A	0.936	0.055	-	annual survival probability adults		34	8

N_J	6	-	Years	Number of juvenile ages	No variation was considered for this parameter	
N_{PB}	4	-	Years	Number of pre-breeding adult ages	No variation was considered for this parameter	
a_B	10	-	Years	Female age at first breeding		9

[1](Lewis *et al.*, 2009); [2](Newell *et al.*, 2013); [3](Newell *et al.*, 2016); [4](Stubbings *et al.*, 2018) [5](Shaw *et al.*, 2002); [6](Thompson & Ollason, 2001); [7](Jenouvrier *et al.*, 2003); [8](Grosbois & Thompson, 2005); [9](Ollason & Dunnet 1978)

Atlantic puffin (*Fratercula arctica*)

The matrix model for the Atlantic puffin (*Fratercula arctica*) is composed of three immature stages, J_{03} (age 0 – 3), J_4 (age 4) and J_5 (age 5), and an adult stage A (age 5+). Immature individuals aged one to three years old are grouped into a single stage, because the estimated survival rate (S_{03}) is identical across these ages. Survival probabilities are different for four (S_4) and five (S_5) year old individuals, and for adults (S_A). Survival and transitions between stages during the non-breeding season are described by the winter transition matrix $\mathbf{A_{w,Fa}}$:

$$\mathbf{A_{w,Fa}} = \begin{pmatrix} \dfrac{S_{03}(1-S_{03}^3)}{(1-S_{03}^{\,4})} & 0 & 0 & 0 \\ \dfrac{S_{03}^{\,4}(1-S_{03})}{(1-S_{03}^{\,4})} & 0 & 0 & 0 \\ 0 & S_4 & 0 & 0 \\ 0 & 0 & S_5 & S_A \end{pmatrix}. \tag{13}$$

Most individuals start breeding when they are at least 6 years old, but some individuals breed earlier. We therefore allow 4 and 5 year old individuals to produce offspring with a separate probability to skip breeding for these life stages (P_{F4} and P_{F5}). Reproduction is modelled by the summer transition matrix $\mathbf{A_{s,Fa}}$:

$$\mathbf{A_{s,Fa}} = \begin{pmatrix} 1 & (1-P_{F4})\dfrac{F_A}{2} & (1-P_{F5})\dfrac{F_A}{2} & (1-P_F)\dfrac{F_A}{2} \\ 0 & 1 & 0 & 0 \\ 0 & 0 & 1 & 0 \\ 0 & 0 & 0 & 1 \end{pmatrix}. \tag{14}$$

Breeding success parameter F_A represents the number of offspring per year, as Atlantic puffin females lay a single egg at a time. The probability that an adult female skips reproduction equals P_F. The annual projection matrix is calculated as $\mathbf{A_{Fa}} = \mathbf{A_{w,Fa}} \cdot \mathbf{A_{s,Fa}}$, with

$$\mathbf{A_{Fa}} = \begin{pmatrix} \dfrac{S_{03}(1-S_{03}^3)}{(1-S_{03}^{\,4})} & (1-P_{F4})\dfrac{F_A}{2}\dfrac{S_{03}(1-S_{03}^3)}{(1-S_{03}^{\,4})} & (1-P_{F5})\dfrac{F_A}{2}\dfrac{S_{03}(1-S_{03}^3)}{(1-S_{03}^{\,4})} & (1-P_F)\dfrac{F_A}{2}\dfrac{S_{03}(1-S_{03}^3)}{(1-S_{03}^{\,4})} \\ \dfrac{S_{03}^{\,4}(1-S_{03})}{(1-S_{03}^{\,4})} & (1-P_{F4})\dfrac{F_A}{2}\dfrac{S_{03}^{\,4}(1-S_{03})}{(1-S_{03}^{\,4})} & (1-P_{F5})\dfrac{F_A}{2}\dfrac{S_{03}^{\,4}(1-S_{03})}{(1-S_{03}^{\,4})} & (1-P_F)\dfrac{F_A}{2}\dfrac{S_{03}^{\,4}(1-S_{03})}{(1-S_{03}^{\,4})} \\ 0 & S_4 & 0 & 0 \\ 0 & 0 & S_5 & S_A \end{pmatrix}. \tag{15}$$

Atlantic puffin parameter values

Parameter values for the Atlantic puffin (Table 43) are mainly based on studies from the UK. Estimates for breeding success were derived from several colonies around the UK. The values for the skipped breeding probability for four and five year olds account for the proportion of individuals that only start breeding at age 6 (Harris & Wanless, 2011). Once breeding starts, Atlantic puffins attempt to breed almost every year (Ashcroft, 1979, Lowther *et al.*, 2020), which translates in the low value for P_F. Values for immature survival are based on a metapopulation study of four colonies in the Gulf of Maine, USA and Canada (Breton *et al.*, 2006). Adult survival rates are based on three UK colonies and two colonies in Norway.

Table 43. Default parameter values Atlantic puffin

Symbol	Mean	SD	Unit	Description	Remark	Years of data	Source
F_A	0.70	0.11	# / year	Fledged offspring		60	1 – 6
P_{F4}	0.6	0.01	-	Skipped breeding probability, 4 year olds			7
P_{F5}	0.3	0.01	-	Skipped breeding probability, 5 year olds			7
P_F	0.078	0.01	-	Skipped breeding probability, adults		3	8
S_{03}	0.71	0.11	-	Annual survival probability juveniles, age 0 – 3		24	9
S_4	0.78	0.092	-	Annual survival probability age 4 individuals		24	9
S_5	0.80	0.083	-	Annual survival probability age 5 individuals		24	9
S_A	0.93	0.057	-	Annual survival probability adults		81	4, 10

[1](Mavor *et al*., 2008); [2](Shaw *et al*., 2002); [3](Newell *et al.*, 2016); [4](Harris *et al.*, 2013); [5](Stubbings *et al.*, 2018); [6](Fayet *et al.*, 2017); [7](Harris & Wanless, 2011); [8](Ashcroft, 1979); [9](Breton *et al.*, 2006); [10](Harris *et al.*, 2005)

Annex 4 Number of casualties for Dutch OWF search areas

*Table 44. Estimated number of casualties due to habitat loss from Dutch OWFs and search areas per OWF id, species and bimonthly period. Areas corresponding to the OWF IDs are shown in **Figure 4-2** and their names can be found in Table 11.*

OWF id	Euring	species	Aug + Sep	Okt + Nov	Dec + Jan	Feb + Mar	Apr + May	Jun + Jul	Total
1	6360	*Alca torda*	0.0	4.4	3.2	2.8	0.0	0.0	10.4
1	6540	*Fratercula arctica*	0.0	0.0	0.3	0.0	0.0	0.0	0.3
1	220	*Fulmarus glacialis*	0.0	0.0	0.4	0.1	0.0	0.0	0.5
1	59	*Gavia sp*	0.0	0.0	0.0	0.1	0.0	0.0	0.1
1	2130	*Melanitta nigra*	0.0	0.0	0.0	0.0	0.0	0.0	0.0
1	710	*Morus bassanus*	0.2	1.0	1.4	1.1	0.1	0.6	4.4
1	720	*Phalacrocorax carbo*	0.0	0.0	0.0	0.0	0.6	0.0	0.6
1	2060	*Somateria mollissima*	0.0	0.0	0.0	0.0	0.0	0.0	0.0
1	6110	*Thalasseus sandvicensis*	0.0	0.0	0.0	0.0	1.7	0.0	1.7
1	6340	*Uria aalge*	0.1	10.8	10.6	12.2	0.1	0.0	33.8
2	6360	*Alca torda*	0.0	1.4	3.3	5.8	0.0	0.0	10.5
2	6540	*Fratercula arctica*	0.0	0.0	0.4	0.0	0.0	0.0	0.4
2	220	*Fulmarus glacialis*	0.0	0.0	0.4	0.1	0.0	0.0	0.5
2	59	*Gavia sp*	0.0	0.0	0.0	0.0	0.0	0.0	0.0
2	2130	*Melanitta nigra*	0.0	0.0	0.0	0.0	0.0	0.0	0.0
2	710	*Morus bassanus*	0.3	1.0	1.7	1.4	0.3	0.0	4.7
2	720	*Phalacrocorax carbo*	0.0	0.0	0.0	0.0	0.9	0.0	0.9
2	2060	*Somateria mollissima*	0.0	0.0	0.0	0.0	0.0	0.0	0.0
2	6110	*Thalasseus sandvicensis*	0.0	0.0	0.0	0.0	0.8	0.0	0.8
2	6340	*Uria aalge*	0.1	6.4	11.4	19.7	0.1	0.0	37.7
3	6360	*Alca torda*	0.0	1.7	2.5	8.9	0.0	0.0	13.1
3	6540	*Fratercula arctica*	0.0	0.0	0.0	0.1	0.0	0.0	0.1
3	220	*Fulmarus glacialis*	0.0	0.1	0.5	0.2	0.0	0.0	0.8
3	59	*Gavia sp*	0.0	0.1	0.0	0.0	0.0	0.0	0.1
3	2130	*Melanitta nigra*	0.0	0.0	0.0	0.0	0.0	0.0	0.0
3	710	*Morus bassanus*	0.1	1.0	1.4	1.6	0.4	0.1	4.6
3	720	*Phalacrocorax carbo*	0.0	0.0	0.0	0.0	0.0	0.0	0.0
3	2060	*Somateria mollissima*	0.0	0.0	0.0	0.0	0.0	0.0	0.0
3	6110	*Thalasseus sandvicensis*	0.0	0.0	0.0	0.0	0.3	0.0	0.3
3	6340	*Uria aalge*	0.0	3.9	9.2	21.6	0.3	0.0	35.0
4	6360	*Alca torda*	0.0	0.1	0.2	0.3	0.0	0.0	0.6
4	6540	*Fratercula arctica*	0.0	0.0	0.0	0.0	0.0	0.0	0.0
4	220	*Fulmarus glacialis*	0.0	0.0	0.0	0.0	0.0	0.0	0.0
4	59	*Gavia sp*	0.0	0.0	0.0	0.0	0.0	0.0	0.0
4	2130	*Melanitta nigra*	0.0	0.0	0.0	0.0	0.0	0.0	0.0
4	710	*Morus bassanus*	0.0	0.0	0.1	0.1	0.0	0.0	0.2
4	720	*Phalacrocorax carbo*	0.0	0.0	0.0	0.0	0.0	0.0	0.0
4	2060	*Somateria mollissima*	0.0	0.0	0.0	0.0	0.0	0.0	0.0
4	6110	*Thalasseus sandvicensis*	0.0	0.0	0.0	0.0	0.0	0.0	0.0
4	6340	*Uria aalge*	0.0	0.1	0.3	0.9	0.0	0.0	1.3
5	6360	*Alca torda*	0.0	0.5	0.9	0.6	0.0	0.0	2.0
5	6540	*Fratercula arctica*	0.0	0.0	0.0	0.0	0.0	0.0	0.0
5	220	*Fulmarus glacialis*	0.0	0.0	0.0	0.0	0.0	0.0	0.0
5	59	*Gavia sp*	0.0	0.1	0.5	0.2	0.0	0.0	0.8
5	2130	*Melanitta nigra*	0.1	0.0	0.0	3.0	3.9	0.0	7.0

5	710	*Morus bassanus*	0.1	0.1	0.0	0.1	0.0	0.3	0.6
5	720	*Phalacrocorax carbo*	0.1	0.4	0.0	0.0	0.2	0.3	1.0
5	2060	*Somateria mollissima*	0.0	0.1	0.0	0.0	0.0	0.0	0.1
5	6110	*Thalasseus sandvicensis*	0.5	0.0	0.0	0.0	0.8	1.2	2.5
5	6340	*Uria aalge*	0.1	7.8	3.6	1.6	0.0	0.0	13.1
6	6360	*Alca torda*	0.0	0.4	0.4	0.3	0.0	0.0	1.1
6	6540	*Fratercula arctica*	0.0	0.0	0.0	0.0	0.0	0.0	0.0
6	220	*Fulmarus glacialis*	0.0	0.0	0.0	0.0	0.0	0.0	0.0
6	59	*Gavia sp*	0.0	0.0	0.0	0.0	0.0	0.0	0.0
6	2130	*Melanitta nigra*	0.0	0.0	0.0	0.0	0.0	0.0	0.0
6	710	*Morus bassanus*	0.0	0.1	0.0	0.1	0.1	0.0	0.3
6	720	*Phalacrocorax carbo*	0.0	0.0	0.0	0.0	0.0	0.0	0.0
6	2060	*Somateria mollissima*	0.0	0.0	0.0	0.0	0.0	0.0	0.0
6	6110	*Thalasseus sandvicensis*	0.0	0.0	0.0	0.0	0.4	0.0	0.4
6	6340	*Uria aalge*	0.0	2.6	3.8	1.3	0.1	0.0	7.8
7	6360	*Alca torda*	0.0	0.2	0.5	1.1	0.0	0.0	1.8
7	6540	*Fratercula arctica*	0.0	0.0	0.0	0.0	0.0	0.0	0.0
7	220	*Fulmarus glacialis*	0.0	0.0	0.0	0.0	0.0	0.0	0.0
7	59	*Gavia sp*	0.0	0.0	0.0	0.2	0.0	0.0	0.2
7	2130	*Melanitta nigra*	0.0	0.0	0.0	0.0	0.0	0.0	0.0
7	710	*Morus bassanus*	0.1	0.0	0.1	0.0	0.1	0.0	0.3
7	720	*Phalacrocorax carbo*	0.0	0.0	0.0	0.0	0.0	0.1	0.1
7	2060	*Somateria mollissima*	0.0	0.0	0.0	0.0	0.0	0.0	0.0
7	6110	*Thalasseus sandvicensis*	0.0	0.0	0.0	0.0	0.1	0.2	0.3
7	6340	*Uria aalge*	0.0	3.1	3.8	1.5	0.1	0.0	8.5
8	6360	*Alca torda*	0.0	0.9	0.8	1.0	0.1	0.0	2.8
8	6540	*Fratercula arctica*	0.0	0.0	0.0	0.0	0.0	0.0	0.0
8	220	*Fulmarus glacialis*	0.9	0.1	0.1	0.0	0.1	0.0	1.2
8	59	*Gavia sp*	0.0	0.0	0.0	0.0	0.2	0.0	0.2
8	2130	*Melanitta nigra*	0.0	0.0	0.0	0.0	0.0	0.0	0.0
8	710	*Morus bassanus*	0.2	0.3	0.0	0.0	0.0	0.1	0.6
8	720	*Phalacrocorax carbo*	0.0	0.0	0.0	0.0	0.0	0.0	0.0
8	2060	*Somateria mollissima*	0.0	0.0	0.0	0.0	0.0	0.0	0.0
8	6110	*Thalasseus sandvicensis*	0.4	0.0	0.0	0.0	0.1	0.0	0.5
8	6340	*Uria aalge*	2.3	2.4	4.3	1.0	0.7	0.3	11.0
9	6360	*Alca torda*	0.0	0.1	0.2	1.0	0.2	0.0	1.5
9	6540	*Fratercula arctica*	0.0	0.0	0.1	0.0	0.0	0.0	0.1
9	220	*Fulmarus glacialis*	0.0	0.0	0.0	0.0	0.1	0.0	0.1
9	59	*Gavia sp*	0.0	0.0	0.0	0.0	0.5	0.0	0.5
9	2130	*Melanitta nigra*	0.0	0.0	0.0	0.0	0.0	0.0	0.0
9	710	*Morus bassanus*	0.0	0.0	0.0	0.0	0.1	0.0	0.1
9	720	*Phalacrocorax carbo*	0.0	0.0	0.0	0.0	0.0	0.0	0.0
9	2060	*Somateria mollissima*	0.0	0.0	0.0	0.0	0.0	0.0	0.0
9	6110	*Thalasseus sandvicensis*	0.1	0.0	0.0	0.0	0.0	0.0	0.1
9	6340	*Uria aalge*	1.9	3.8	2.3	0.3	1.0	0.0	9.3
10	6360	*Alca torda*	0.0	1.9	1.8	3.7	0.2	0.0	7.6
10	6540	*Fratercula arctica*	0.0	0.0	0.0	0.0	0.0	0.0	0.0
10	220	*Fulmarus glacialis*	0.0	0.0	0.0	0.1	0.0	0.0	0.1
10	59	*Gavia sp*	0.0	0.0	1.1	0.9	0.1	0.0	2.1
10	2130	*Melanitta nigra*	0.0	0.0	0.0	0.0	0.0	0.0	0.0
10	710	*Morus bassanus*	0.4	0.2	0.1	0.0	0.3	0.2	1.2
10	720	*Phalacrocorax carbo*	0.0	0.0	0.0	0.0	0.0	0.3	0.3
10	2060	*Somateria mollissima*	0.0	0.0	2.0	0.0	0.0	0.0	2.0
10	6110	*Thalasseus sandvicensis*	0.6	0.0	0.0	0.0	0.6	0.4	1.6
10	6340	*Uria aalge*	0.1	8.0	13.8	3.7	0.4	0.4	26.4

11	6360	*Alca torda*	0.0	5.0	1.2	0.5	0.1	0.0	6.8
11	6540	*Fratercula arctica*	0.0	0.0	0.0	0.0	0.0	0.0	0.0
11	220	*Fulmarus glacialis*	0.0	0.0	0.0	0.0	0.0	0.0	0.0
11	59	*Gavia sp*	0.0	0.0	0.0	0.0	0.0	0.0	0.0
11	2130	*Melanitta nigra*	0.0	0.0	0.0	0.1	0.0	0.0	0.1
11	710	*Morus bassanus*	0.0	0.2	0.5	0.0	0.1	0.0	0.8
11	720	*Phalacrocorax carbo*	0.0	0.0	0.0	0.0	0.0	0.0	0.0
11	2060	*Somateria mollissima*	0.0	0.0	1.8	0.0	0.0	0.0	1.8
11	6110	*Thalasseus sandvicensis*	0.6	0.0	0.0	0.0	0.2	0.1	0.9
11	6340	*Uria aalge*	0.0	18.3	9.0	3.4	0.2	0.0	30.9
12	6360	*Alca torda*	0.0	0.9	1.2	0.6	0.0	0.0	2.7
12	6540	*Fratercula arctica*	0.0	0.0	0.0	0.0	0.0	0.0	0.0
12	220	*Fulmarus glacialis*	0.0	0.0	0.0	0.0	0.0	0.0	0.0
12	59	*Gavia sp*	0.0	0.0	0.2	0.0	0.0	0.0	0.2
12	2130	*Melanitta nigra*	0.0	0.0	0.0	0.0	0.0	0.0	0.0
12	710	*Morus bassanus*	0.0	0.2	0.4	0.0	0.2	0.0	0.8
12	720	*Phalacrocorax carbo*	0.0	0.0	0.0	0.0	0.0	0.0	0.0
12	2060	*Somateria mollissima*	0.0	0.0	0.3	0.0	0.0	0.0	0.3
12	6110	*Thalasseus sandvicensis*	0.0	0.0	0.0	0.0	0.4	0.1	0.5
12	6340	*Uria aalge*	0.0	8.6	8.0	2.2	0.0	0.0	18.8
13	6360	*Alca torda*	0.0	1.0	1.6	1.0	0.0	0.0	3.6
13	6540	*Fratercula arctica*	0.0	0.0	0.0	0.0	0.0	0.0	0.0
13	220	*Fulmarus glacialis*	0.0	0.0	0.0	0.0	0.0	0.0	0.0
13	59	*Gavia sp*	0.0	0.0	0.2	0.2	0.1	0.0	0.5
13	2130	*Melanitta nigra*	0.0	0.0	0.0	0.0	0.0	0.0	0.0
13	710	*Morus bassanus*	0.2	0.2	0.1	0.1	0.3	0.1	1.0
13	720	*Phalacrocorax carbo*	0.0	0.0	0.0	0.0	0.0	0.0	0.0
13	2060	*Somateria mollissima*	0.0	0.0	0.0	0.0	0.0	0.0	0.0
13	6110	*Thalasseus sandvicensis*	0.3	0.0	0.0	0.0	0.6	0.1	1.0
13	6340	*Uria aalge*	0.0	9.3	12.0	2.8	0.2	0.0	24.3
14	6360	*Alca torda*	0.0	2.3	2.1	3.7	0.0	0.0	8.1
14	6540	*Fratercula arctica*	0.0	0.0	0.0	0.0	0.0	0.0	0.0
14	220	*Fulmarus glacialis*	0.0	0.0	0.5	0.1	0.0	0.0	0.6
14	59	*Gavia sp*	0.0	0.0	0.0	0.2	0.0	0.0	0.2
14	2130	*Melanitta nigra*	0.0	0.0	0.0	0.0	0.0	0.0	0.0
14	710	*Morus bassanus*	0.1	1.0	1.5	1.4	0.2	0.3	4.5
14	720	*Phalacrocorax carbo*	0.0	0.0	0.0	0.0	0.0	0.0	0.0
14	2060	*Somateria mollissima*	0.0	0.0	0.0	0.0	0.0	0.0	0.0
14	6110	*Thalasseus sandvicensis*	0.1	0.0	0.0	0.0	1.3	0.0	1.4
14	6340	*Uria aalge*	0.0	7.8	6.4	11.5	0.3	0.0	26.0
15	6360	*Alca torda*	0.0	3.8	3.6	8.2	0.3	0.0	15.9
15	6540	*Fratercula arctica*	0.0	0.2	0.0	0.1	0.0	0.0	0.3
15	220	*Fulmarus glacialis*	0.0	0.0	0.1	0.1	0.0	0.0	0.2
15	59	*Gavia sp*	0.0	0.0	0.2	0.0	0.0	0.0	0.2
15	2130	*Melanitta nigra*	0.0	0.0	0.0	0.0	0.0	0.0	0.0
15	710	*Morus bassanus*	0.2	0.6	0.1	0.5	0.0	0.3	1.7
15	720	*Phalacrocorax carbo*	0.0	0.0	0.0	0.0	0.0	0.0	0.0
15	2060	*Somateria mollissima*	0.0	0.0	0.0	0.0	0.0	0.0	0.0
15	6110	*Thalasseus sandvicensis*	0.8	0.0	0.0	0.0	1.4	1.5	3.7
15	6340	*Uria aalge*	0.5	27.9	22.5	6.9	2.4	0.1	60.3
bw4	6360	*Alca torda*	0.1	1.6	1.8	2.7	0.1	0.0	6.3
bw4	6540	*Fratercula arctica*	0.0	0.0	0.1	0.0	0.0	0.0	0.1
bw4	220	*Fulmarus glacialis*	0.6	0.0	0.1	0.1	0.0	0.0	0.8
bw4	59	*Gavia sp*	0.1	0.0	0.0	0.1	0.1	0.0	0.3
bw4	2130	*Melanitta nigra*	0.0	0.0	0.0	0.0	0.0	0.0	0.0
bw4	710	*Morus bassanus*	0.2	0.4	0.1	0.0	0.1	0.1	0.9

bw4	720	*Phalacrocorax carbo*	0.0	0.0	0.0	0.0	0.0	0.0	0.0
bw4	2060	*Somateria mollissima*	0.0	0.0	0.0	0.0	0.0	0.0	0.0
bw4	6110	*Thalasseus sandvicensis*	0.9	0.0	0.0	0.0	0.1	0.0	1.0
bw4	6340	*Uria aalge*	8.0	3.0	7.9	2.1	2.7	0.7	24.4
bw6	6360	*Alca torda*	0.2	7.9	9.1	34.8	0.8	0.0	52.8
bw6	6540	*Fratercula arctica*	0.0	0.1	0.3	1.2	0.0	0.0	1.6
bw6	220	*Fulmarus glacialis*	0.9	0.5	1.4	1.2	0.8	0.6	5.4
bw6	59	*Gavia sp*	0.0	0.0	0.2	0.0	0.0	0.0	0.2
bw6	2130	*Melanitta nigra*	0.0	0.0	0.0	0.0	0.0	0.0	0.0
bw6	710	*Morus bassanus*	0.8	2.4	2.3	0.8	0.9	0.3	7.5
bw6	720	*Phalacrocorax carbo*	0.0	0.0	0.0	0.0	0.0	0.0	0.0
bw6	2060	*Somateria mollissima*	0.0	0.0	0.0	0.0	0.0	0.0	0.0
bw6	6110	*Thalasseus sandvicensis*	0.3	0.1	0.0	0.0	2.7	0.2	3.3
bw6	6340	*Uria aalge*	5.3	30.4	34.4	54.0	48.8	2.6	175.5
bw7	6360	*Alca torda*	0.0	2.1	4.5	10.9	0.0	0.0	17.5
bw7	6540	*Fratercula arctica*	0.0	0.1	0.0	0.1	0.0	0.0	0.2
bw7	220	*Fulmarus glacialis*	0.0	0.1	0.2	0.5	0.0	0.1	0.9
bw7	59	*Gavia sp*	0.0	0.0	0.2	0.0	0.0	0.0	0.2
bw7	2130	*Melanitta nigra*	0.0	0.0	0.0	0.0	0.0	0.0	0.0
bw7	710	*Morus bassanus*	0.3	0.7	0.3	0.4	0.5	0.1	2.3
bw7	720	*Phalacrocorax carbo*	0.0	0.0	0.0	0.0	0.0	0.0	0.0
bw7	2060	*Somateria mollissima*	0.0	0.0	0.0	0.0	0.0	0.0	0.0
bw7	6110	*Thalasseus sandvicensis*	0.1	0.0	0.0	0.0	0.5	0.0	0.6
bw7	6340	*Uria aalge*	0.9	15.4	13.5	10.5	4.4	0.0	44.7
bw8	6360	*Alca torda*	0.0	1.1	2.4	7.2	0.0	0.0	10.7
bw8	6540	*Fratercula arctica*	0.0	0.0	0.0	0.1	0.0	0.0	0.1
bw8	220	*Fulmarus glacialis*	0.0	0.0	0.1	0.1	0.0	0.1	0.3
bw8	59	*Gavia sp*	0.0	0.1	0.1	0.0	0.0	0.0	0.2
bw8	2130	*Melanitta nigra*	0.0	0.0	0.0	0.0	0.0	0.0	0.0
bw8	710	*Morus bassanus*	0.1	0.3	0.0	0.1	0.2	0.0	0.7
bw8	720	*Phalacrocorax carbo*	0.0	0.0	0.0	0.0	0.0	0.0	0.0
bw8	2060	*Somateria mollissima*	0.0	0.0	0.0	0.0	0.0	0.0	0.0
bw8	6110	*Thalasseus sandvicensis*	0.0	0.0	0.0	0.0	0.1	0.0	0.1
bw8	6340	*Uria aalge*	0.0	8.5	6.9	5.8	1.3	0.0	22.5
258	6360	*Alca torda*	0.2	14.7	24.3	8.1	0.5	0.1	47.9
258	6540	*Fratercula arctica*	0.0	0.2	0.4	0.4	0.6	0.0	1.6
258	220	*Fulmarus glacialis*	1.0	0.5	0.9	0.3	0.3	0.4	3.4
258	59	*Gavia sp*	0.0	0.0	1.2	3.0	0.7	0.0	4.9
258	2130	*Melanitta nigra*	0.0	0.0	0.0	0.0	0.0	0.0	0.0
258	710	*Morus bassanus*	1.3	2.7	0.5	0.2	0.0	1.2	5.9
258	720	*Phalacrocorax carbo*	0.0	0.0	0.0	0.0	0.0	0.0	0.0
258	2060	*Somateria mollissima*	0.0	0.0	0.0	0.0	0.0	0.0	0.0
258	6110	*Thalasseus sandvicensis*	0.1	0.0	0.0	0.0	0.4	0.0	0.5
258	6340	*Uria aalge*	52.9	43.4	135.9	23.7	32.7	16.0	304.6
263o	6360	*Alca torda*	1.0	6.2	5.7	2.8	0.7	0.0	16.4
263o	6540	*Fratercula arctica*	0.0	0.2	0.2	0.1	0.5	0.0	1.0
263o	220	*Fulmarus glacialis*	2.8	0.8	0.9	6.9	0.2	0.5	12.1
263o	59	*Gavia sp*	0.0	0.9	0.3	1.1	0.0	0.0	2.3
263o	2130	*Melanitta nigra*	0.0	0.0	0.0	0.0	0.0	0.0	0.0
263o	710	*Morus bassanus*	0.9	2.2	0.9	0.1	0.4	0.6	5.1
263o	720	*Phalacrocorax carbo*	0.0	0.0	0.0	0.0	0.0	0.0	0.0
263o	2060	*Somateria mollissima*	0.0	0.0	0.0	0.0	0.0	0.0	0.0
263o	6110	*Thalasseus sandvicensis*	1.4	0.0	0.0	0.0	0.7	0.0	2.1
263o	6340	*Uria aalge*	56.0	10.2	24.8	6.4	7.5	13.4	118.3
270	6360	*Alca torda*	0.0	6.4	13.2	17.9	0.4	0.0	37.9

270	6540	*Fratercula arctica*	0.0	0.1	0.1	0.2	0.0	0.0	0.4
270	220	*Fulmarus glacialis*	0.1	0.4	0.6	0.1	0.1	0.1	1.4
270	59	*Gavia sp*	0.0	0.0	0.0	0.2	0.6	0.0	0.8
270	2130	*Melanitta nigra*	0.0	0.0	0.0	0.0	0.0	0.0	0.0
270	710	*Morus bassanus*	0.4	1.4	0.9	0.2	0.4	0.2	3.5
270	720	*Phalacrocorax carbo*	0.0	0.0	0.0	0.0	0.0	0.0	0.0
270	2060	*Somateria mollissima*	0.0	0.0	0.0	0.0	0.0	0.0	0.0
270	6110	*Thalasseus sandvicensis*	0.3	0.0	0.0	0.0	0.6	0.2	1.1
270	6340	*Uria aalge*	1.6	25.3	34.0	21.4	28.8	1.1	112.2
272	6360	*Alca torda*	0.1	4.5	10.6	7.3	0.4	0.0	22.9
272	6540	*Fratercula arctica*	0.0	0.0	0.1	0.2	0.0	0.0	0.3
272	220	*Fulmarus glacialis*	0.4	0.4	0.5	0.2	0.3	0.2	2.0
272	59	*Gavia sp*	0.0	0.0	0.0	2.9	0.6	0.0	3.5
272	2130	*Melanitta nigra*	0.0	0.0	0.0	0.0	0.0	0.0	0.0
272	710	*Morus bassanus*	0.4	1.5	0.9	0.1	0.2	0.1	3.2
272	720	*Phalacrocorax carbo*	0.0	0.0	0.0	0.0	0.0	0.0	0.0
272	2060	*Somateria mollissima*	0.0	0.0	0.0	0.0	0.0	0.0	0.0
272	6110	*Thalasseus sandvicensis*	0.0	0.0	0.0	0.0	0.0	0.0	0.0
272	6340	*Uria aalge*	9.4	17.0	32.2	11.0	20.0	1.7	91.3
274	6360	*Alca torda*	0.2	44.4	10.6	13.1	2.7	0.0	71.0
274	6540	*Fratercula arctica*	0.0	0.1	0.1	0.0	0.0	0.0	0.2
274	220	*Fulmarus glacialis*	0.1	0.3	0.3	0.8	0.2	0.4	2.1
274	59	*Gavia sp*	0.0	0.0	0.3	0.5	1.5	0.0	2.3
274	2130	*Melanitta nigra*	0.0	0.0	0.0	0.0	0.0	0.0	0.0
274	710	*Morus bassanus*	1.6	1.9	0.7	1.4	0.9	0.7	7.2
274	720	*Phalacrocorax carbo*	0.0	0.0	0.0	0.0	0.0	0.0	0.0
274	2060	*Somateria mollissima*	0.0	0.0	0.0	0.0	0.0	0.0	0.0
274	6110	*Thalasseus sandvicensis*	1.4	0.1	0.0	0.0	1.3	0.2	3.0
274	6340	*Uria aalge*	27.5	42.2	45.8	31.9	27.8	6.0	181.2

Wageningen Marine Research

T +31 (0)317 48 7000

E: marine-research@wur.nl

www.wur.eu/marine-research

Visitors' address

- Ankerpark 27 1781 AG Den Helder
- Korringaweg 7, 4401 NT Yerseke
- Haringkade 1, 1976 CP IJmuiden

With knowledge, independent scientific research and advice, **Wageningen Marine Research** substantially contributes to more sustainable and more careful management, use and protection of natural riches in marine, coastal and freshwater areas.

Wageningen Marine Research is part of Wageningen University & Research. Wageningen University & Research is the collaboration between Wageningen University and the Wageningen Research Foundation and its mission is: 'To explore the potential for improving the quality of life'